

1975

Frame stability and design of columns in unbraced multistory steel frames, July 8, 1975 (77-27)

L. W. Lu

Erkan Ozer

J. H. Daniels

Omer S. Okten

Follow this and additional works at: <http://preserve.lehigh.edu/engr-civil-environmental-fritz-lab-reports>

Recommended Citation

Lu, L. W.; Ozer, Erkan; Daniels, J. H.; and Okten, Omer S., "Frame stability and design of columns in unbraced multistory steel frames, July 8, 1975 (77-27)" (1975). *Fritz Laboratory Reports*. Paper 2036.
<http://preserve.lehigh.edu/engr-civil-environmental-fritz-lab-reports/2036>

This Technical Report is brought to you for free and open access by the Civil and Environmental Engineering at Lehigh Preserve. It has been accepted for inclusion in Fritz Laboratory Reports by an authorized administrator of Lehigh Preserve. For more information, please contact preserve@lehigh.edu.

Effective Column Length and Frame Stability

FRAME STABILITY AND DESIGN OF COLUMNS IN UNBRACED MULTISTORY STEEL FRAMES

by

Le-Wu Lu

Erkan Ozer

J. Hartley Daniels

Omer S. Okten

Shosuke Morino

This work has been carried out as part of an investigation sponsored by the American Iron and Steel Institute.

Reproduction of this report in whole or in part is permitted for any purpose of the United States Government.

Fritz Engineering Laboratory

Lehigh University

Bethlehem, Pennsylvania

July 8, 1975

Fritz Engineering Laboratory Report No. 375.2

ABSTRACT

The strength and drift characteristics of unbraced multi-story steel frames subjected to combined gravity and wind loads are studied with special emphasis on the effect of overall frame instability. Seven frames having dimensions and working loads typical of those commonly found in apartment and office structures were selected for detailed study. Four designs were made for each frame: three stress-controlled designs and one drift-controlled design. The stress designs were all based on the allowable-stress provisions of the AISC Specification; the main difference is in the design columns. In two of these designs, the effect of frame instability was not considered and the columns were proportioned as if the frame had been laterally braced. In the third design this effect was included by following the AISC provisions for columns in an unbraced frame. The drift design was made to satisfy approximately a drift limitation of 0.002 at working load.

The frames were then analyzed for their response in the elastic and elastic-plastic range under proportioned and non-proportioned gravity and wind loads. The latter involved constant gravity load and increasing (or decreasing) wind. In most cases, the levels of gravity load used in the non-proportional analysis were the working load and 1.30 times the working load. Both first- and second-order analysis were carried out to determine the various characteristic loads, including maximum loads and the first plastic hinge load, and the characteristic drifts, including drifts at working

and factored loads. In the second-order analysis, the reduction of member stiffness due to axial force and effect of frame instability were included. →
s. 6

The results show that even though the strength of the structures is reduced considerably by frame instability, all stress designs are sufficiently strong to achieve a wind load factor equal to or greater than 1.40 under proportional loads, 2.06 under non-proportional loads with gravity load maintained at the working value, and 1.66 with gravity load maintained at 1.30 times the working value. Also, the stress design having columns proportioned in accordance with the AISC provisions for unbraced frames do not show significant increase in load-carrying capacity when compared with the designs in which frame instability effect is neglected. The drift design frames have large wind load-carrying capacity, with load factors ranging from a low of 1.45 for proportional loading condition to more than 4.0 for non-proportional loading condition, depending on the gravity load on the beams.

Based on the results obtained, a simple design procedure is recommended for unbraced frames with geometry, loads, and drift characteristics similar to those of the frame studied. This procedure recognizes that adequate strength and stability can be assured when the working load drift is held to within a certain limit.

TABLE OF CONTENTS

	<u>Page</u>
ABSTRACT	i
1. INTRODUCTION	1
1.1 Limit Loads of Multistory Frames	2
1.2 Current Approach in Allowable-Stress Design	3
1.3 Frame Designed for Drift Control	5
1.4 Objectives and Scope of Study	6
2. DESIGN OF FRAMES	8
2.1 Selection of Frames and Working Loads	8
2.2 Design Assumptions	9
2.3 Design Procedure and Criteria	10
2.3.1 Stress-Controlled Designs	11
2.3.2 Drift-Controlled Design	12
2.4 Preliminary Design Procedure	13
2.5 Final Stress Design Procedure	15
2.6 Drift Design Procedure	16
2.7 Member Sizes Selected	16
3. ANALYSIS OF FRAMES	18
3.1 Analysis Procedure	18
3.1.1 Second-Order Proportional Load Analysis (SOFRAN-LIN)	19
3.1.2 Second-Order Non-Proportional Load Analysis (SOFRAN-DIN)	19
3.2 Analysis Performed	19
3.3 Summary of Results	21
4. DISCUSSION OF RESULTS	23
4.1 Identifying Parameters of Frames	23
4.2 Comparison of Proportional and Non-Proportional Load-Drift Curves	23
4.3 General Behavior and Load-Drift Characteristics	25
4.3.1 Analyses 1, 2 and 3	25
4.3.2 Analysis 5	28
4.3.3 Lower Bound to Frame Strength	28

4.4	Strength Characteristics of Frames	29
4.4.1	Maximum Loads from First-and Second-Order Analyses	29
4.4.2	First Plastic Hinge Load	30
4.4.3	Design I Versus Design II	31
4.4.4	Design I Versus Design III	32
4.4.5	Frame 3 Versus Frame 4	32
4.4.6	Frame 1 Versus Frame 6	33
4.4.7	Frame 4 Versus Frame 7	34
4.5	Drift Characteristics of Frames	34
4.5.1	Working Load Drift of Stress-Controlled Designs	34
4.5.2	First-Order Versus Second-Order Drift	35
4.5.3	Design I Versus Design II	35
4.6	P-Delta Moments in Frames	36
4.6.1	Development of ϕ and $\bar{\phi}$ Factors	36
4.6.2	P-Delta Moments at Working and Factored Loads	37
4.7	Plastic Hinge Patterns	39
4.8	Relationships Between Maximum Strength and Working Load Drift	40
4.9	Comments on Columns in Stress-Controlled Designs	41
4.9.1	Governing Column Formulas in Designs I and III and in Design II	42
4.9.2	Maximum Axial Stress Ratios and Column Slenderness Ratios	43
4.9.3	Relative Column Weights	44
5.	DESIGN RECOMMENDATIONS	45
5.1	Review of Results	45
5.2	Recommendations for Allowable-Stress Design	47
6.	SUMMARY AND CONCLUSIONS	48
7.	ACKNOWLEDGEMENTS	51
8.	APPENDIXES	52
	Appendix A Preliminary Design of Design I, Frame 1	53

Appendix B	Second-Order Frame Analysis--Load Increment Program (SOFRAN-LIN)	61
Appendix C	Second-Order Frame Analysis--Drift Increment Program (SOFRAN-DIN)	62
Appendix D	Effect of Variation of Modulus of Elasticity	63
Appendix E	Effect of Residual Stresses	64
9.	NOMENCLATURE	65
10.	TABLES AND FIGURES	68
11.	REFERENCES	133

1. INTRODUCTION

When allowable-stress method is used in designing unbraced multi-story steel frames, the columns are usually proportioned as isolated members utilizing the "effective length concept". The effective column length, always greater than the actual length, is determined from an elastic buckling analysis of the frame under gravity load. The analysis assumes that the frame buckles in the sidesway mode at the critical load. Strictly speaking, the effective length thus determined can be rationally used only in the design of frames which are loaded by gravity load that causes no bending moment in the members (load acting along the axes of the columns).⁽¹⁾ When the gravity load is applied to the beams, or when, in addition to the gravity load, lateral load is also applied, bending moment occurs in the frame. The columns must therefore be designed for the combined effect of axial thrust and bending moment. The effective column length approach becomes inadequate when bending moment, as well as axial thrust, must be considered in the design process.

For the case of combined gravity and lateral loads, frame drift occurs as soon as the lateral load is applied. At a given level of the applied loads, each story of the frame has a definite value of drift Δ (delta). Due to this drift, an additional secondary bending moment, known as the P- Δ (P-delta) moment, is developed in each story, where P is the total gravity load above the story. This moment introduces the effect of frame instability into the structure. At high levels of the applied loads the bending moment due to the applied loads together with the P-Delta moment causes yielding in the critical parts of the frame. Eventually the structure fails by the combined

influence of frame instability and yielding. The behavior is similar to that of a beam-column. Thus, the problems, which must be carefully considered in developing design method, is the effect of the P-Delta moment at both the working load and the maximum load levels. Also, the ultimate strength of a multistory frame can be closely evaluated only when both effects of yielding and instability are taken into account. Any elastic analysis, regardless how refined, can not give a realistic assessment of strength of the frame.

1.1 Limit Loads of Multistory Frames

Figure 1 shows the lateral load vs. drift relationships of a frame subjected to proportionally increasing gravity and lateral loads, the proportionality constant being equal to α . Two types of frame analysis can be performed. The first-order analysis in which the effect of P-Delta moment is ignored, and the second-order analysis in which this effect is included. If the frame is perfectly elastic, the first-order analysis gives a linear relationship, shown as (a) in Fig. 1. The second-order analysis leads to the non-linear load vs. deflection curve (b) which approaches the elastic stability limit load of the frame when the drift becomes very large (equal to infinity in theory). It has been shown that the gravity load represented by the elastic stability limit load is equal to the elastic buckling load of the frame. (2) That is, the presence of the lateral load does not reduce the gravity load carrying capacity of the structure. This load can therefore be determined simply from a frame buckling analysis for the sidesway mode, and it has an engineering significance only if the structure remains entirely elastic. A study of the yield stress levels of the structural steels and the dimensions and loads commonly en-

countered in building design has indicated that for frames of practical proportions this load is usually several times higher than the load which will cause initial yielding in the structures.⁽³⁾ The elastic stability limit load, therefore, gives only a qualitative indication of the stable (or unstable) characteristic of a structure, and the effective column length determined from this load obviously has only limited significance in frame design.

When the effect of yielding is included in the analysis, the load vs deflection relationships shown as curves (c) and (d) in Figure 1 are obtained. The first-order curve becomes horizontal at the plastic limit load. This is the load at which the frame will deform continuously as a kinematic mechanism if the effect of deformation and the associated P-Delta moment is not present. The "real" behavior of the structure is closely represented by curve (d) obtained from the second-order elastic-plastic analysis in which the combined effects of yielding and P-Delta moment are taken into account.⁽⁴⁾ The peak of the curve corresponds to the inelastic stability limit load (or simply the stability limit load), and it usually does not coincide with the formation of a plastic mechanism. The strength of multistory frames designed by different approaches can best be studied using this load as the basis of comparison.

1.2. Current Approach in Allowable-Stress Design

The effect of frame instability is taken into account in the current practice by modifying the basic beam-column interaction formulas. The basic formulas given in the AISC Specification for proportioning columns in a braced planar frame are;⁽⁵⁾

$$\frac{f_a}{F_a} + \frac{C_m f_b}{\left(1 - \frac{f_a}{F_e'}\right) F_b} \leq 1.0 \quad (1)$$

and

$$\frac{f_a}{0.6F_y} + \frac{f_b}{F_b} \leq 1.0 \quad (2)$$

in which f_a and f_b are, respectively, the computed axial and bending stresses, and

F_a = allowable axial stress if axial force alone existed

F_b = allowable compressive bending stress if bending moment alone existed

F_e' = elastic Euler buckling stress divided by a factor of safety. It is always computed for the in-plane case of buckling.

$C_m = 0.6 - 0.4 \frac{M_1}{M_2} \geq 0.4$ where $\frac{M_1}{M_2}$ is the ratio of the

smaller to the larger moments applied at the ends of the member. It is positive when the member is bent in reverse curvature.

The first formula takes into account the member instability effect occurring within the individual beam-columns, and the second is to safe guard against yielding at the ends (or braced points) of the members. The use of these formulas in column design is discussed more fully in Chapter 2.

Two modifications are required when the frame under consideration is not laterally braced. The first is the use of an in-plane

effective column length factor K in computing F_a and F_e' and the second is to assign a C_m value of 0.85 (instead of the much smaller values given by the formula above). The validity of these modifications has long been questioned and a need therefore exists for a systematic evaluation of the strength of unbraced multistory frames designed according to the current approach. More broadly, a need also exists for a comprehensive study of the behavior of unbraced frames in the elastic-plastic range and near the maximum load. A thorough understanding of the significance of the P-Delta effect appears necessary in an effort to develop alternate methods for frame design.

1.3 Frames Designed For Drift Control

In addition to the stress criteria, the design of most practical unbraced frames must also satisfy a working load drift criterion which is imposed by the designer and found from experience. For frames more than ten to twenty stories in height the drift criterion usually would require an increase in the member sizes over those selected to satisfy the stress requirements. Since the amount of P-Delta moment existing in each story is a direct function of frame drift, increased frame stiffness results in a reduction of the P-Delta moment and, consequently, leads to an increase in the load-carrying capacity. A relationship therefore exists between frame strength (as determined by the stability limit load) and frame stiffness. A thorough study of the strength of frames designed for

drift control is needed in order to establish such a relationship.

1.4 Objectives and Scope of Study

The objectives of this study are:

1. To select a small group of seven unbraced multistory frames for investigation. This group of seven frames is to be representative of a much larger group of similar frames commonly encountered in apartment and office type structures, with respect to geometry, loading and performance parameters.

2. To study the strength and drift characteristics the selected frames where the columns are proportioned to meet the 1969 AISC allowable-stress criteria but with no consideration being given to the effect of frame instability. The frames are therefore designed as if they were laterally braced. An evaluation of the load-carrying capacity of these frames due to frame instability effect is also made.

3. To investigate the strength and drift characteristics of the frames where the columns are proportioned to meet all AISC allowable-stress criteria (that is, using K in computing F_a and F_e' and $C_m = 0.85$).

4. To investigate the strength and drift characteristics of the frames which are designed to meet drift as well as stress criteria.

5. To evaluate the P-Delta moment in a story in relation to the moment due to the applied lateral load.

6. To develop new method of column design in unbraced frames subjected to combined loads.

In this study, seven different unbraced frames, ranging from 10-story, 5-bay to 40-story, 2-bay, were selected for detailed design and analysis. Included are two apartment and five office type frames. These frames differ in height-to-width ratios, bay widths, story heights, number of bays and stories, and level of working loads. The frames are designed to satisfy either the stress provisions of the AISC Specification or a drift index criterion of 0.002.* The columns are designed as discussed above. A large number of first-order and second-order proportional and non-proportional load analyses are then carried out using computer programs developed for this purpose at the Fritz Laboratory. All second-order analyses determine the strength and drift characteristics of the frames in the elastic and elastic-plastic range.

* This value is in accordance with the recommendation made in Ref. 6.

2. DESIGN OF FRAMES

2.1 Selection of Frames and Working Loads

Figure 2 shows the dimensions and working loads of the seven unbraced multistory steel frames selected for the study. The selection drew heavily upon the experience and judgment of the members of a task committee which was organized by the AISI to provide technical advice to this study.* The main consideration was to assemble a small number of different unbraced frames for design and analysis which would represent a much larger class of unbraced frames commonly encountered in the design of many office and apartment type structures in the United States.

The parameters considered significant in the selection of the frames were: (1) overall height-to-widths ratios, (2) individual bay widths, (3) individual story heights, (4) number of bays and stories for a given frame, (5) spacing of the frames, and (6) magnitude of the working loads.

Frames 1 and 6 represent frames found in relatively low apartment type structures. The story heights, bay widths and working loads are considered to be fairly representative for such structures. Frames 2, 4, 5 and 7 represent frames found in low-to-medium height office type structures. Again, the story heights, bay widths, and working loads are considered to be representative.

*The names of the Committee members are given in the Acknowledgement.

Frame 3 represents a medium height office type structure having slightly larger working loads.

Specifically, Frames 3 and 4 were selected to study the effect of variation in gravity loads. Frames 1 and 6 were selected to provide a comparison of the effect of the number of bays on the behavior of a relatively low frame. Also, Frames 4 and 7 were selected to provide a comparison of the effect of number of stories.

Two loading conditions were considered: (1) gravity loads alone, and (2) gravity plus wind loads. The gravity loads consisted of the dead and live floor loads (including partitions), dead and live roof loads, exterior wall loads and the parapet load (3-ft. high parapet assumed). The gravity loads on the beams are uniform and symmetrical about the frame centerlines. The wind loads are constant over the entire height and can act from the left or right.*

2.2 Design Assumptions

1. A36 steel is used for beams and columns.
2. All members are oriented with their web in the plane of the frames and are subjected to strong-axis bending.
3. The frames are braced in the out-of-plane direction at the joints. In one of the three stress designs of each frame, the columns are also assumed to be braced against weak-axis buckling.

*A moderate wind load intensity of 20psf is used throughout this study. It is believed that in frames designed for higher levels of wind the influence of P-Delta moment (and the effect of frame instability) would be less critical.

4. Lateral-torsional buckling of the beams is prevented by the floor system.

5. Local buckling of flanges and webs does not occur.

6. Member lengths are defined by their centerlines.

7. The ANSI live load reduction formula is used to compute the beam and column loads.⁽⁷⁾

8. Wall and parapet loads are applied as concentrated loads at the exterior joints.

9. Wind loads are applied as concentrated loads at the exterior joints.

10. No composite action occurs between the beams and the floor system.

11. Behavior of frames is assumed to be linear and elastic, and P-Delta effect is ignored. (See Art. 2.5).

12. Stress-controlled designs are in accordance with the 1969 AISC Specification; exceptions are as explained in Art. 2.3.1.

13. Drift-controlled designs are as described in Art. 2.3.2.

2.3 Design Procedure and Criteria

The design of the frames is based on the procedure described in the book "Structural Steel Design"⁽⁸⁾ and the selection of member sizes is in accordance with the AISC Specification. The design of the frames was partly done by hand and partly carried out on the computer using a program prepared in the course of the investigation.

2.3.1 Stress-Controlled Designs

Stresses for the gravity loading condition are computed using the loads shown in Fig. 1. For the gravity plus win (combined) loading condition both loads are multiplied by 0.75, instead of increasing the allowable stress by one-third as prescribed by the AISC Specification. (5,8)

The maximum calculated bending stress in the beams is compared with the AISC allowable stress, for both loading conditions. The basic AISC interaction equations for beam-columns are used in the design of all columns for both loading conditions. However, for the combined loading case the selection of effective column length K and the method of computing the coefficient C_m leads to three different stress-controlled designs for each frame as follows (Table 1):

Design I: For both the in-plane and out-of-plane (lateral) directions K is assumed to be unity ($K_x = 1.0$, $K_y = 1.0$). Lateral bracing of the columns is provided only at the beam-to column joints. All columns are proportioned to satisfy both Formulas (1) and (2). In Formula (1) F_a is computed using $\frac{h}{r_y}$, F'_e using $\frac{h}{r_x}$, and the coefficient C_m is determined as if the frame was braced. The effect of frame instability is therefore completely ignored in this design.

Design II: For the in-plane direction K is computed using the AISC alignment chart for the sidesway permitted case. For the out-of-plane direction K is assumed to be unity ($K_y = 1.0$). The frames are again assumed to be braced at the beam-to-column joint only. The F_a term is computed using the larger of the two slenderness

ratios, $\frac{Kh}{r_x}$ and $\frac{h}{r_y}$ and F'_e is based on $\frac{Kh}{r_x}$. The coefficient of C_m is equal to 0.85 as recommended by AISC. (5) This design complies with all the AISC Specification requirements with regard to frame instability.

Design III: For the in-plane direction K is assumed to be unity ($K_x = 1.0$). In the out-of-plane direction the columns are considered to be braced continuously against lateral-torsional buckling. Therefore only the effect of in-plane strong-axis bending is considered in the column design. The slenderness ratio $\frac{h}{r_x}$ is used in computing both F_a and F'_e . The AISC formula for braced frames is again used to obtain the coefficient C_m .

2.3.2 Drift-Controlled Design

The criterion for drift used in this investigation is the working load drift index for the frame as a whole. That is, the relative roof to base drift at combined working loads, divided by the total frame height. One drift controlled design is performed for each frame as follows:

Design IV: The member sizes determined in Design I are modified using a simplified optimization procedure (9) to achieve a working load drift index of 0.002 (1/500). This procedure leads to member sizes which are close to those required by a theoretical minimum weight design. In most instances this requires an increase in beam size but no change in column size. For Frames 4 and 7 the column sizes are also increased slightly.

2.4 Preliminary Design Procedure

The bending moments in each beam due to the gravity loads alone are computed taking the end restraints into account in an approximate manner. The wind moments in the beams and columns are determined using a conventional Portal analysis.⁽⁸⁾ Axial thrusts in the columns due to gravity loads are computed using tributary column areas, and axial thrusts in the columns due to wind are determined from a conventional Cantilever analysis.⁽⁸⁾ No P-Delta effect is considered.

The preliminary design procedure is illustrated in Appendix A using Frame 1 - Design I as an example. (A more complete explanation of the procedure is given in Ref. 8).

Step 1 in Appendix A shows the assignment of loads for Frame 1. Also shown are the live load reduction factors for the beams and the columns.

Step 2 shows the Portal analysis of the frame assuming that wind load is applied as a concentrated load at each level. The distribution factor for column shear due to wind is assumed to be proportional to the aisle width.

Step 3 shows a typical beam design at Level 10 of Frame 1. Calculations 10 and 11 determine the positive and negative bending moments due to gravity load, considering the effect of elastic restraint provided by the adjacent columns. For the computation of stress under combined wind and gravity loads (Calculations 12 to 18), the stress resultants (moments, etc.) are taken as 3/4 of those produced by the working loads to account for the 1/3 increase in allowable

stress permitted by AISC. Calculations 17 and 18 give the value of positive and negative bending moment in a beam under the combined loads. Final beam sizes are chosen according to the largest bending moment given in calculations 19 or 20.

Step 4 shows the gravity load thrusts in the columns at every other story. Note that the live load reduction factors computed in Step 1 are used here.

The bending moments in the columns due to gravity load alone are shown in Step 5. The column moments are obtained by distributing the beam moments equally above and below a joint.

Axial thrusts in columns due to wind are computed in Step 6 using a Cantilever analysis.

In Step 7, the bending moments in the columns due to wind are computed using a Portal analysis.

In Step 8 the axial thrusts and bending moments in the columns are summarized. Axial thrusts due to combined loads are obtained by multiplying the summation of those due to gravity load and to wind load (Step 6) by 0.75.

Step 9 illustrates the design of an exterior column between levels 10 and 11 for both the gravity and the gravity plus wind loading conditions. A column section W8x58 is chosen for the first trial, and section properties are shown in Calculations 5 to 10. Note that K is assumed to be unity. Stresses caused by axial thrust and bending moment are given in Calculations 11 and 12. The allowable

bending stress is equal to 60% of the yield stress as shown in Calculation 16. The allowable stress for the axial thrust is given in Calculation 19.

Computation of the interaction formulas starts from Calculation 20. Note that the formula to compute C_m given in Calculation 23 is for a braced frame.

2.5 Final Stress Design Procedure

The frames obtained in the preliminary design are analyzed on a first-order basis, under both gravity and combined gravity and wind loading conditions. For the beams the computed stresses are compared with the AISC allowable stresses. These stresses are kept to within $\pm 5\%$ of the allowable stresses (about ± 1.1 ksi for A36 steel) consistent with the availability of sections. The columns are checked using the appropriate modified AISC interaction equation as discussed in Art. 2.3.1. Computed values are within the range of 1.05 to 0.80 for the sum of the interaction equation terms. Most columns, however, this sum is maintained within 1.05 to 0.9.

A second-order elastic-plastic computer program (based on proportional loading condition and using the load increment approach^{(10)*}) is employed to obtain the approximate first-order wind load versus drift curve of all sevel frames. This curve is generated in each case by a linear projection of the response obtained at a load factor of 0.25. Stress resultants at 75% of the working loads for the combined load condition are also based on a linear projection of the results at the 0.25 load factor level. A small error is introduced

* A description of this program is given in Appendix B

due to the small second-order effects actually present at the 0.25 load factor level and reflected in the first-order results. This error was examined however and found to be only about 2 to 3%. In addition, drift computations for Frame 4 based on this program and the STRESS programs indicated a negligible difference.

This second-order program is also used to find the stress resultants under gravity load alone by specifying zero wind load.

A computer program (COLCHK) was developed specifically to design the columns of the frames used in the study. It makes use of the end moments and axial force obtained from the first-order analysis. The program provides several possible shapes and allows the final selection to be made by the designer.

2.6 Drift Design Procedure

Fleischer's procedure by which drift and material-optimized drift adjustments for unbraced frames can be closely estimated is used to achieve drift-controlled designs⁽⁹⁾ In all cases Design I is used as the initial design. Whenever the calculated column adjustment factor is close to unity the column sizes are unchanged.

2.7 Member Sizes Selected

The member sizes selected for the seven frames designed four different ways are shown in Tables 2 to 8. All frames are symmetrically proportioned since geometry and gravity load conditions are symmetrical and wind loads can occur from either direction. An attempt was made also to follow accepted design office rules of standard practice when proportioning each frame. The following rules apply to the

selection of member sizes for all frames:

- 1) All beams on the same level have same member size.
- 2) All exterior columns in the two consecutive stories have same member size (that is, exterior columns in the first and second stories have same member size etc.)
- 3) All interior columns in the two consecutive stories have same member size.

As shown in Tables 4, 5, 6, and 8 Designs I and III for Frames 3, 4, 5, and 7 are identical. This is because in both designs the column sizes are controlled by the stress formula $\frac{f_a}{0.6F_y} + \frac{f_b}{F_b} \leq 1.0$. Since the stress design of Frame 6, Design I, already met the working load drift criterion of 0.002 discussed in Art. 2.3.2, Design IV for Frame 6 was not performed. (See also Fig. 20.)

3. ANALYSIS OF FRAMES

The complete analytical results of this study for all frame designs (23 separate designs and 99 analyses) are shown in Figs. 3 through 25. The figures show the relationships between wind load factor W/W_0 and drift index Δ/H (W is the applied wind load, W_0 the working wind load, Δ the roof level drift, and H the total frame height). Each frame design is subjected to as many as five separate and different analyses. The lateral load versus drift results are shown by numbered curves in the figures. The analysis procedure used to obtain each curve will be described in detail in Art. 3.1. The first occurrence of a plastic hinge is indicated on each curve by the open or solid circle, triangle, or square.

In all the figures, the load-drift curves for stress-controlled frames begin at zero wind load factor. The curves for all drift-controlled frames begin at a wind load factor of one.

3.2 Analysis Procedure

Following the final design of each frame, as described in Chapter 2, up to five additional independent analyses are then performed by computer to obtain the load vs drift relationships of each frame under proportional and nonproportional combined gravity and wind loads. A summary of these analyses is given in Table 9. Two computer programs (SOFRAN-LIN and SOFRAN-DIN) previously developed at Fritz Laboratory and significantly improved during this investigation are used for this purpose. These programs are briefly described in Appendix B and C.

3.1.1 Second-Order, Proportional Load Analysis (SOFRAN-LIN)

The analysis of each frame is initiated at a load factor of 0.25 as described in Appendix B. (These results were previously used in the final design stage as described in Chapter 2). Subsequent analyses are obtained at 0.25 increments up to the working load level (L.F. = 1.0). Between the working load level and the maximum load level increments of 0.05 in load factor are used. The load-drift behavior of each frame under proportional loads is shown as Curve 3 in Figs. 3 through 25.

3.1.2 Second-Order, Non-Proportional Load Analysis (SOFRAN-DIN)

The gravity loads are first applied to the beams and plastic hinges, if any, noted. Lateral wind loads are then applied following the drift increment technique developed in Ref. 11 and briefly described in Appendix C. The load-drift behavior of each frame under non-proportional loads is shown as Curves 1, 2 and 5 in Figs. 3 through 25. In each of these curves the designated load factor for gravity loads GLF is 1.3, 1.0 and 1.2 respectively. For Curve 5 the yield stress level of the steel beams and columns is assumed to be 90% of that for A36 steel or 32.4 ksi. Curve 5 therefore includes the effect of a material strength factor as well as load factor. This analysis is carried out only for the Frame 2 designs and for the Frame 5 designs.

3.2 Analyses Performed

The complete investigation of each frame required the following major analyses, performed in the following order (Table 9):

Analysis 1: A second-order elastic-plastic analysis is performed for non-proportional loads with a gravity load factor of 1.3 (Curve 1, Figs. 3 through 25). Depending on the refinement of the final design a complete load-drift curve (with ascending and descending portions) may or may not be achieved. In a few cases, no descending portion of the curve is obtained because the axial load in the critical column exceeds the axial yield load, that is, $P > P_y$. When this happens, the analysis is terminated and corresponding load is recorded as the maximum load.

Analysis 2: This is also a second-order elastic-plastic analysis for non-proportional loading condition but with the gravity load factor reduced to 1.0 (Curve 2). Since the loading condition is less severe than in Analysis 1, a higher maximum wind load is always obtained.

Analysis 3: A second-order elastic-plastic analysis is performed for the proportional loading case and the results are shown as Curve 3.

Analysis 4: This is a first-order elastic analysis and makes use of the results of Analysis 3 for a load factor of 0.25. As described in Art. 2.5, the first-order analysis results were used to check the adequacy of the trial member sizes in the final stage of frame design. The elastic load-drift relationship is given as Curve 4.

Analysis 5: This analysis is made for the non-proportional loading condition using a gravity load factor of 1.2 and a yield stress

level equal to 90% of the specified yield stress, as discussed in Art. 3.1.2. The results are shown as Curve 5 in Figs. 7, 8, 9, 10, 17, 18, and 19.

A first-order elastic-plastic analysis is also made under proportional loads for all the Design I frames. The results of this analysis may be compared with those of Analysis 3 to assess the reduction in the load-carrying capacity due to frame instability.

In all the analysis performed a modulus of elasticity E equal to 29,000 ksi is used and all members in the frames are assumed to be free of residual stress. Appendix D contains the results of a study made to examine the effect of changing E values on the load-drift relationship. The influence of cooling residual stress has also been studied and the results are given in Appendix E.

3.3 Summary of Results

A summary of the analytical results is presented in Tables 10 to 13 inclusive. Tables 10, 11 and 12 contain a summary of the results of the three stress designs of each frame. Table 13 is a summary of the results of the one drift design of each frame.

Column 2 of each table shows the working load-drift index of each frame (roof top drift at wind load factor of one divided by frame height) resulting from the first-order elastic analysis (Analysis 4). Columns 3, 6, 9 and 12 show the working load-drift index of each frame as determined by Analyses 3, 2, 5 and 1, respectively. Similarly Columns 4, 7, 10 and 13 show the values of

the wind load factor at the formation of the first plastic hinge in each frame, and Columns 5, 8, 11 and 14 show the maximum load (stability limit load) factor achieved for each frame, as determined by the various analyses performed.

Table 14 shows a comparison between the maximum load (plastic limit load) factors of the Design I frames from the first-order elastic-plastic analysis and those from Analysis 3.

4. DISCUSSION OF RESULTS

4.1 Identifying Parameters of Frames

As previously stated in Art. 1.4, the small group of seven frames selected for this study is considered to be representative of a much larger class of similar frames commonly encountered in apartment and office type structures. It may be assumed that any unbraced steel frame, designed for use in such structures and within the general geometric, loading and performance parameters of the frames investigated in this report, will have analytical characteristics similar to those presented in this report. Geometric parameters include: (1) number of stories, (2) number of bays, (3) frame height-to-width ratio, (4) story height, (5) bay width, and (6) panel aspect ratios (story height divided by bay width). Loading parameters include: (1) roof and floor dead and live loads, (2) wall and parapet loads, and (3) wind loads. Performance parameters include: (1) frame drift index (roof top drift divided by frame height) and (2) story drift index (story drift divided by story height).

4.2 Comparison of Proportional and Non-Proportional Load-Drift Curves

Figure 26 shows qualitative load-drift curves of an unbraced frame subjected to combined gravity and wind loads. Each numbered curve represents the results of one of the four analyses explained in Art. 3.2 (Analyses 1, 2, 3 or 4). The location of the first plastic hinge in the figure is represented by an open or solid circle or a solid triangle as also shown in Figs. 3 through 25.

Figure 26 will be used to explain the relationships between the load-drift curves as determined by proportional and non-proportional load analyses.

In the figure the first plastic hinges for Analysis 2 (non-proportional, gravity load factor of 1.0) and Analysis 3 (proportional) are both assumed to occur above a wind load factor of 1.0 (working). In this case Curves 2 and 3 must coincide at a wind load factor of 1.0 (point (a)).

Curve 3 must be initially tangent to Curve 4 (first-order) and lies to the left of Curve 2 prior to the working load level. Beyond this point Curve 2 must lie above Curve 3.

The same observation also holds if the first plastic hinges for Analysis 1 (non-proportional, gravity load factor of 1.3) and Analysis 3 both lie above a wind load factor of 1.3. Referring to Curve 3 and Curve 1 in Fig. 26, these curves must coincide at a wind load factor of 1.3 (point (b)). In this case Curve 3 lies to the left of Curve 1 prior to the 1.3 load factor level. Beyond this point Curve 1 must lie above Curve 3.

The following general observations have been found valid with regard to frame strength under proportional and non-proportional loads:

1. For each consecutive non-proportional load analysis, as the level of the constant gravity load factor is increased the maximum wind load factor for the frame (maximum strength) is reduced, due to increased P-Delta effect and earlier plastic hinge formation.

2. If the maximum load factor for a proportional load analysis equals or exceeds 1.3 (say) then the maximum load factor for a non-proportional analysis with 1.3 gravity load factor must also exceed a wind load factor of 1.3 and will tend to be larger than the maximum achieved under the proportional load analysis. This results from the fact that above a load factor of 1.3, the gravity load in a proportional load analysis exceeds a 1.3 load factor thus reducing the maximum strength of the frame under the proportional load analysis.

3. Conversely, if the maximum load factor for a proportional load analysis does not achieve 1.3 then the maximum load factor for a non-proportional analysis with 1.3 gravity load factor cannot achieve a wind load factor of 1.3 and will tend to be lower than the maximum achieved under the proportional load analysis. This results from the fact that the gravity load in the non-proportional load analysis (1.30 times work value) is higher than that in the proportional load analysis, thus reducing the maximum strength of the frame under the non-proportional load analysis.

4.3 General Behavior and Load-Drift Characteristics

4.3.1 Analyses 1, 2, and 3

The results of Analyses 1, 2 and 3 performed on the seven frames are shown in Columns 3 to 8 and 12 to 14 of Tables 10 to 13, and the load-drift curves are labeled 1, 2 and 3 in Figs. 3 to 25. These results can be examined in the light of the discussion presented in the previous article.

Columns 4 and 7 of these tables indicate that no plastic hinges occur prior to the working wind load. The corresponding values of drift index in Columns 3 and 6 should therefore be identical. An examination of the values given shows that they are nearly the same. The small differences which do occur can be explained as follows. First, two different computer programs (SOFRAN-LIN and SOFRAN-DIN) are used to generate the load-drift output. Small differences can be expected as a result of variations in program execution such as convergence criteria adopted, round-off errors, etc. Secondly, SOFRAN-DIN generates load-drift output data only at the formation of plastic hinges. Therefore the values in Column 6 of the tables are computed using a linear extension of the load-drift curve from the origin to the point corresponding to the first plastic hinge. The criterion on achieving identical drift values as stated above was used, in fact, as a check on the accuracy of the results of the two computer programs.

Values of drift index corresponding to a wind load factor of 1.3 are not shown in Tables 10 to 13. However, examination of Figs. 3 to 25 indicate that where plastic hinges do not occur prior to 1.3 load factor, the corresponding values of drift index as determined by Analyses 1 and 3 are essentially the same.

Further examination of Figs. 3 to 25 shows that the load-drift behavior of the frames by Analyses 1, 2 and 3 are nearly the same up to a wind load factor of about 1.3. Beyond 1.3, there is a marked separation of the curves. For all frames, the highest wind load factor is achieved by Analysis 2 (gravity load

factor = 1.0), followed by Analysis 1 (gravity load factor = 1.30). The lowest maximum wind load factor occurs for Analysis 3 (proportional). The maximum wind load factors achieved under the three loading conditions are shown in Columns 5, 8 and 14 of Tables 10 to 13.

A characteristic of the load-drift curves in Figs. 3 to 25, for the non-proportional loading conditions (Analyses 1 and 2) is the relatively large values of drift index at the maximum wind load factor. Considerable ductility (deformability) is also evident beyond the maximum capacity as shown for the stress-controlled design of Frames 3, 4, 5 and 7. In a non-proportional load analysis, the load-drift behavior of the frame after attainment of the maximum load is a function of the load-drift behavior of the individual stories. If plastic hinges concentrate in one or two stories in the lower portion of the frame, the load-drift curve of the frame will reach a peak and suddenly drop or even reverse direction as shown for example in Figs. 5, 14, 19, 21 and 22. This behavior is the result of instability failure in the one or two lower stories. In these stories drift increases even under reduced wind loading. However the remainder of the frame responds elastically under the reduced wind loading. Under certain circumstances the drift at the top of the frame can reverse direction after attainment of the maximum strength. In a well proportioned frame (that is, with respect to the plastic strength of each story of the frame) plastic hinges will be distributed throughout the frame and the non-proportional load-drift curve can be nearly horizontal at the maximum load and considerable ductility can be achieved as shown in

Figs. 9, 12, 14, 15, 17, 18, 23 and 24.

4.3.2 Analysis 5

Analysis 5 is a non-proportional load analysis in which the gravity load factor is 1.2 and the yield stress level of the steel beams and columns is assumed to be $0.9 F_y$ (Art. 3.2). This analysis was performed only for Frames 2 and 5. The results are summarized in Columns 9, 10 and 11 of Tables 10 to 13. The load-drift curves shown in Figs. 7 to 10 and Figs. 17 to 19 as Curve 5 are similar to those obtained from Analyses 1, 2 and 3.

This analysis was undertaken to explore in a preliminary way the effect of variations of both load and resistance factors on the load-drift behavior of unbraced frames. The gravity load factor of 1.2 and resistance factor of 0.9 were selected arbitrarily. It is apparent from an examination of the load-drift curves for Frames 2 and 5 that the choice of resistance factor has a significant effect on the maximum strength of the frames. If no reduction in yield stress level were considered, Curve 5 for both frames would lie between Curves 1 and 2 and probably would be a little closer to Curve 1 than Curve 2.

4.3.3 Lower Bound to Frame Strength

For the discussion to follow in Art. 4.4 on the strength characteristics of the frames included in this investigation, strength must be defined. A study of Figs. 3 to 25 indicates that the least maximum wind load factor is always achieved under a proportional load analysis (Analysis 3). This is true even for the non-proportional

load analysis with a reduced yield stress level. A conservative estimate of frame strength can therefore be made by using the maximum load obtained from the proportional load analysis. This strength will be used frequently as the basis for strength comparison in Art. 4.4. (See also Art. 4.8 and Fig. 42.)

4.4 Strength Characteristics of Frames

4.4.1 Maximum Loads from First-and Second-Order Analyses

As mentioned in Art. 3.2, in addition to the several types of second-order analysis, first-order elastic-plastic analyses have been performed on all the Design I frames and the results are given in Table 14. The load (plastic limit load) factors achieved under proportional load range from 1.60 for Frame 3 to 2.05 for Frame 5 with an average of 1.71. The corresponding load factors of the second-order analyses vary from 1.40 for Frames 3, 4 and 7 to 1.60 for Frame 5 (Table 14 and Column 5, Table 10), the average being 1.45. These results show that the reduction in strength due to frame instability effect amounts to about 15.2% for the seven frames studied.

When the results of all the stress-controlled designs (Designs I, II and III) are considered (Columns 5, Tables 10 to 13), the range of the load factors from the second-order proportional load analyses is from 1.40 to 1.75.

For the non-proportional loading condition with gravity load factor of unity, the wind load factor achieved is in the range of 2.06 and 3.06 with an average of 2.40 (Column 8, Tables 10, 11, 12). This

means that under working gravity loads the frames are capable of resisting a maximum wind equal to 2 to 3 times the working wind. When the gravity loads acting on the frames increase to 1.30 times the working values, the range of load factor reduces to between 1.66 to 2.45 with an average value of 1.92. These values are substantially higher than the recommended load factor of 1.30 given in the AISC Specification.

The drift-controlled frames (Design IV) always achieve load factors higher than those achieved by the stress-controlled designs. The range load factors achieved is from 1.45 to 2.05 for the proportional loading condition. These frames are modifications of the Design I frames. For Frames 1, 2, 3, and 5 only the beam sizes are increased to reduce the working load drift index to the desired value of about 0.002. For these frames a drift reduction of up to 41% results in an increase in strength of up to 19%. For Frames 4 and 7 some columns also required increasing in size as well as the beams. For these frames a drift reduction of up to 46% results in an increase in strength of up to 47%.

The results of Frames 1, 2, 3 and 5 indicate that the stability of an unbraced frame may be improved by increasing its beam sizes, with column sizes unchanged. In the current AISC procedure (Design II) the increase is usually in the columns.

4.4.2 First Plastic Hinge Load

The load factor corresponding to the formation of the first plastic hinge is summarized in Column 4 of Tables 10 to 13, for the proportional load case. For the three stress-controlled designs, this

load factor falls in a narrow range from 1.20 to 1.35. With the exception of Frame 3, the first plastic hinge load is the same for all the three designs. The relative uniformity of the load factor at the formation of the first plastic hinge is a consequence of the allowable-stress design requirements, and the fact that the first plastic hinge almost always occurs in a beam.

In the drift-controlled designs, most beams are selected based on stiffness considerations, and usually have different maximum stresses for the same factored load. The load factor corresponding to the first plastic hinge therefore tends to vary over a wider range. For the seven selected frames, this range is from 1.35 to 1.80 with an average of 1.52.

4.4.3 Design I Versus Design II

Figures 27 and 28 compare load-drift curves for stress-controlled Designs I and II of Frames 5 and 6 under proportional loading (Analysis 3). No significant difference in strength and in load-drift characteristics can be observed between these two designs. Similar results are obtained for all other frames included in this study. The conclusion is that the use of κ factors larger than one and a C_m factor equal to 0.85 in column design does not lead to significantly stronger frames. The same conclusion was first reached by Lu⁽¹²⁾ and, subsequently, in an independent study by Liapunov.⁽¹³⁾ These results, when compared with those given in Table 14, indicate that the current design method is not fully effective to account for the P-Delta moment in an unbraced frame.

Column 5 on Tables 8 and 9 shows that Design I frames always achieve a slightly lower load factor than Design II frames. The difference is due to the larger sizes required for some of the columns in Design II. It is significant that the load factor for all Design I frames always equals or exceeds 1.40 which is higher than the value of 1.30 given in the AISC Specification.

4.4.4 Design I Versus Design III

Tables 2 to 8 show that beam and column sizes are identical for Designs I and III of Frames 3, 4, 5 and 7. The reason for this will be discussed in Art. 4.9.1. Design I of Frames 1, 2 and 6 has a few columns whose sizes are larger than those of Design III. But these changes do not effect the maximum loads of the frames (Column 5, Tables 10 and 12). Figure 28 compares the load-drift curves of Designs I and III of Frame 6 (Analysis 3). The curves are nearly the same. This is because the drift characteristics of a frame are influenced more significantly by the beams than by the columns.

4.4.5 Frame 3 Versus Frame 4

Frames 3 and 4 were selected partly for the purpose of providing a comparative study of load-drift characteristics for two levels of working gravity loads which are commonly encountered in the design of office structures. The two frames have identical geometry and wind loads. However, the gravity loads for Frame 4 are smaller than those for Frame 3, as shown in Fig. ~~V~~². The resulting beams and columns for Frame 4 are smaller than for Frame 3 as shown in Tables 4 and 5. Since both frames are designed to satisfy the same allowable-

stress requirements the maximum loads of the frames should be approximately the same, except for differences introduced by the P-Delta effect and different plastic hinge patterns. With the same exceptions the first plastic hinge in each frame should also occur at about the same load. Examination of Figs. 11 and 12 and Figs. 14 and 15 show that the above is indeed correct for the stress-controlled designs. Therefore, within the variations in gravity loads considered in this study, there is very little effect of the level of gravity loads on the maximum strength of frames designed by the allowable-stress method.

4.4.6 Frame 1 Versus Frame 6

The two frames are identical except that Frame 1 has three bays and Frame 6 five bays. They were selected to study the effect of the number of bays on the strength and drift behavior of a relatively low apartment type structure. The beam and column sizes are mostly smaller in Frame 6, because each member in this frame is designed for a lesser amount of the applied load. The maximum loads of all the designs for both frames, however, are essentially the same under proportional loads (Column 5, Tables 10 to 13). The drift is considerably less for Frame 6 and, because of the smaller working load drift, Design IV was not carried out for this frame.

This study indicates that when two frames of same height and bay width are designed by the allowable-stress method for identical working loads, their strength is not affected significantly by the number of bays in each frame, although the stiffness of the frame with more bays is higher.

4.4.7 Frame 4 Versus Frame 7

The only difference between the two frames is in the number of stories; Frame 4 is a 30 story office structure and Frame 7 a 40 story office structure. The results of these frames can therefore be used to study the effect of increasing the number of stories. The member sizes of Frame 4 as shown in Table 5 are almost identical to those of the upper 30 stories of Frame 7. Tables 10 and 11 indicate that the load-carrying capacities of the stress-controlled designs of the two frames are nearly the same, but the working load drift of Frame 7 is about 12% larger.

The drift-controlled designs of the two frames have somewhat different member sizes, and, consequently, different maximum loads and drift indexes. For both frames the beams as well as the columns have to be substantially increased in order to satisfy the drift requirement, and the maximum loads of these frames are therefore much higher than those of Frames 1, 2, 3 and 6 (Table 13).

4.5 Drift Characteristics of Frames

4.5.1 Working Load Drift of Stress-Controlled Designs

The second-order working (wind) load-drift index for each stress-controlled frame design is summarized in Columns 3, 6, 9 and 12 of Tables 10 to 12. Values obtained vary from a low of 0.00226 for Frame 6, Design II, Analysis 3 (frame with the smallest height-to-width ratio) to a high of 0.00478 for Frame 7, Design I, Analysis 1 (frame with the largest height-to-width ratio). If only proportional

loading (Analysis 3) is considered, as in Art. 4.4, the range reduces slightly from a low of 0.00226 for Frame 6, Design II, to a high of 0.00460 for Frame 7, Design III. The range, considering only proportional loading and Design I, is from 0.00237 for Frame 6 to 0.00460 for Frame 7.

Considering that the frame height-to-width ratios differ by by a factor of over eight and considering the differences in frame configuration and maximum strengths the range of second-order working load-drift index is quite small. In fact, this range is probably centered around accepted values of frame-drift index used by designers with an upper value close to the practical upper limit.

4.5.2 First-Order Versus Second-Order Drift

The first-order drift index for each stress-controlled design is summarized in Column 2 of Tables 10 to 13. A comparison of these values with those shown in Column 3 of the same tables indicates that second-order drift is from 7.2% (Frame 5, Design I) to 10.8% (Frame 3, Design III) larger than the corresponding first-order drift. Considering only Design I, the range is from 7.2% (Frame 5) to 10.6% (Frame 7).

4.5.3 Design I Versus Design II

Referring to Columns 2 and 3 of Tables 10 and 11 it is evident that very little difference exists in the working load-drift index between Design I and the AISC Design II. In fact, Design I drift values exceed Design II drift by a maximum of only 4.9%.

4.6 P-Delta Moments in Frames

4.6.1 Development of ϕ and $\bar{\phi}$ Factors

The ϕ factor is defined as the ratio of wind plus P-Delta moment to wind moment in a story. That is,

$$\phi = \frac{\Sigma W \cdot h + \Sigma P \cdot \Delta}{\Sigma W \cdot h} \quad (3)$$

in which ΣW is the cumulative wind shear, ΣP the cumulative gravity loads, h the story height, and Δ the story drift. This factor can be generated by introducing a fictitious wind increment δW at each floor level. That is

$$\phi = \frac{\Sigma W \cdot h + \Sigma \delta W \cdot h}{\Sigma W \cdot h} \quad (4)$$

for the case of constant W and P applied at all stories, combination of Eqs. (3) and (4) gives

$$\Sigma P \cdot \Delta = \Sigma W \cdot h(\phi - 1) = \Sigma \delta W \cdot h \quad (5)$$

or

$$W(\phi - 1) = \delta W \quad (6)$$

The increment of wind load δW can also be expressed in terms of the gravity load P per story used to generate Eq. 3 as follows:

$$\delta W = \bar{\phi} P = \bar{\phi} w_g Ls \quad (7)$$

where w_g is the uniformly distributed dead plus live gravity loads in a story (assumed constant), L is the total width of the frame in its plane and s is the tributary width perpendicular to the frame. Since

$$W = w_w h s \quad (8)$$

where w_w is the uniformly distributed wind load, substitution of Eqs.

7 and 8 into Eq. 6 yields,

$$\bar{\phi} = \frac{w_w}{w_g} \frac{h}{L} (\phi - 1) \quad (9)$$

The factor ϕ represents the amount of wind increment δH per level in terms of the gravity load per story P required in a first-order analysis to yield the same story moments as those obtained from a second-order analysis.

4.6.2 P-Delta Moments at Working and Factored Loads

Figures 29 to 35 show the calculated ϕ factors at factored loads (GLF = 1.30) for all the stories of each stress and drift design of the seven frames (the design number is shown circled). These factors are determined using Eq. 3 from the results of a proportional load analysis (Analysis 3). The figures show the amount of second-order P-Delta moment in each story as a ratio of the wind moment.

The figures can also be interpreted in a different way. For constant values of wind loading, story height and gravity loads over the height of a frame the ϕ factor is proportional to the story slope, that is the story drift divided by the story height. Thus the profile of the frame at factored loads can easily be visualized from the ϕ factor information by starting at the bottom of the frame where the slope is zero.

The main observations from Figs. 29 to 35 are as follows:

1. The story P-Delta moment ratios (or story slopes) are smallest near the top and bottom of each frame as expected.

2. The story P-Delta moment ratios for the three stress designs of each frame are nearly the same.

3. For all the seven frames, the P-Delta moment ratios for Design II are generally slightly smaller than those for Designs I and III.

4. The P-Delta moment ratios for the drift-controlled frames are substantially less than those for the stress-controlled frames. This correlates with the higher load factors achieved by the drift-controlled frames.

Table 15 summarizes the calculated average and maximum ϕ and $\bar{\phi}$ factors for Design I (stress) and Design IV (drift). The average ϕ factor ϕ_{ave} shown in Columns 5 and 9 are calculated neglecting the bottom one or two stories and top three to ten stories of a frame depending on the height of the frame. The selection is based on the results of the individual frames shown in Figs. 29 to 35. For example, the bottom two and top ten stories were neglected in computing ϕ_{ave} for Frame 3. The ϕ_{max} and $\bar{\phi}_{max}$ shown in the table are the maximum values attained in an individual story.

Figures 36 and 37 compare the ϕ factors at working and factored loads of Design I, Frames 1 and 7. The results show that the distribution of the ϕ factors throughout the height is quite similar at working and factored loads, and that the ratio of ϕ factors at factored loads to ϕ factors at working loads is about 1.30.

It is customary in some design offices to add a small percentage of the gravity loads in each story to the wind loads when

calculating working load frame drift on a first-order basis in order to compensate for the P-Delta effect. It is not uncommon for designers to add 1 or 2 percent of the gravity loads to the wind loads. Columns 7 and 8 of Table 15 indicate that for the Design I frames less than one percent is acceptable. The range varies from about 0.4 to 0.7 percent. For the Design IV frames (drift designs) the range is from about 0.3 to 0.4 percent.

4.7 Plastic Hinge Patterns

Figures 38 to 41 show the locations of the plastic hinges for selected frames, and design and analysis conditions. In each case the wind loads are assumed to act from the left.

The plastic hinge patterns shown in Fig. 38 are those existing in Design I, Frame 1 immediately after reaching the maximum loads. The corresponding load factors are 2.4 for Analysis 2 and 1.8 for Analysis 1. In each case, loss of strength and stiffness in the lower portion of the frame results in failure by inelastic frame instability.

In Fig. 39 the plastic hinge patterns of Designs I, II and III, Frame 4 corresponding to the maximum loads from Analyses 1 and 2 are shown. The load-drift relationships given in Figs. 14 and 15 show no sharp unloading after the attainment of the maximum load. Plastic hinges are distributed through almost the entire height of the structure, with more forming in Design I and III frame than in Design II frame.

The plastic hinge patterns at maximum loads of Designs I

and II, Frame 5 are given in Fig. 40. The load-drift relationships show significant deformability before and after reaching the maximum load (Figs. 17 and 18). Again, more hinges form in Design I frame than in Design II frame; in the latter structure only 13 hinges are found and are all in the beams.

Figure 41 shows the relatively fewer plastic hinges (107) existing in Frame 7 at the maximum load under a proportional load analysis. In the non-proportional load analysis considerably more plastic hinges (143) are evident. The concentration of plastic hinges in the central columns of tall bay frames (such as Frames 3, 4 and 7) was consistently found in this study.

4.8 Relationships Between Maximum Strength and Working Load Drift

Figure 42 shows the relationships between the maximum load factor of the stress-controlled frame designs and their working load drift index. For each frame the maximum wind load factor attained in Analyses 1, 2, or 3 is plotted against the first-order working load (wind load factor of 1.0) drift index as computed by Analysis 4.

In the figure the squares correspond to Analysis 1 results, the triangles to Analysis 2 results, and the solid circles to Analysis 3 results. Also shown in the figure are the empirical straight line relationships for the three groups of plotted points.

Figure 42 clearly shows that the lower bound frame strength is determined by a proportional load analysis (Art. 4.3.3). The range of strengths varies from 1.4 to about 1.75 load factor as noted in

Art. 4.4.1. The range of working load drift index is small, varying from about 0.002 to about 0.004. The average slope through these points show that the frame strength under proportional loads is relatively insensitive within the range of geometric, loading and performance parameters of the seven frames (see Arts. 4.1 and 5.1).

The above result is not unexpected. For the frames studied, the P-Delta effect at working loads is not large. Allowable stress design of the frames therefore should result in a first plastic hinge formation (approximately first yielding) at a load factor of about 1.25* (see Tables 10 to 12). The maximum load cannot greatly exceed that value since the combination of plastic hinge formation (reduced frame stiffness) and increasing gravity loads and P-Delta moment causes the structure to fail rapidly by frame instability.

In non-proportional load analysis, where the gravity loads are constant, significantly higher strengths can be achieved as indicated in Fig. 42. In this case, however, the range of parameters describing the seven frames studied has a more pronounced effect on the frame strength as evidenced by the wider scattering of the plotted results. Combinations of parameters leading to higher frame drifts often result in a substantial lowering of frame strength.

4.9 Comments on Columns in Stress-Controlled Designs

4.9.1 Governing Column Formulas in Designs I and III and in Design II

The 1969 AISC Specification requires that all columns in a

* This value is based on an allowable bending stress of $0.6F_y$ adjusted for a one-third increase permitted for the combined loading case.

frame be proportioned to satisfy the two formulas given as Eqs. 1 and 2 in Art. 1.2. In unbraced frame design, the use of an effective length factor K greater than unity in computing F_a and F'_e and a C_m value of 0.85 makes Eq. 1 more critical than Eq. 2. In fact, almost all the columns in Design II frames are selected based on Eq. 1. Equation 1, however, may become less critical than Eq. 2 when the actual column length ($K = 1.0$) is used in computing F_a and F'_e and when a C_m value given by the formula $C_m = 0.6 - 0.4 \frac{M_1}{M_2} \geq 0.4$ is adopted. For the seven frames studied Eq. 2 governs the selection of much more columns than does Eq. 1 in Designs I and III. Figure 43 shows the loading condition and the column formula that govern the size of each of the columns in Designs II and III, Frame 1. Also shown is the governing loading condition for each beam.

As mentioned in Art. 1.2, Eq. 2 is a stress criterion (as opposed to stability criterion) and its use is to safeguard against yielding at the ends (or braced points) of a column. It becomes the controlling design criterion in a situation where the beam-column instability effect is not an overriding failure condition. Studies on the strength of beam-columns commonly encountered in building frame design have shown that this is indeed the case for many beam-columns subjected to bending moments causing double curvature deformation.⁽¹⁴⁾ The various analyses performed on the selected frames indicate that, under combined gravity and wind loads, the bending moments in most columns do produce double curvature deformation.

Figure 44 shows the moment diagram and the location of the critical section in such a column. The maximum moment that can be resisted by the column is equal to its full plastic moment (reduced for the effect of axial thrust).

In cases where Eq. 2 controls the design, the columns in Designs I and III have identical sizes.

4.9.2 Maximum Axial Stress Ratios and Column Slenderness Ratios

In Eqs. 1 and 2, the significant parameters showing the influence of axial force in column design are: (1) the axial stress ratios f_a/F_a and $f_a/0.6 F_y$ and (2) the column slenderness ratios h/r_x and h/r_y . Since this study is concerned primarily with in-plane stability of planar frames, the h/r_x ratio is used to characterize the column strength. The values of these parameters were recorded and their influence on column size selection were carefully examined in the final design of the seven selected frames. The largest value of $f_a/0.6 F_y$ value was about 0.75 and occurred in several columns in the lower part of Frame 7, Design III under combined loads. A maximum f_a/F_a value of 0.75 also occurred in this frame, but it did not control the column design, because as previously explained, Eq. 1 was not as critical as Eq. 2.

The largest value of h/r_x was around 42 and occurred in Design III, Frame 2.

Since Design I columns are on the average slightly larger than Design III columns (in some cases they are identical), the

corresponding values of f_a/F_a , $f_a/0.6 F_y$, and h/r_x are slightly lower.

4.9.3 Relative Column Weights

Figure 45 shows the relative column weights for the stress-controlled designs of the seven frames. In each case the column weight for the AISC design (Design II) is taken as 100%. The column weights for Designs I and III are shown relative to Design II.

Design I columns are from 7 to 11% lighter than Design II columns. Design III columns are from 7 to 14% lighter than Design II columns. Since the beams for all the stress-controlled designs of each frame are nearly identical, the difference in weight for a given frame is attributed mainly to the columns.

5. RECOMMENDATIONS

5.1 Review of Results

As stated in Art. 1.4, one of the objectives of this study is to develop a new method of column design in unbraced frames subjected to combined gravity and wind loads based on the information obtained from the seven selected frames. The major results that are useful in developing design recommendations are embodied in Fig 42 and in the statements contained in Arts. 4.4, 4.5 and 4.8. The results show that, even though the strength of the frames is reduced considerably by frame instability, all stress-controlled designs are sufficiently strong to achieve a wind load factor equal to or greater than 1.40 under proportional loads, 2.06 under non-proportional loads with a gravity load factor of unity, and 1.66 with a gravity load factor equal to 1.30. This is because of the large reserve strength in the plastic range in redundant rigid steel framed structures. It is significant that all the Design I and III frames, which were designed with the effect of frame instability completely neglected, can achieve an average wind load factor of 1.45 under proportional loads and that the increase in strength of the Design II frames, whose columns were proportioned to satisfy the AISC Specification requirements, amounts to only about seven percent (corresponding to an increase of load factor of 0.10). These results suggest that unbraced frames with geometry, working loads and drift characteristics

similar to those of the seven frames included in this study may be designed as if they were properly braced. The geometry, loads and drift characteristics of these frames have been described in Arts. 4.1 and 4.5; they are further identified as follows:

Geometric

1. Number of stories: 10 to 40
2. Number of bays: 1 to 5
3. Frame height-to-width ratio: 0.95 to 8.0
4. Story height: 9.5 to 14.0 feet
5. Bay width: 20 to 56 feet
6. Panel aspect ratios: 0.25 to 0.475
(story height to bay width)

Loading

1. Gravity: Roof -live 30 to 40 psf
-dead 40 to 50 psf

Floor -live 40 to 100 psf
-dead 50 to 75 psf
2. Wind: 20 psf (uniform over entire height)

Drift Characteristics

1. First-order working load frame drift index (frame drift divided by frame height): 0.00208 to 0.00417.
2. First-order working load story drift index (story drift divided by story height) may exceed the frame drift index by 10 to 30 percent.

5.2 Recommendations for Allowable-Stress Design

The results of this investigation show that adequate strength and stability can be assured under combined gravity and wind loads when unbraced rigid frames are designed to meet the following criteria:

1. The columns are to be designed in accordance with the provisions of the 1969 Specification except that:
 - a) The effective length factor K is assumed equal to unity in the calculation of F_a and F_e .
 - b) The coefficient C_m is computed as for braced frames.
2. The maximum column axial stress ratios $\frac{f_a}{F_a}$ and $\frac{f_a}{0.60F_y}$ do not exceed 0.75.
3. The maximum in-plane column slenderness ratio h/r_x does not exceed 35.
4. The bare frame first-order working load drift index Δ/H does not exceed 0.004.

The limitations specified in Items 2,3 and 4 above are close to the maximum values encountered in this study. Further research may result in changes to these limiting values. Item 4 does not intend to suggest drift limits for serviceability.

6. SUMMARY AND CONCLUSIONS

Seven unbraced multistory frames were selected for detailed study with particular emphasis on the effect of frame instability. Included were two apartment and five office type frames. The frames differed in number of stories and bays, height-to-width ratios, story heights, bay widths, and level of working loads. They were designed to satisfy either the stress provisions of the AISC Specification or a specified drift criterion. A large number of first-order and second-order proportional and non-proportional load analyses were performed using computer programs developed previously for studying frame strength.

The major conclusions based on the results of this investigation are as follows. They are applicable to unbraced frames whose overall characteristics are similar to those of the frames included in this study.

1. Under proportional loads, the presence of P-Delta moment reduces the load-carrying capacity of all the frames studied by about 12 to 22 percent.
2. There is an appreciable difference between the load-drift relationships from the second-order proportional and non-proportional analyses. The P-Delta moment included in these analyses is the primary reason for this difference.

3. In the second-order non-proportional analysis, the amount of gravity load acting on the beams affects significantly the wind load carrying capacity of the frames.
4. For the frames studied, a conservative (lower bound) estimate of the maximum strength is determined from a proportional analysis.
5. The stress-controlled Designs I and III, whose columns are proportioned as if the frames were laterally braced can achieve a load factor ranging from 1.40 to 1.60 under proportional loads. A minimum load factor of 1.40, therefore, can be achieved using the 1969 AISC column design rules but using the actual column length and the C_m value for braced frames.
6. The load factors of the Design II frames, whose columns are proportioned to meet all the AISC Specification requirements (using effective length factor K and $m = 0.85$), are only slightly higher than those of Design I and III frames.
7. Under non-proportional loads, all the stress-controlled designs can achieve a wind load factor ranging from 2.06 to 3.06 for a gravity load factor of 1.0 and from 1.66 to 2.45 for a gravity factor of 1.30.

8. For all the stress-controlled designs, the first plastic hinge forms at an average load factor of 1.29 under proportional loads and 1.60 under non-proportional loads with a gravity load factor of 1.0.
9. Frames designed to meet a drift limitation of 0.002 have large wind load carrying capacity. The wind factor of the drift-controlled frames varies from a low of 1.45 for a proportional analysis to more than 4.0 for a non-proportional analysis, depending upon the gravity load on the beams.
10. The first-order working load drift index of the stress-controlled frames is in the range of 0.00208 to 0.00417. The P-Delta moment increases the working load drift by about 7 to 10 percent.
11. The average P-Delta moment in a story amounts to about 14 to 20 percent of the wind moment in the stress-controlled designs and about 7 to 14 percent in the drift-controlled designs.
12. A simple procedure is recommended in designing unbraced frames similar to those studied. This procedure recognizes that frame stability considerations are such that so long as the working load drift index is less than 0.004 frame stability need not be considered.

7. ACKNOWLEDGMENTS

The research reported herein was conducted at the Fritz Engineering Laboratory, Department of Civil Engineering, Bethlehem, Pennsylvania. Lynn S. Beedle is Director of Fritz Engineering Laboratory, and David A. VanHorn is Chairman of the Department of Civil Engineering. The research was co-directed by Le-Wu Lu and J. Hartley Daniels.

The investigation was sponsored by the Committee of Structural Steel Producers and the Committee of Steel Plate Producers of the American Iron and Steel Institute. The contribution of the AISI Task Force on Project 174 is gratefully acknowledged. The Task Force members are W. C. Hansell, AISI Project Supervisor, S. P. Asrow, T. V. Galambos, I. Hooper, W. A. Milek, Jr., I. M. Viest, and G. Winter. The study was originally suggested by I. Hooper.

The results of the first-order elastic-plastic analysis were obtained by Dr. Francois Cheong-Siat-Moy.

The manuscript was carefully typed by Mrs. Ruth Grimes, Miss Debra Zappasodi and Mrs. Sheila Novak. The figures were prepared by Mr. Jack Gera and his staff.

8. APPENDIXES

APPENDIX APRELIMINARY DESIGN OF DESIGN I, FRAME I

(Refer also to Ref. 8)

Step 1 - Assignment of Loads

Using the loading in Fig. 1, the distributed live load w_L and dead load w_D on the roof beam are calculated as follows:

$$w_L = 30 \times 20 = 600 \text{ lb/ft.} = 0.60 \text{ k/ft.}$$

$$w_D = \frac{40 \times 20 = 800}{1,400 \text{ lb/ft}} = \frac{0.80}{1.40} \text{ k/ft.}$$

Similarly, the distributed live and dead loads on the floor girders are calculated as follows:

$$w_L = 40 \times 20 = 800 \text{ lb/ft.} = 0.80 \text{ k/ft.}$$

$$w_D = \frac{55 \times 20 = 1,100}{1,900 \text{ lb/ft.}} = \frac{1.10}{1.90} \text{ k/ft.}$$

Maximum Reduction (Ref. 7)

$$R_{\max} = \frac{100(95)}{4.33(40)} = 55\%$$

Live Load Reduction

	Left	Center	Right	
Girder	A-B	B-C	C-D	
Floor area served (sq. ft.)	400	400	400	
% L.L. Red. (0.08 x area)	32	32	32	
Column	A	B	C	D
Floor area served/story	200	400	400	200
% L.L. Red. Roof	0	0	0	0
Level 2	16	32	32	32
Level 3	32	55	55	32
Level 4	48.0	55.0	55.0	48.0
Level 5 thru 10	55	55	55	55

?
16

Step 6 - Columns - Wind Load Thrust in Columns

The column thrust due to wind load is obtained by a cantilever analysis assuming equal column areas, as

$$I = \sum x^2 A = (30^2 + 10^2 + 10^2 + 30^2) A = 2000 \text{ ft}^2 A$$

$$\text{Column thrust} = A \frac{Mx}{I} = \frac{Mx}{2000}$$

Column No. Thrust	A 0.0150M	B 0.0050M	C 0.0050M	D 0.0150M	
Levels	M(k-ft)	Thrust (kips)	Thrust (kips)	Thrust (kips)	Thrust (kips)
1-2	14.75	+0.221	+0.074	-0.074	-0.221
2-3	62.30	+0.935	+0.312	-0.312	-0.935
3-4	146.0	+2.19	+0.73	-0.73	-2.19
4-5	365.5	+3.99	+1.33	-1.33	-3.99
5-6	420.0	+6.30	+2.10	-2.10	-6.30
6-7	614.0	+9.20	+3.07	-3.07	-9.20
7-8	844.0	+12.70	+4.23	-4.23	-12.70
8-9	1107.0	+16.60	+5.53	-5.53	-16.60
9-10	1405.0	+21.00	+7.00	-7.00	-21.00
10-11	1740.0	+26.10	+8.70	-8.70	-26.10

Step 7 - Wind Moment in Columns

Bending moments in columns due to wind load are obtained by portal analysis shown in Step 2. Moments at column top M_{Top} and bottom M_{Btm} are as follows:

$$M_{\text{Top}} = M_{\text{Btm}} = (\% \text{ shear}) \times (\text{shear}) \times 4.75'$$

Level	Moment (k-ft)	
	A	B
1-2	2.45	4.90
2-3	5.49	10.98
3-4	8.50	17.00
4-5	11.50	23.00
5-6	14.50	29.00
6-7	17.50	35.00
7-8	21.35	42.70
8-9	23.60	47.20
9-10	26.50	53.00
10-11	29.60	59.20

Step 8 - Summary of Wind Load Thrust and Moment in Columns

Level	Gravity				Gravity & Wind*			
	A		B		A		B	
	P (k)	M (k-ft)	P (k)	M (k-ft)	P (k)	M (k-ft)	P (k)	M (k-ft)
2-3	55	15	62	0	42	15.4	47	8.2
		15		0		15.4		8.2
4-5	106	15	122	0	83	19.9	94	17.3
		15		0		19.9		17.3
6-7	156	15	182	0	124	24.4	139	26.2
		15		0		24.4		26.2
8-9	207	15	243	0	169	29.0	186	35.5
		15		0		29.0		35.5
10-11	258	15	304	0	214	33.5	234	44.5
		15		0		33.5		44.5

*Take 0.75 of P and M shown in Steps 4 to 8 in design calculations

Step 9 - Column design: Column A Level 10 to 11 $F_y = 36$ ksi (Design I)

Calculation	Units	Gravity	Gravity & Wind
① Design Thrust P	k	258	214
② Design Moment M_1	k-ft.	15	34
③ Design Moment M_2	k-ft.	15	34
④ Trial Column		<u>W8x58</u>	<u>W8x58</u>
⑤ A	in. ²	17.1	17.1
⑥ I_x	in. ⁴	227	227
⑦ S_x	in. ³	52.0	52.0
⑧ r_x	in.	3.65	3.65
⑨ r_y	in.	2.10	2.10
⑩ K	---	<u>1.0</u>	<u>1.0</u>
⑪ $f_a = \textcircled{1} \div \textcircled{5}$	ksi	15.1	12.5
⑫ $f_b = \{12 \times \textcircled{2} \text{ or } \textcircled{3}\} \textcircled{7}$	ksi	3.5	7.85
⑬ $C_b = 1.75 + 1.05 (M_1/M_2) + 0.3(M_1/M_2)^2 \leq 2.3$		2.3	2.3
⑭ L_d/A_f	---	151	151
⑮ $F_b = 12000 \times \textcircled{13} \div \textcircled{14}$	ksi	183	183
⑯ $F_b = 0.60 F_y$	ksi	22	22
⑰ $L/r_x = 12 \times \text{Length} \div \textcircled{8}$	---	31.2	31.2
⑱ $L/r_y = 12 \times \text{Length} \div \textcircled{9}$	---	54.5	54.5
⑲ F_a (AISC Table 1) $\textcircled{18}$	ksi	17.95	17.95
⑳ F'_e (AISC Table 2) $\textcircled{17}$	ksi	153	153
㉑ $f_a/F'_e \textcircled{11} \div \textcircled{20}$	---	0.099	0.082
㉒ $1.0 - \textcircled{21}$	---	0.901	0.918
㉓ $C_m = 0.60 - 0.40 M_1/M_2 \geq 0.4$	---	0.40	0.40
㉔ $\textcircled{23} \times \textcircled{12} \div \textcircled{22} \times \textcircled{15} \text{ or } \textcircled{16}$	---	0.071	0.155
㉕ $f_a/F_a = \textcircled{11} \div \textcircled{19}$	---	0.840	0.695
㉖ $\textcircled{24} + \textcircled{25}$	---	0.911	0.850
㉗ OK or NG (Is $\textcircled{26} \leq 1.0$?)	---	<u>OK</u>	<u>OK</u>
㉘ $f_a/0.6 F_y = \textcircled{11} \div \textcircled{16}$	---	0.685	0.570
㉙ $f_b/F_b = \textcircled{12} \div \textcircled{15} \text{ or } \textcircled{16}$	---	0.159	0.357
㉚ $\textcircled{28} + \textcircled{29}$	---	0.844	0.927
㉛ OK or NG (Is $\textcircled{30} \leq 1.0$?)	---	<u>OK</u>	<u>OK</u>

APPENDIX B
SECOND-ORDER FRAME ANALYSIS --
LOAD INCREMENT PROGRAM (SOFRAN-LIN)

The program prepared by B. P. Parikh (designated program SOFRAN-LIN*) was developed essentially to obtain the structural response such as bending moments and joint displacements, under a specific intensity of applied load.⁽¹⁰⁾ The program is based on the slope-deflection equations which govern the member behavior under combined axial force and bending moment. The member stiffness are modified to take into account the effects of axial force and yielding. The plastic hinge moment, M_{pc} , is defined by the relationships:

$$M_{pc} = M_p \quad 0 \leq \frac{P}{P_y} \leq 0.15$$

$$M_{pc} = 1.18 \left(1 - \frac{P}{P_y}\right) M_p \quad 0.15 \leq \frac{P}{P_y} \leq 1.0$$

The program repeatedly solves the frame until the structural response converges. If the user specifies a series of proportionally increasing gravity and wind loads, the load-drift curve of the frame under proportional loads can be traced up to the maximum values of the two loads. The program does not detect the loads at which the various plastic hinges form.

APPENDIX C
SECOND-ORDER FRAME ANALYSIS --
DRIFT INCREMENT PROGRAM (SOFRAN-DIN)

The complete load-deflection curve of a frame under constant gravity load and increasing (or decreasing) wind load can be generated by a program, developed by S. W. Kim (designated program (SOFRAN-DIN*)), which traces the plastic hinge formations including the descending portion of load-drift curve that occurs after the frame reaches its stability limit.⁽¹¹⁾ This program is unique in that it employs an incremental drift procedure rather than the incremental load procedure as used in program SOFRAN-LIN. Program SOFRAN-DIN first assumes a small drift increment, of a particular story and then searches for the necessary wind load increment which causes the assumed drift increment. Once the wind load increment is found, the drift at each story of the frame is determined consistent with the wind load increment. Specifically, to reduce computation the drift increments chosen are defined by the formation of each successive plastic hinge to the next, and the computation is terminated at the convenience of the programmer; for instance, when a plastic mechanism forms in the frame or when the applied load is reduced to a certain level after reaching the stability limit load, or some other criterion.

The member stiffnesses are modified in the same manner as in SOFRAN-LIN. The plastic hinge moment, M_{pc} , is defined by the same relationships as given in Appendix B.

*Second-Order FRame ANalysis --Drift INcrement

APPENDIX DEFFECT OF VARIATION OF MODULUS OF ELASTICITY

At an early stage in the investigation a comparative study was made of the effect on the load-drift curves of several frames of a variation of the modulus of elasticity, E . Figure 46 for example compares the load-drift behavior of Frame 5, Design I for $E = 29,000$ ksi and $E = 30,000$ ksi. The study concluded that the value of the modulus of elasticity, within the above range, does not significantly affect the ultimate load capacity. As a result of this study all frame analyses were performed assuming $E = 29,000$ ksi.

APPENDIX EEFFECT OF RESIDUAL STRESSES

At an early stage of this investigation a comparative study was made of the effect on the load-drift curves of several frames of an assumed residual stress pattern. Figure 47 for example compares the load-drift behavior of Frame 5, Design I for two levels of residual stress, $\sigma_{rc} = 0$ and $\sigma_{rc} = 0.3 \sigma_y$, where σ_{rc} is the maximum cooling residual stress level and σ_y is the yield stress level. Cooling residual stresses were approximated by the idealized pattern as shown in Fig. 48. The study indicates that the effect of residual stresses on the ultimate load capacity is small. As a result of this study all frame analyses were performed assuming zero residual stress.

9. NOMENCLATURE

- A = Cross sectional area of column
- C_m = Coefficient used in Formula (1.6 - 1a) of the 1969 AISC Specification (see Eq. 1 of this report)
- C_b = Coefficient used in Formula (1.5 - 6a) of the 1969 AISC Specification
- E = Modulus of elasticity
- F_a = Allowable axial stress if axial force alone existed in a beam-column (see Eqs. 1 and 2)
- F_b = Allowable compressive bending stress if bending moment alone existed in a beam-column (see Eqs. 1 and 2)
- F'_e = Elastic buckling stress divided by a factor of safety (see Eq. 1)
- F_y = Yield stress
- \bar{F}_y = Reduced yield stress (90 percent of F_y)
- f_a = Computed axial stress in a beam-column
- f_b = Computed bending stress in a beam-column
- H = Total roof-to-base frame height
- h = Story height
- I = Moment of inertia of column
= Moment of inertia of column areas (in cantilever analysis)
- I_e = Moment inertia of elastic core
- K = Effective length factor of column, subscripts x and y refer to strong and weak axes, respectively
- L = Total in-plane frame width
- M = Column end moment, subscripts refer to end 1 or end 2, top or bottom
= Moment at midheight of column (in cantilever analysis)
- M_{max} = Maximum moment in column

- M_p = Plastic hinge moment
 M_{pc} = Plastic hinge moment modified to include the effect of axial force
 M_w = Wind moment
 P = Total gravity load above a story (cumulative)
 Gravity load in one story within the tributary area of the frame (non-cumulative)
 P_y = Axial yield load of column (AF_y)
 R = Live Load reduction factor
 r = Radius of gyration, subscripts x and y refer to strong and weak axes, respectively
 S = Section modulus
 s = Tributary width perpendicular to the frame for wind load
 W = Concentrated wind load at a floor level
 W = Working value of W
 w_D = Unit dead load
 w_g = Unit gravity load ($w_D + w_L$)
 w_L = Unit live load
 w_w = Unit wind load
 α = proportionality constant
 Δ = Story drift
 = Roof level frame drift
 δ = Deflection of column
 ϕ = Ratio of second-order story moment to first-order story moment (see Eq. 3)
 = Curvature
 $\bar{\phi}$ = Ratio of wind plus equivalent P-Delta wind load to wind load (see Eq. 7)

- ϕ = Curvature corresponding to M_{pc} (M_{pc}/EI)
- σ_{rc} = Compressive residual stress
- σ_{rt} = Tensile residual stress

10. TABLES AND FIGURES

TABLE 1: SUMMARY OF DESIGNS

Design		K_x	K_y	C_m
Stress Designs	I	1.0	1.0	$0.6 - 0.4 \frac{M_1}{M_2} \geq 0.4$
	II (AISC)	K	1.0	0.85
	III	1.0	0.0	$0.6 - 0.4 \frac{M_1}{M_2} \geq 0.4$
Drift Design	IV	Design I but working load drift index reduced to 0.002		

TABLE 2: MEMBER SIZES FOR FRAME 1

Beams					Columns				
Levels	Design I	Design II	Design III	Design IV	Levels	Design I	Design II	Design III	Design IV
1	W12x22	W12x22	W12x22	W14x26	1-3 EXT	W8x20	W8x24	W8x20	W8x20
2	W14x22	W14x22	W14x22	"	INT	W8x17	W8x17	W8x15	W8x17
3	"	"	"	W16x31	3-5	W8x31	W8x35	W8x31	W8x31
4	"	"	"	"		W8x28	W8x31	W8x28	W8x28
5	W14x26	W14x26	W14x26	"	5-7	W8x40	W8x48	W8x40	W8x40
6	"	"	"	"		W8x40	W8x48	W8x40	W8x40
7	W14x30	W14x30	W14x30	W18x35	7-9	W8x48	W8x58	W8x48	W8x48
8	"	"	"	"		W8x58	W8x58	W8x58	W8x58
9	W16x31	W16x31	W16x31	W18x40	9-11	W8x58	W8x67	W8x58	W8x58
10	"	"	"	"		W8x67	W10x66	W8x67	W8x67

TABLE 3: MEMBER SIZES FOR FRAME 2

Beams					Columns				
Levels	Design I	Design II	Design III	Design IV	Levels	Design I	Design II	Design III	Design IV
1	W21x49	W21x49	W21x49	W24x 55	1-3 EXT	W8x 67	W8x 67	W8x 58	W8x 67
2	W21x55	W21x55	W21x55	W24x 68	INT	W8x 35	W8x 35	W8x 28	W8x 35
3	"	"	"	"	3-5	W12x 79	W12x 85	W12x 65	W12x 79
4	"	"	"	"		W12x 65	W12x 79	W12x 65	W12x 65
5	"	"	"	"	5-7	W14x 95	W14x103	W14x 84	W14x 95
6	W24x61	W24x61	W24x61	W24x 84		W14x 95	W14x103	W14x 95	W14x 95
7	"	"	"	"	7-9	W14x119	W14x127	W14x111	W14x119
8	W24x68	W24x68	W24x68	W27x 84		W14x119	W14x136	W14x119	W14x119
9	"	"	"	"	9-11	W14x136	W14x150	W14x127	W14x136
10	"	"	"	"		W14x158	W14x167	W14x158	W14x158
11	W24x76	W24x76	W24x76	W27x 94	11-13	W14x158	W14x184	W14x158	W14x158
12	"	"	"	"		W14x184	W14x202	W14x184	W14x184
13	W24x84	W24x84	W24x84	"	13-15	W14x176	W14x202	W14x176	W14x176
14	"	"	"	"		W14x211	W14x237	W14x211	W14x211
15	"	"	"	"	15-17	W14x202	W14x237	W14x202	W14x202
16	"	"	"	"		W14x246	W14x287	W14x246	W14x246
17	W27x84	W27x84	W27x84	W30x 99	17-19	W14x219	W14x264	W14x219	W14x219
18	"	"	"	"		W14x287	W14x314	W14x287	W14x287
19	"	"	"	"	19-21	W14x246	W14x287	W14x246	W14x246
20	W27x94	W27x94	W27x94	W30x108		W14x314	W14x342	W14x314	W14x314
21	"	"	"	"	21-23	W14x287	W14x314	W14x287	W14x287
22	"	"	"	"		W14x342	W14x370	W14x342	W14x342
23	"	"	"	"	23-25	W14x314	W14x342	W14x314	W14x314
24	"	"	"	"		W14x370	W14x398	W14x370	W14x370
25	"	"	"	"	25-27	W14x370	W14x370	W14x342	W14x370
26	"	"	"	"		W14x426	W14x426	W14x398	W14x426

TABLE 4: MEMBER SIZES FOR FRAME 3

Beams					Columns				
Levels	Design I	Design II	Design III	Design IV	Levels	Design I	Design II	Design III	Design IV
1	W24x55	W24x55		W24x84	1-3 EXT	W14x74	W14x74		W14x74
2	W24x68	W24x76		W27x94	INT	W14x43	W14x43		W14x43
3	"	"		"	3-5	W14x103	W14x111		W14x103
4	W24x76	"		W30x99		W14x78	W14x84		W14x78
5	"	"		"	5-7	W14x127	W14x142		W14x127
6	"	"		"		W14x119	W14x127		W14x119
7	"	"		"	7-9	W14x158	W14x176		W14x158
8	W24x84	W24x84		W30x108		W14x158	W14x167		W14x158
9	"	"		"	9-11	W14x184	W14x211		W14x184
10	W27x84	W27x84		W30x116		W14x202	W14x211		W14x202
11	"	"		"	11-13	W14x211	W14x246		W14x211
12	W27x94	W29x94		W33x118		W14x237	W14x264		W14x237
13	"	"		"	13-15	W14x237	W14x287		W14x237
14	"	"		"		W14x287	W14x314		W14x287
15	W30x99	W30x99		W36x135	15-17	W14x287	W14x342		W14x287
16	"	"		"		W14x314	W14x342		W14x314
17	"	"		"	17-19	W14x314	W14x370		W14x314
18	W30x108	W30x108		"		W14x370	W14x398		W14x370
19	"	"		"	19-21	W14x342	W14x398		W14x342
20	"	"		W36x150		W14x398	W14x426		W14x398
21	W30x116	W30x116		"	21-23	W14x370	W14x455		W14x370
22	"	"		"		W14x455	W14x455		W14x455
23	"	"		"	23-25	W14x426	W14x500		W14x426
24	W33x118	W33x118		W36x170		W14x500	W14x500		W14x500
25	"	"		"	25-27	W14x455	W14x550		W14x455
26	"	"		"		W14x550	W14x550		W14x550
27	"	"		W36x182	27-29	W14x500	W14x605		W14x500
28	"	"		"		W14x550	W14x605		W14x550
29	"	"		"	29-31	W14x605	W14x605		W14x605
30	"	"		"		W14x665	W14x730		W14x665

Same as Design I

Same as Design I

TABLE 5: MEMBER SIZES FOR FRAME 4

Beams					Columns				
Levels	Design I	Design II	Design III	Design IV	Levels	Design I	Design II	Design III	Design IV
1	W21x44	W21x44		W24x76	1-3 EXT	W10x54	W10x60		W10x66
2	W21x55	W21x55		W27x84	INT	W10x33	W10x39		W10x39
3	"	"		"	3-5	W14x68	W14x78		W14x84
4	"	"		"		W14x68	W14x68		W14x84
5	W24x61	W24x61		W30x99	5-7	W14x95	W14x103		W14x119
6	W24x68	W24x68		W30x108		W14x95	W14x103		W14x119
7	"	"		"	7-9	W14x119	W14x127		W14x142
8	W24x76	W24x76		W30x116		W14x127	W14x142		W14x158
9	"	"		"	9-11	W14x142	W14x150		W14x176
10	"	"	Same as Design I	"		W14x158	W14x176	Same as Design I	W14x193
11	W24x84	W24x84		W33x118	11-13	W14x167	W14x184		W14x202
12	"	"		"		W14x193	W14x211		W14x237
13	W27x84	W27x84		W36x135	13-15	W14x193	W14x211		W14x237
14	"	"		"		W14x219	W14x237		W14x264
15	W27x94	W27x94		W36x150	15-17	W14x219	W14x246		W14x264
16	"	"		"		W14x246	W14x287		W14x287
17	"	"		"	17-19	W14x246	W14x287		W14x287
18	W30x99	W30x99		W36x170		W14x287	W14x314		W14x342
19	"	"		"	19-21	W14x287	W14x314		W14x342
20	"	"	"		W14x314	W14x342	W14x370		
21	"	"	"	21-23	W14x314	W14x342	W14x370		
22	W30x108	W30x108	W35x182		W14x342	W14x370	W14x398		
23	"	"	"	23-25	W14x342	W14x370	W14x398		
24	"	"	"		W14x398	W14x426	W14x455		
25	W30x116	W30x116	W35x194	25-27	W14x370	W14x398	W14x426		
26	"	"	"		W14x426	W14x455	W14x500		
27	"	"	"	27-29	W14x398	W14x455	W14x455		
28	"	"	"		W14x455	W14x500	W14x550		
29	"	"	"	29-31	W14x500	W14x500	W14x605		
30	"	"	"		W14x550	W14x550	W14x665		

Wall loads acting on exterior columns are;

$$\text{Level 1 (3' parapet)} \quad P = 3/9.5 \times 0.475 \times 20 = 3.0^k$$

$$\text{Levels 2 to 10} \quad P = 0.475 \times 20 = 9.5^k$$

Concentrated wind loads at each level are;

$$\text{Level 1} \quad W_o = (4.75 + 3.00) \times 20 \times 0.020 = 3.1^k$$

$$\text{Levels 2 to 10} \quad W_o = 9.50 \times 20 \times 0.020 = 3.8^k$$

Step 2 - Portal Analysis

Cumulative shear at each story due to the wind loads calculated in Step 1 is shown below:

<u>Level</u>	<u>Wind Load (kips)</u>	<u>Cumulative Wind Shear (kips)</u>
1	3.1	3.1
2	3.8	6.9
3	3.8	10.7
4	3.8	14.5
5	3.8	18.3
6	3.8	22.1
7	3.8	25.9
8	3.8	29.7
9	3.8	33.5
10	3.8	37.3
11		

The distribution factors of wind shear to each column in a story are as follows:

	A	B	C	D
Aisle width	10'	20'	20'	10'
% of total shear	16.7	33.3	33.3	16.7

Based on the cumulative wind shear and the distribution factors, the following bending moments M_w in beams due to wind load are obtained.

$$\begin{aligned}
 \text{Level 1: } M_w &= \frac{1}{6} (3.1 \times 4.75) = 2.45 \text{ k-ft} \\
 \text{Level 2: } M_w &= \frac{1}{6} (3.1 \times 9.5 + 3.8 \times 4.75) = 7.91 \\
 \text{Level 3: } M_w &= \frac{1}{6} (6.9 \times 9.5 + 3.8 \times 4.75) = 13.95 \\
 \text{Level 4: } M_w &= \frac{1}{6} (10.7 \times 9.5 + 3.8 \times 4.75) = 20.0 \\
 \text{Level 5: } M_w &= \frac{1}{6} (14.5 \times 9.5 + 3.8 \times 4.75) = 26.0 \\
 \text{Level 6: } M_w &= \frac{1}{6} (18.3 \times 9.5 + 3.8 \times 4.75) = 32.0 \\
 \text{Level 7: } M_w &= \frac{1}{6} (22.1 \times 9.5 + 3.8 \times 4.75) = 38.0 \\
 \text{Level 8: } M_w &= \frac{1}{6} (25.9 \times 9.5 + 3.8 \times 4.75) = 44.0 \\
 \text{Level 9: } M_w &= \frac{1}{6} (29.7 \times 9.5 + 3.8 \times 4.75) = 50.0 \\
 \text{Level 10: } M_w &= \frac{1}{6} (33.5 \times 9.5 + 3.8 \times 4.75) = 56.0
 \end{aligned}$$

Step 3 - Beam Design - Level 10

Calculation	Operation	Units	Girder A-B
①	Span L	ft.	20
②	Live Load w_L	k/ft.	0.80
③	Dead Load w_D	k/ft.	1.10
④	Live Load Reaction $w_L L/2$	k	8.0
⑤	Dead Load Reaction $w_D L/2$	k	11.0

Calculation	Operation	Units	A-B
⑥	% LL used (1.0-Red.)	%	68.0
⑦	% LL x $w_L L^2$	k-ft.	217.5
⑧	$w_D L^2$	k-ft.	440.0
⑨	⑦+⑧ = $\Sigma w L^2$	k-ft	657.5
<u>Gravity Moments</u>			
⑩	(+) 0.08 x ⑨	k-ft.	52.6
⑪	(-) 0.045 x ⑨	k-ft.	29.6
<u>Wind & Gravity Moments</u>			
⑫	Wind Moment M_w (Portal)	k-ft.	56.0
⑬	$0.09375 \times \text{⑨} = 3/4 \times w L^2/8$	k-ft.	61.70
⑭	$1.50 \times \text{⑫}^2 \div \text{⑨}$	k-ft.	7.15
⑮	$0.75 \times \text{⑪}$	k-ft.	22.20
⑯	$0.75 \times \text{⑫}$	k-ft.	42.0
⑰	(+) ⑬ + ⑭ - ⑮	k-ft.	46.65
⑱	(-) ⑮ + ⑯	k-ft.	64.20
<u>Design</u>			
⑲	(+) Design M ⑩ or ⑰	k-ft.	52.6
⑳	(-) Design M ⑪ or ⑱	k-ft.	64.20
㉑	Section for $F_y = 36$ ksi		W14x26

Step 4 - Columns - Gravity Load Thrust in Columns

Tier	Computation	Thrust (kips)	
		Col.A	Col.B
Levels 1-3	Level 1 - $(w_D + w_L) \times \text{Aisle}$	14.00	28.00
	Level 2 - $w_L \times (1\text{-Red}) \times \text{Aisle}$	6.72	10.88
	$w_D \times \text{Aisle}$	11.00	22.00
	Column - Est. 50 lb/ft. - 2 stories	0.95	0.95
	Wall - 2 stories & parapet	<u>22.00</u>	<u>0</u>
		54.67	61.83

Levels 3-5	Level 3 - w_L x (1-Red) x Aisle	5.44	7.20
	w_D x Aisle	11.00	22.00
Levels 4	w_L x (1-Red) Aisle	4.16	7.20
	w_D x Aisle	11.00	22.00
	Column - Est. 75 lb/ft. - 2 stories	1.42	1.42
	Wall - 2 stories	<u>19.00</u>	<u>0</u>
		106.69	121.65
Levels 5-7	2 Levels - w_L x (1-Red) Aisle	7.20	14.40
	w_D x Aisle	22.00	44.00
	Column - Est. 100 lb/ft. - 2 stories	1.90	1.90
	Wall - 2 stories	<u>19.00</u>	<u>0</u>
		156.79	181.95
Levels 7-9	2 Levels	29.20	58.40
	Column - Est. 125 lb/ft. - 2 stories	2.37	2.37
	Wall - 2 stories	<u>19.00</u>	<u>0</u>
		207.26	242.62
Levels 9-11	2 Levels	29.20	58.40
	Column - Est. 150 lb/ft. - 2 stories	2.85	2.85
	Wall - 2 stories	<u>19.00</u>	<u>0</u>
		258.31	303.87

Step 5 - Columns - Gravity Load Moments in Columns

Bending moments in columns due to the gravity loads are obtained by distributing the bending moments in beams equally in columns above and below the joint to which that beam is attached.

Tier		Moment (k-ft)	
		Col. A	Col. B
Levels 2-3	Moment below level 2	14.8	0
	Moment above level 3	14.8	0
All other levels		14.8	0

TABLE 6: MEMBER SIZES FOR FRAME 5

Beams					Columns					
Levels	Design I	Design II	Design III	Design IV	Levels	Design I	Design II	Design III	Design IV	
1	W30x99	W30x99		W36x150	1-3	W14x136	W14x136		W14x136	
2	W33x130	W33x130		W36x230						
3	"	"		"	3-5	W14x158	W14x184		W14x158	
4	"	"		"						
5	"	"		"	5-7	W14x202	W14x228		W14x202	
6	"	"		"						
7	W36x135	W36x135	Same as Design I	W36x260	7-9	W14x246	W14x264	Same as Design I	W14x246	
8	"	"		"						
9	W36x150	W36x150		W36x300	9-11	W14x314	W14x314		W14x314	
10	"	"		"						
11	W36x160	W36x160		W36x300*	11-13	W14x342	W14x370		W14x342	
12	"	"		"						
13	W36x170	W36x170		"	13-15	W14x398	W14x426		W14x398	
14	W36x182	W36x182		W36x300**						
15	"	"		"	15-17	W14x426	W14x500		W14x426	
16	W36x194	W36x194		"						
17	"	"	"	17-19	W14x500	W14x550	W14x500			
18	"	"	"							
19	W36x230	W36x230		W36x300***	19-21	W14x605	W14x605	W14x605		
20	"	"		"						

*Section W36x300 + 2(1/2"x12") cover plates
 **Section W36x300 + 2(3/4"x15") cover plates
 ***Section W36x300 + 2(1-1/4"x15") cover plates

TABLE 7: MEMBER SIZES FOR FRAME 6

Beams					Columns				
Levels	Design I	Design II	Design III	Design IV	Levels	Design I	Design II	Design III	Design IV
1	W12x22	W12x22	W12x22	Same as Design I	1-3 EXT	W8x20	W8x24	W8x20	Same as Design I
2	W14x22	W14x22	W14x22		INT	W8x17	W8x17	W8x13	
3	"	"	"		3-5	W8x28	W8x35	W8x28	
4	"	"	"			W8x28	W8x28	W8x24	
5	"	"	"		5-7	W8x35	W8x48	W8x35	
6	"	"	"			W8x35	W8x40	W8x35	
7	W14x26	W14x26	W14x26		7-9	W8x48	W8x58	W8x48	
8	"	"	"			W8x48	W8x48	W8x48	
9	"	"	"		9-11	W8x58	W8x67	W8x58	
10	"	"	"			W8x58	W8x67	W8x58	

TABLE 8: MEMBER SIZES FOR FRAME 7

Beams					Columns				
Levels	Design I	Design II	Design III	Design IV	Levels	Design I	Design II	Design III	Design IV
1	W21x44	W21x44		W24x76	1-3 EXT	W10x54	W10x60		W10x77
2	W21x55	W21x55		W27x84	INT	W10x33	W10x39		W10x45
3	"	"		"	3-5	W12x79	W12x85		W14x95
4	W24x61	W24x61		W30x99		W12x65	W12x72		W14x78
5	"	"		"	5-7	W14x95	W14x103		W14x142
6	W24x68	W24x68		W30x108		W14x95	W14x103		W14x142
7	"	"		"	7-9	W14x119	W14x127		W14x176
8	W24x76	W24x76		W30x116		W14x127	W14x136		W14x184
9	"	"		"	9-11	W14x142	W14x150		W14x211
10	W24x84	W24x84		W33x118		W14x158	W14x176		W14x228
11	"	"		"	11-13	W14x176	W14x176		W14x246
12	"	"		"		W14x193	W14x211		W14x287
13	W27x94	W27x94		W36x135	13-15	W14x193	W14x219		W14x287
14	"	"		"		W14x219	W14x237		W14x314
15	"	"		"	15-17	W14x228	W14x246		W14x342
16	W30x99	W30x99		W36x160		W14x264	W14x287		W14x370
17	"	"		"	17-19	W14x264	W14x287		W14x370
18	"	"		"		W14x287	W14x314		W14x398
19	"	"		"	19-21	W14x287	W14x314		W14x398
20	W30x108	W30x108		W36x170		W14x314	W14x342		W14x426

Same as Design I

Same as Design I

TABLE 8 (Continued)

Beams					Columns				
Levels	Design I	Design II	Design III	Design IV	Levels	Design I	Design II	Design III	Design IV
21	W30x108	W30x108		W36x170	21-23 EXT	W14x314	W14x370		W14x426
22	"	"		"	INT	W14x370	W14x370		W14x500
23	W30x116	W30x116		W36x194	23-25	W14x342	W14x398		W14x455
24	"	"		"		W14x398	W14x398		W14x550
25	"	"		"	25-27	W14x370	W14x426		W14x500
26	"	"		"		W14x426	W14x426		W14x605
27	W33x118	W33x118	Same as Design I	W36x230	27-29	W14x398	W14x455	Same as Design I	W14x550
28	"	"		"	W14x455	W14x455	W14x605		
29	"	"		"	W14x426	W14x500	W14x605		
30	"	"		"	W14x500	W14x500	W14x665		
31	W33x130	W33x130		W36x245	31-33	W14x455	W14x550		W14x605
32	"	"		"	W14x500	W14x550	W14x665		
33	"	"		"	33-35	W14x500	W14x550		W14x665
34	"	"		"	W14x550	W14x550	W14x730		
35	"	"		"	35-37	W14x550	W14x605		W14x730
36	"	"		"	W14x605	W14x605	W14x730*		
37	"	"	"	37-39	W14x605	W14x665	W14x730*		
38	"	"	"	W14x605	W14x665	W14x730*			
39	"	"	"	39-41	W14x730	W14x730	W14x730***		
40	"	"	"	W14x665	W14x730	W14x730**			

*Section W14x730 + 2(1"x15") cover plates
 **Section W14x730 + 2(1¹/₂"x15") cover plates
 ***Section W14x730 + 2(2"x15") cover plates

TABLE 9: SUMMARY OF ANALYSES

Analysis 1	Second-Order, Elastic-Plastic, Non-proportional Gravity Load Factor=1.3, Computer Program used: SOFRAN-DIN
Analysis 2	Second-Order, Elastic-Plastic, Non-proportional Gravity Load Factor=1.0, Computer Program used: SOFRAN-DIN
Analysis 3	Second-Order, Elastic-Plastic, Proportional Computer Program used: SOFRAN-LIN
Analysis 4	First-Order, Linear-Elastic
Analysis 5	Second-Order, Elastic-Plastic, Non-proportional Gravity Load Factor=1.2, Yield Stress Level = $0.9 F_y$ Computer Program used: SOFRAN-DIN

TABLE 10: SUMMARY OF ANALYSES FOR DESIGN I (STRESS DESIGN)

Frame	First-Order Analysis	Second-Order Analysis Proportional Loading			Second-Order Analyses: Nonproportional Loading								
					1.0 Gravity L.F.			1.2 Gravity L.F.			1.3 Gravity L.F.		
	Δ/H	Δ/H	Load Factor		Δ/H	Load Factor		Δ/H	Load Factor		Δ/H	Load Factor	
	Working	Working	1st Hinge	Max.	Working	1st Hinge	Max.	Working	1st Hinge	Max.	Working	1st Hinge	Max.
1	2	3	4	5	6	7	8	9	10	11	12	13	14
1	0.00296	0.00318	1.30	1.45	0.00313	1.81	2.51	----	--	--	0.00323	1.17	1.87
2	0.00267	0.00293	1.35	1.45	0.00293	1.69	2.52	0.00301	1.10	1.69	0.00305	1.31	1.97
3	0.00297	0.00328	1.25	1.40	0.00328	1.45	2.34	----	--	--	0.00343	1.09	1.65
4	0.00370	0.00404	1.25	1.40	0.00406	1.41	2.07	----	--	--	0.00423	0.83	1.72
5	0.00345	0.00370	1.30	1.60	0.00369	1.55	2.49	0.00379	1.16	2.13	0.00382	1.29	2.36
6	0.00217	0.00237	1.30	1.45	0.00237	1.89	2.73	----	--	--	0.00247	1.14	1.90
7	0.00417	0.00460	1.25	1.40	0.00459	1.34	2.06	----	--	--	0.00478	1.18	1.66

TABLE 11: SUMMARY OF ANALYSES FOR DESIGN II (AISC STRESS DESIGN)

Frame	First-Order Analysis	Second-Order Analysis Proportional Loading			Second-Order Analyses: Nonproportional Loading								
					1.0 Gravity L.F.			1.2 Gravity L.F.			1.3 Gravity L.F.		
	Δ/H	Δ/H	Load Factor		Δ/H	Load Factor		Δ/H	Load Factor		Δ/H	Load Factor	
	Working	Working	1st Hinge	Max.	Working	1st Hinge	Max.	Working	1st Hinge	Max.	Working	1st Hinge	Max.
1	2	3	4	5	6	7	8	9	10	11	12	13	14
1	0.00283	0.00304	1.30	1.55	0.00300	1.87	2.68	---	--	--	0.00310	1.23	2.13
2	0.00257	0.00282	1.35	1.55	0.00278	1.73	2.67	0.00284	1.12	2.01	0.00289	1.32	2.14
3	0.00282	0.00310	1.20	1.50	0.00307	1.47	2.44	---	--	--	0.00316	0.94	2.33
4	0.00356	0.00389	1.25	1.50	0.00387	1.47	2.19	---	--	--	0.00398	1.07	1.82
5	0.00336	0.00360	1.30	1.75	0.00360	1.60	2.61	0.00362	1.16	2.20	0.00365	1.31	2.45
6	0.00208	0.00226	1.30	1.55	0.00227	1.89	3.06	---	--	--	0.00236	1.26	2.32
7	0.00398	0.00437	1.25	1.45	0.00432	1.39	2.13	---	--	--	0.00446	1.17	1.93

TABLE 12: SUMMARY OF ANALYSES FOR DESIGN III (STRESS DESIGN)

Frame	First-Order Analysis	Second-Order Analysis Proportional Loading			Second-Order Analyses: Nonproportional Loading								
					1.0 Gravity L.F.			1.2 Gravity L.F.			1.3 Gravity L.F.		
	Δ/H	Δ/H	Load Factor		Δ/H	Load Factor		Δ/H	Load Factor		Δ/H	Load Factor	
	Working	Working	1st Hinge	Max.	Working	1st Hinge	Max.	Working	1st Hinge	Max.	Working	1st Hinge	Max.
1	2	3	4	5	6	7	8	9	10	11	12	13	14
1	0.00305	0.00330	1.30	1.45	0.00325	1.81	2.41	-----	--	--	0.00335	1.16	1.85
2	0.00271	0.00298	1.35	1.45	0.00296	1.70	2.65	0.00303	1.10	1.72	0.00307	1.30	1.89
3	-----	-----	--	--	-----	--	--	-----	--	--	-----	--	--
4	-----	-----	--	--	-----	--	--	-----	--	--	-----	--	--
5	-----	-----	--	--	-----	--	--	-----	--	--	-----	--	--
6	0.00224	0.00245	1.30	1.45	0.00246	1.89	2.69	-----	--	--	0.00256	1.13	1.82
7	-----	-----	--	--	-----	--	--	-----	--	--	-----	--	--

TABLE 13: SUMMARY OF ANALYSES FOR DESIGN IV (DRIFT DESIGN)

Frame	First-Order Analysis	Second-Order Analysis Proportional Loading			Second-Order Analyses: Nonproportional Loading								
					1.0 Gravity L.F.			1.2 Gravity L.F.			1.3 Gravity L.F.		
		Δ/H	Δ/H	Load Factor		Δ/H	Load Factor		Δ/H	Load Factor		Δ/H	Load Factor
Working	Working	1st Hinge	Max.	Working	1st Hinge	Max.	Working	1st Hinge	Max.	Working	1st Hinge	Max.	
1	2	3	4	5	6	7	8	9	10	11	12	13	14
1	0.00234	0.00249	1.45	1.55	0.00245	2.24	2.71	----	--	--	0.00251	1.68	2.06
2	0.00211	0.00227	1.40	1.50	0.00229	2.32	3.20	0.00233	1.43	1.89	0.00236	1.63	2.13
3	0.00210	0.00224	1.35	1.45	0.00223	2.47	2.97	----	--	--	0.00235	1.41	2.24
4	0.00205	0.00216	1.60	1.80	0.00216	3.24	3.92	----	--	--	0.00219	2.49	3.18
5	0.00202	0.00211	1.50	1.90	0.00206	2.61	3.82	0.00209	1.70	2.84	0.00210	1.95	3.15
6	----	----	--	--	----	--	--	----	--	--	----	--	--
7	0.00224	0.00235	1.80	2.05	0.00235	3.37	4.08	----	--	--	0.00237	3.09	3.85

TABLE 14. COMPARISON OF MAXIMUM LOADS FROM FIRST-ORDER
AND SECOND-ORDER ANALYSES UNDER PROPORTIONAL
LOADS, DESIGN I FRAMES

Frame	First- Order Analysis	Second- Order Analysis	Percent Difference
1	1.70	1.45	14.7
2	1.65	1.45	12.1
3	<u>1.60</u>	<u>1.40</u>	12.5
4	1.65	1.40	15.6
5	<u>2.05</u>	<u>1.60</u>	22.0
6	1.70	1.45	14.7
7	1.65	1.40	15.1

TABLE 15: SUMMARY OF ϕ AND $\bar{\phi}$ FACTORS FOR DESIGNS I AND IV

Frame	h/L	w_w psf	w_g^* psf	Design I				Design IV			
				ϕ_{ave}	ϕ_{max}	$\bar{\phi}_{ave}$	$\bar{\phi}_{max}$	ϕ_{ave}	ϕ_{max}	$\bar{\phi}_{ave}$	$\bar{\phi}_{max}$
1	2	3	4	5	6	7	8	9	10	11	12
1	0.1583	20	95	1.15	1.16	0.0050	0.0053	1.11	1.12	0.0037	0.0040
2	0.1333	20	125	1.19	1.20	0.0040	0.0043	1.14	1.15	0.0030	0.0032
3	0.2000	20	175	1.20	1.21	0.0046	0.0048	1.13	1.14	0.0030	0.0032
4	0.2000	20	125	1.17	1.18	0.0054	0.0058	1.09	1.10	0.0029	0.0032
5	0.2500	20	125	1.14	1.16	0.0056	0.0064	1.07	1.08	0.0028	0.0032
6	0.0950	20	95	1.18	1.20	0.0036	0.0040	—	—	—	—
7	0.2000	20	125	1.19	1.22	0.0061	0.0070	1.09	1.11	0.0029	0.0035

* w_g used in calculating $\bar{\phi}$'s is the total dead plus live loads, the latter does not include a live load reduction factor.

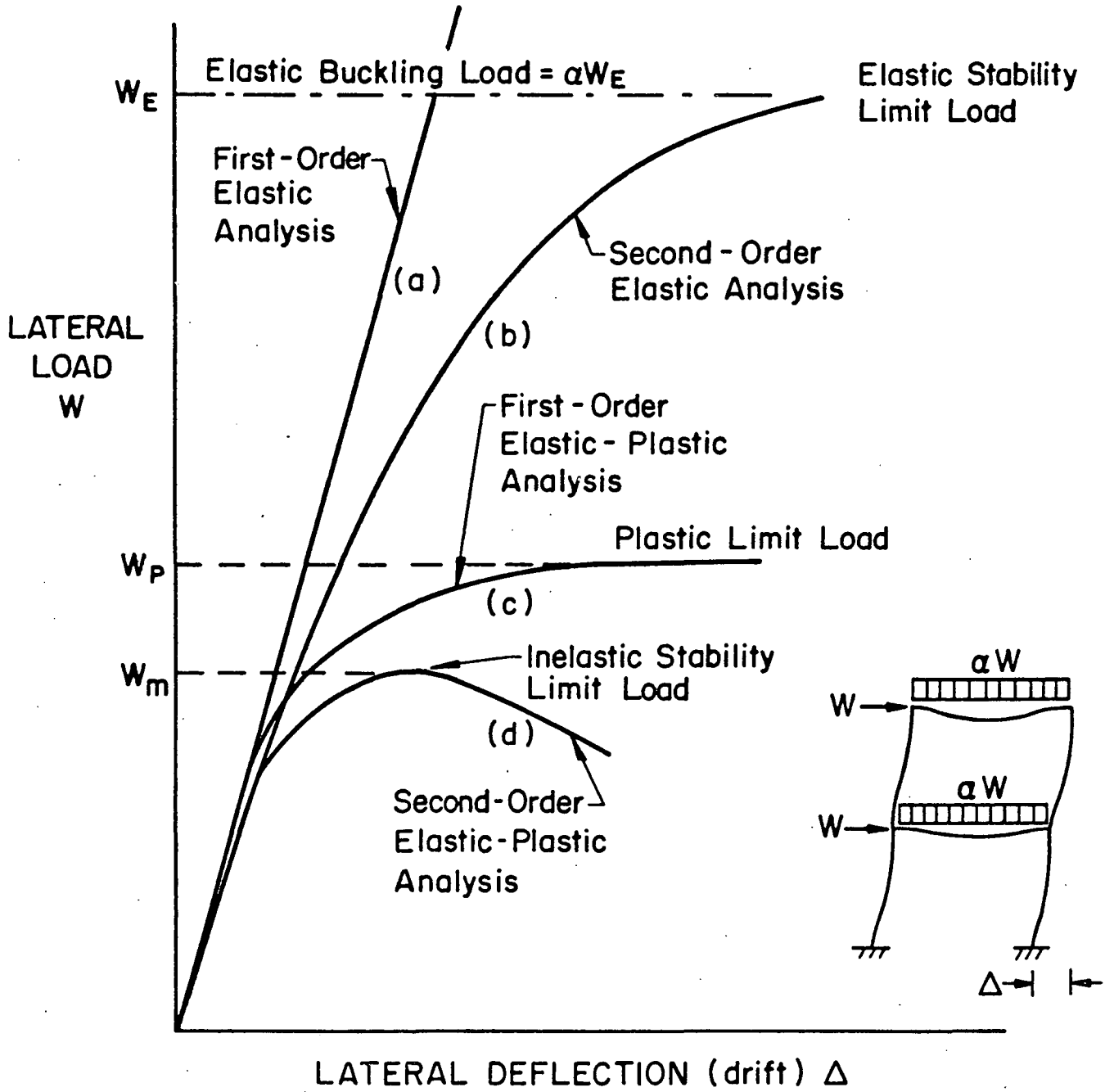


Fig. 1 Load-Deflection Curves of a Frame under Proportional Loads

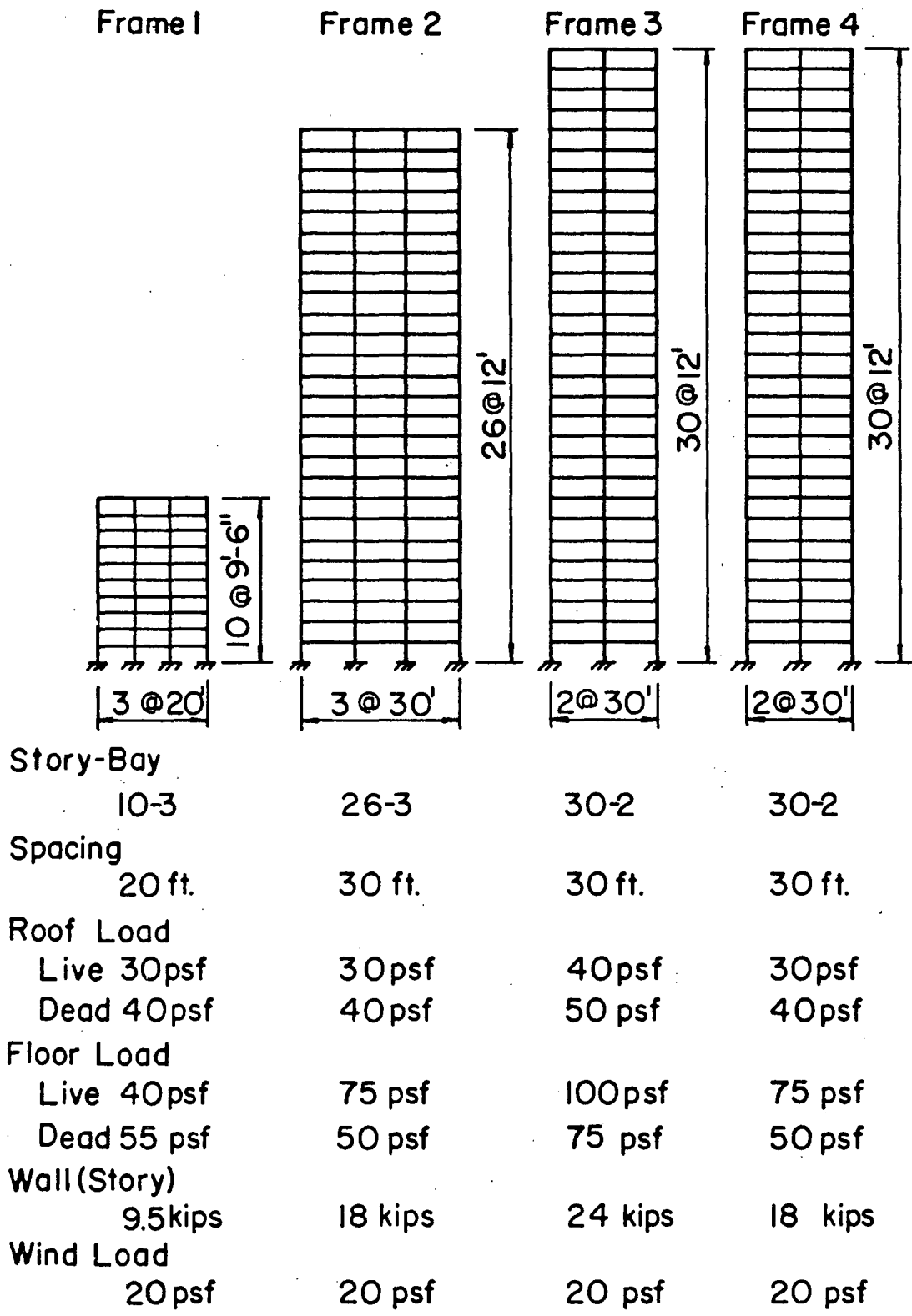


Fig. 2 Frame Dimensions and Loads

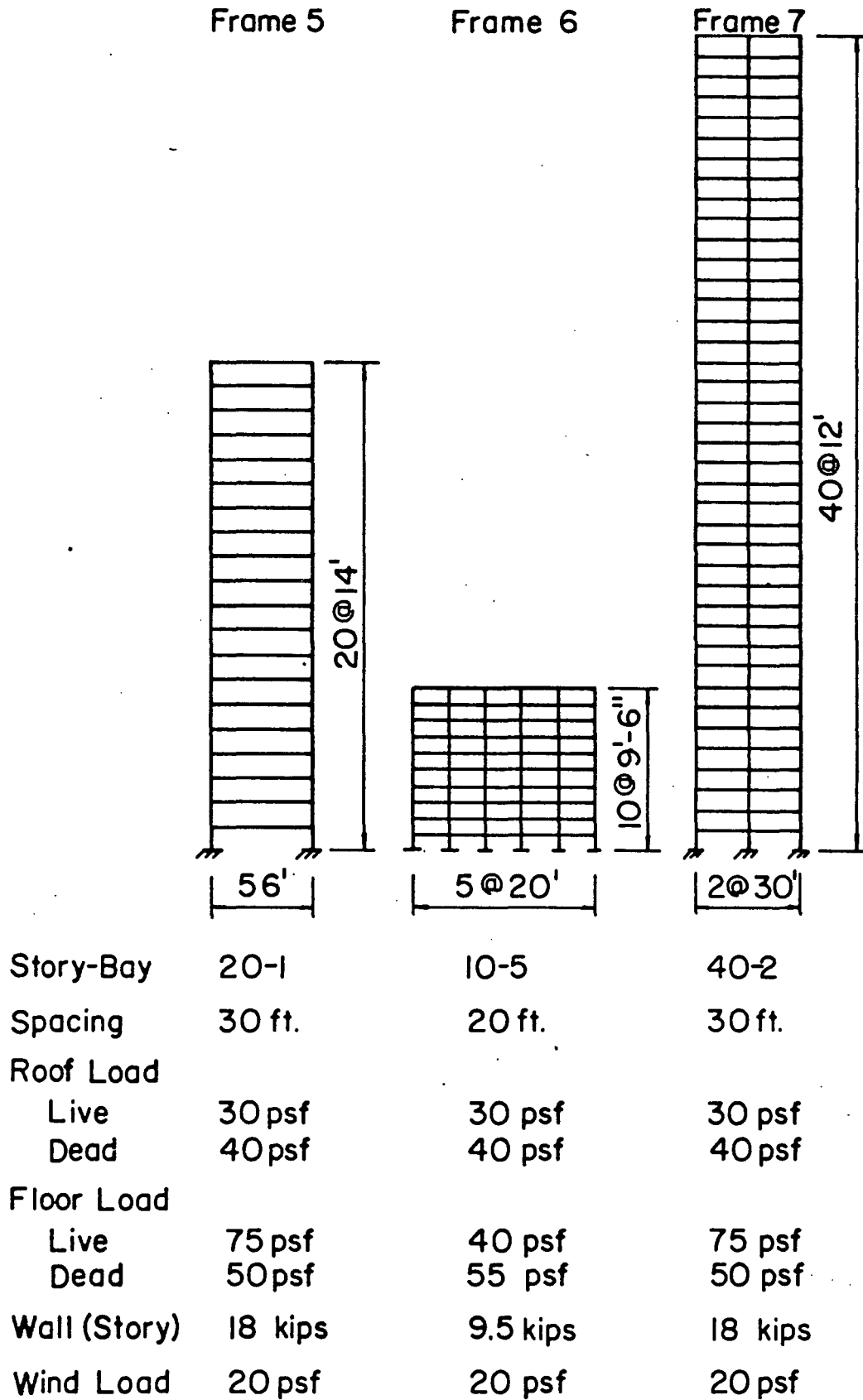


Fig. 2 Frame Dimensions and Loads (continued)

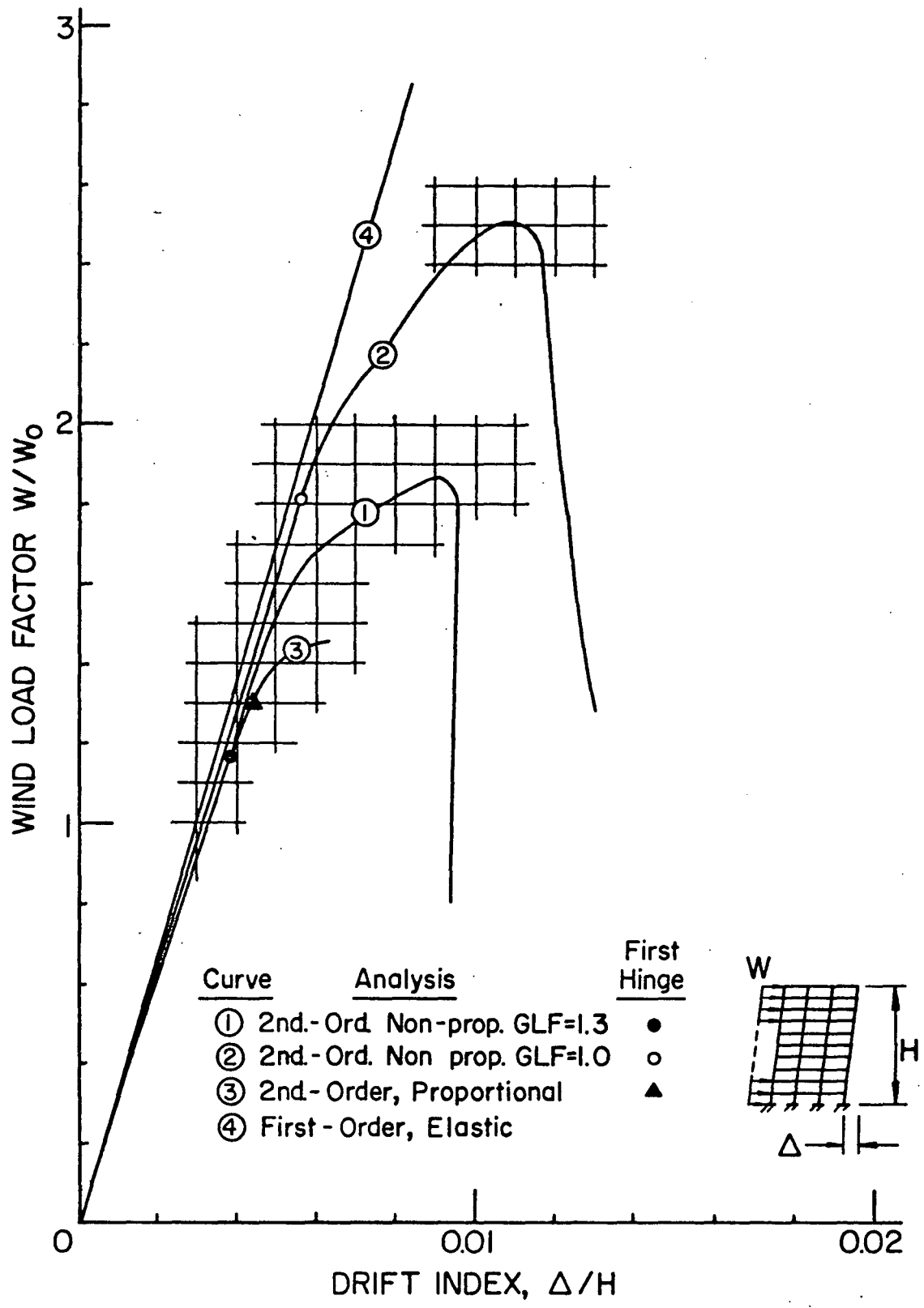


Fig. 3 Load - Drift Curves of Frame 1 - Design I

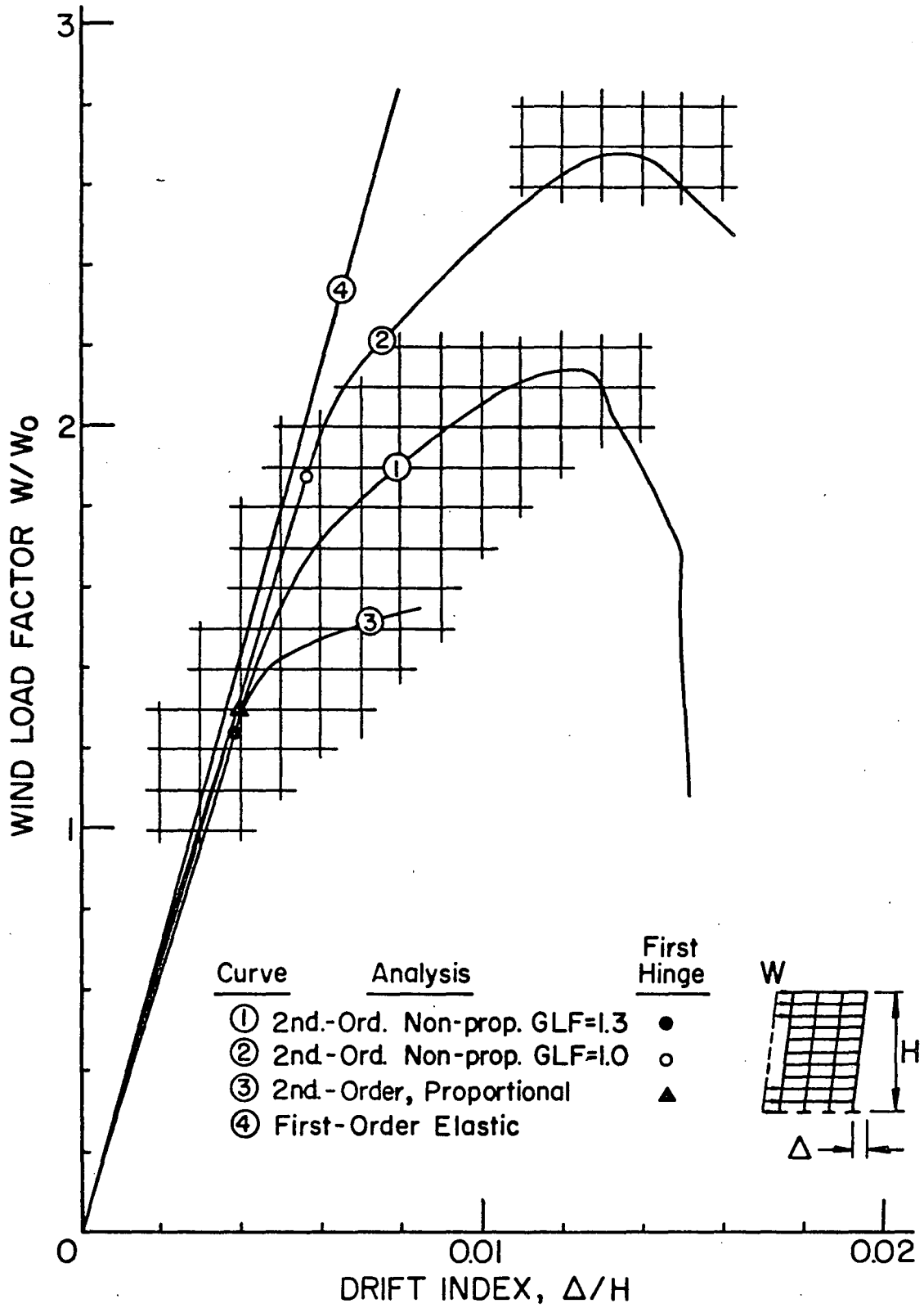


Fig. 4 Load - Drift Curves of Frame 1 - Design II

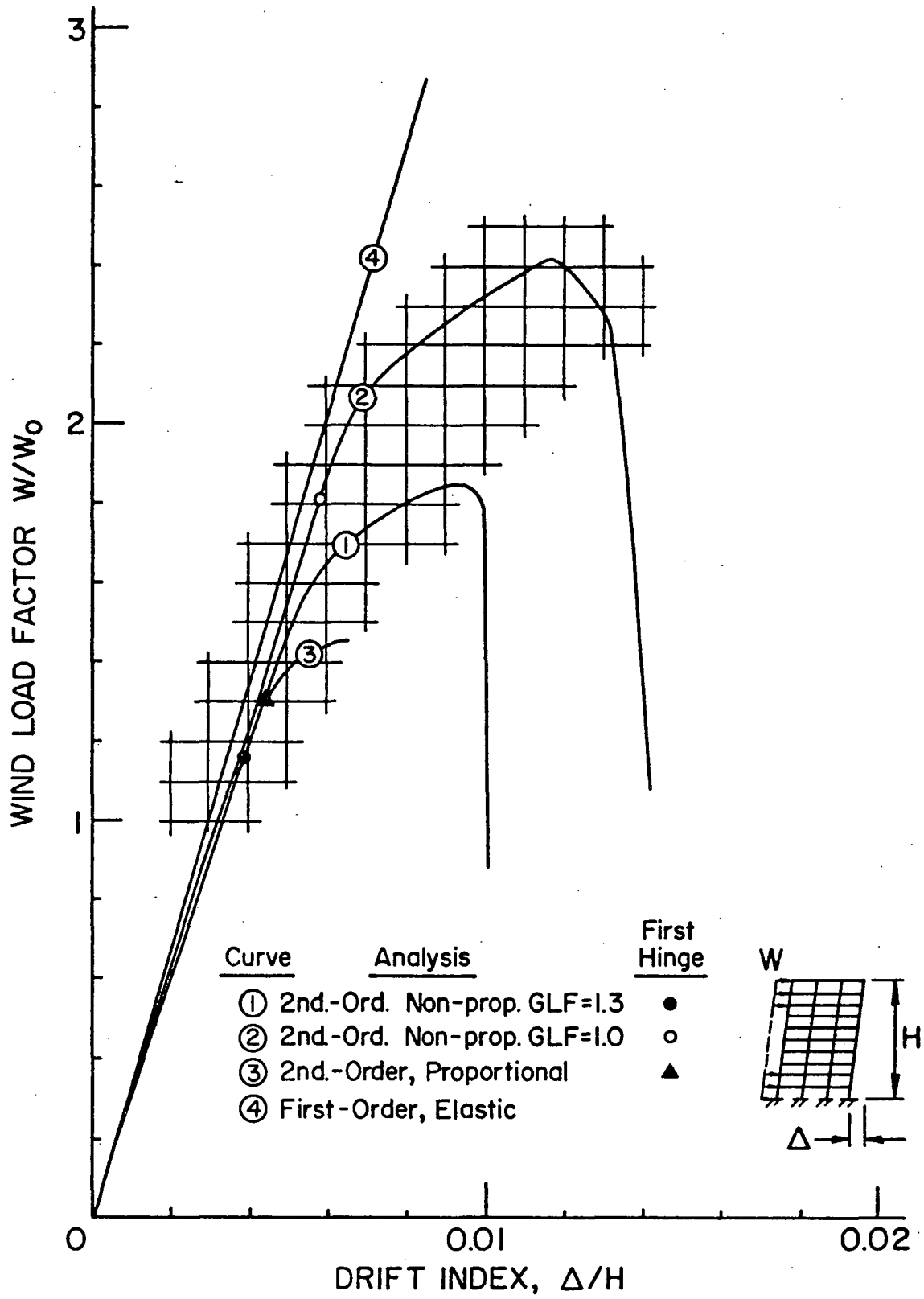


Fig. 5 Load - Drift Curves of Frame 1 - Design III

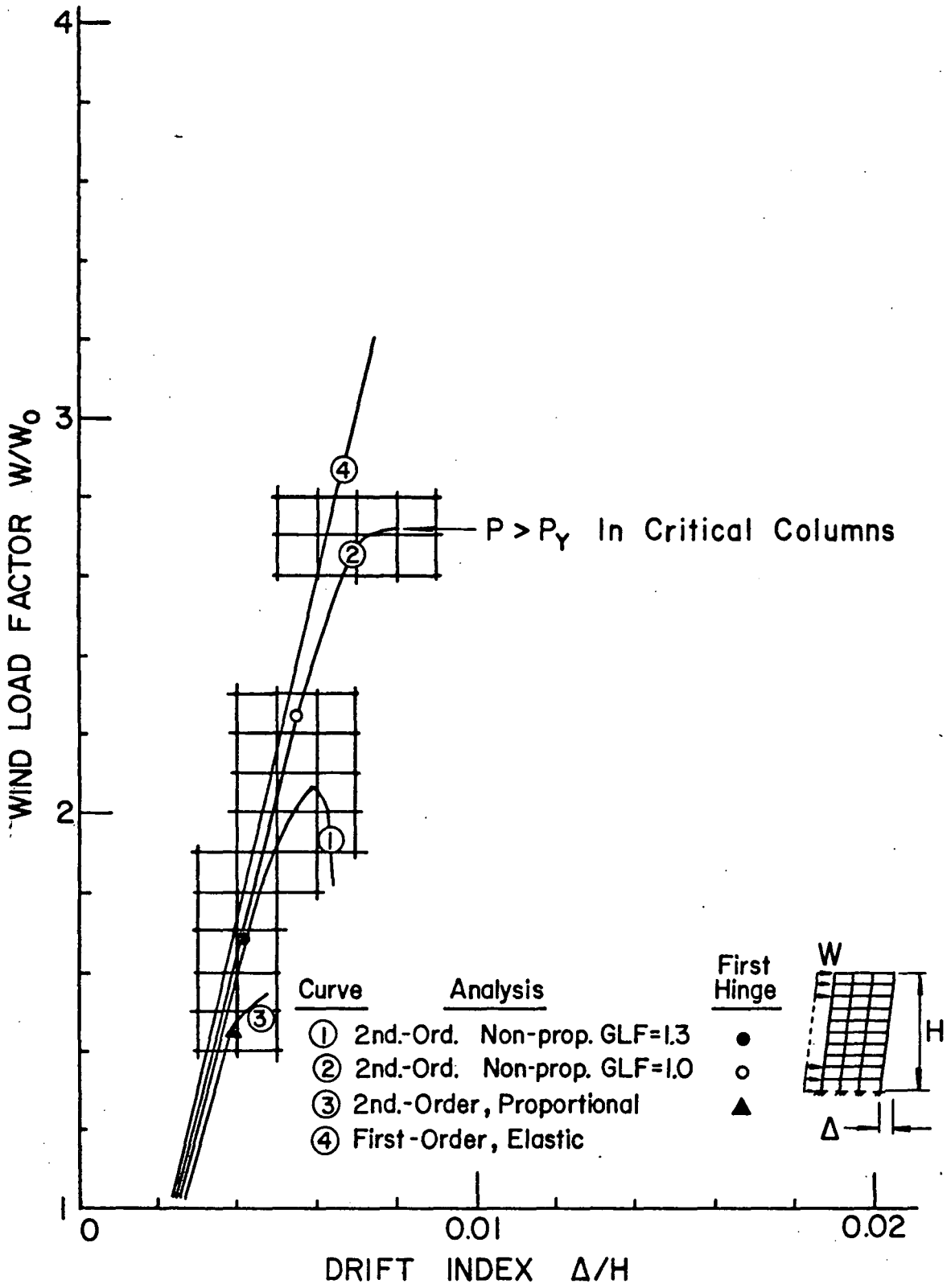


Fig. 6 Load - Drift Curves of Frame 1 - Design IV

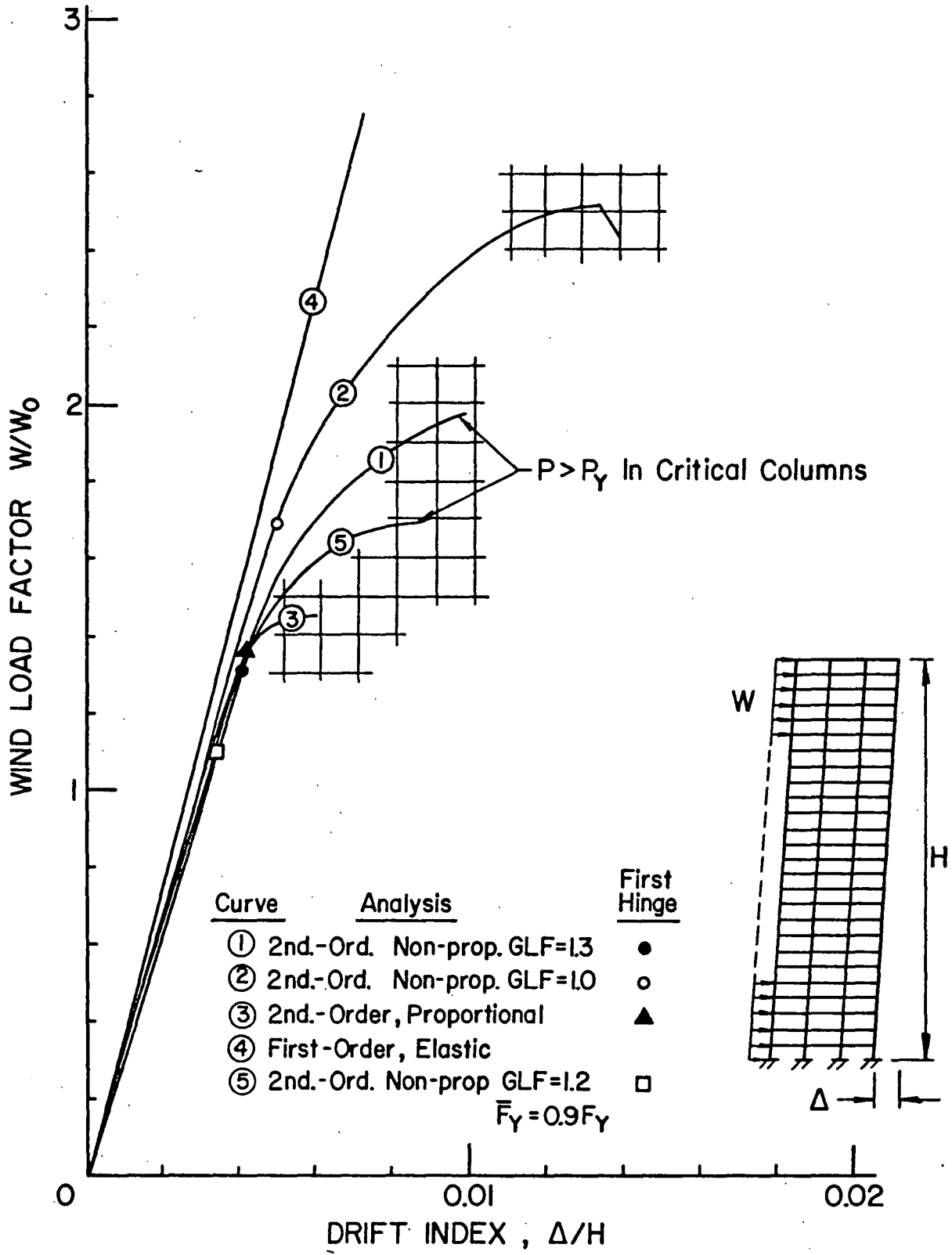


Fig. 7 Load - Drift Curves of Frame 2 - Design I

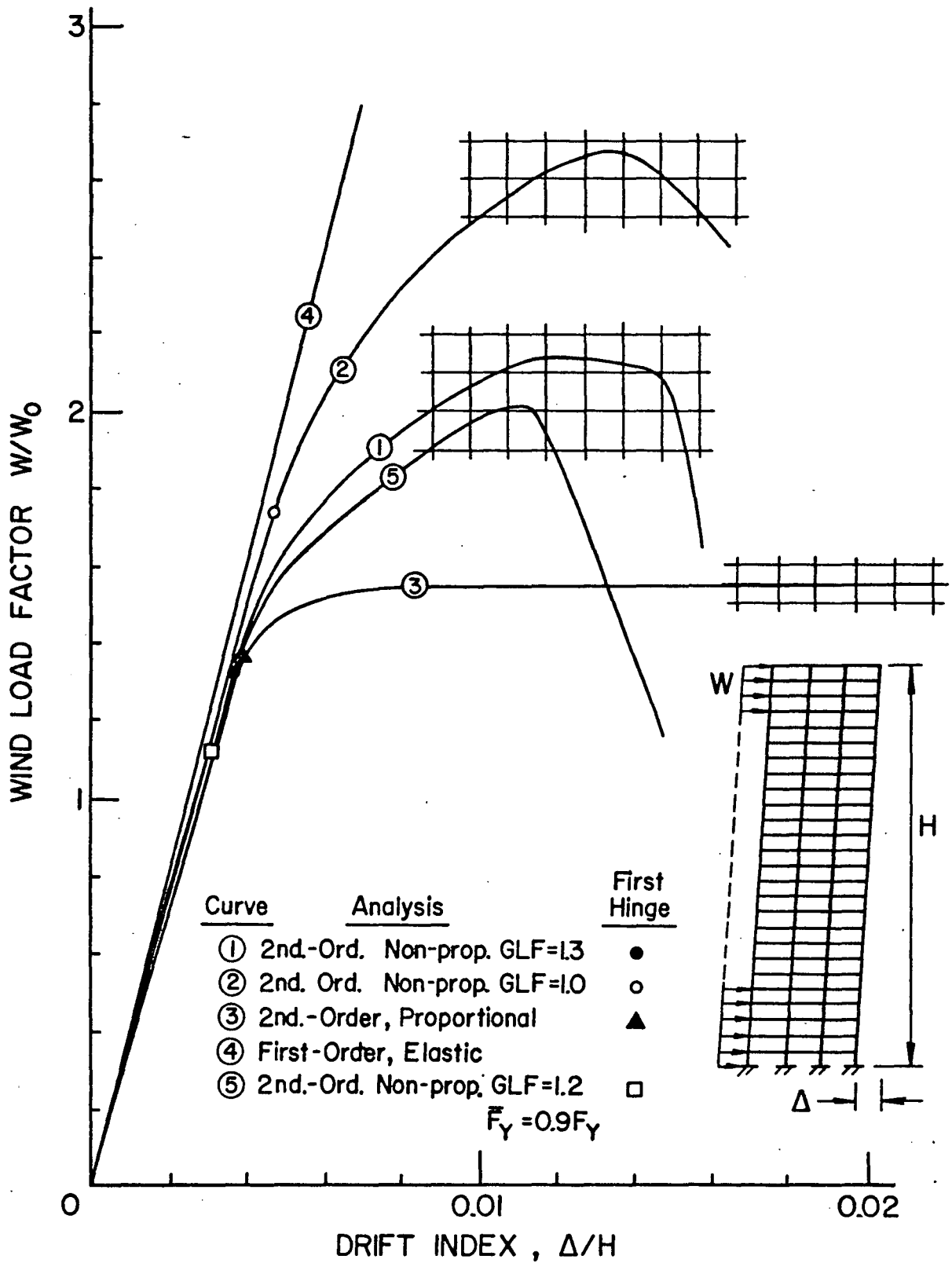


Fig. 8 Load - Drift Curves of Frame 2 - Design II

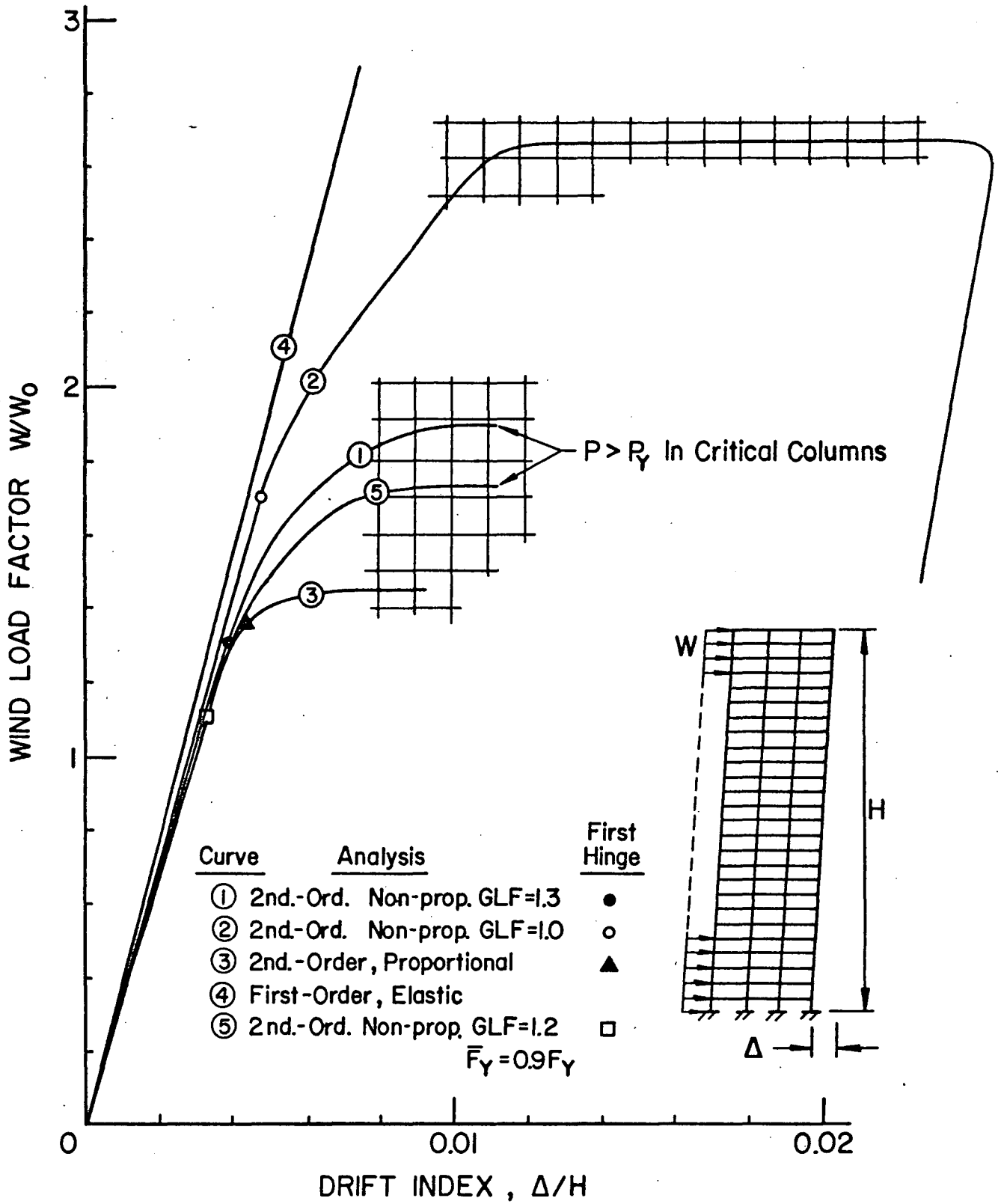


Fig. 9 Load - Drift Curves of Frame 2 - Design III

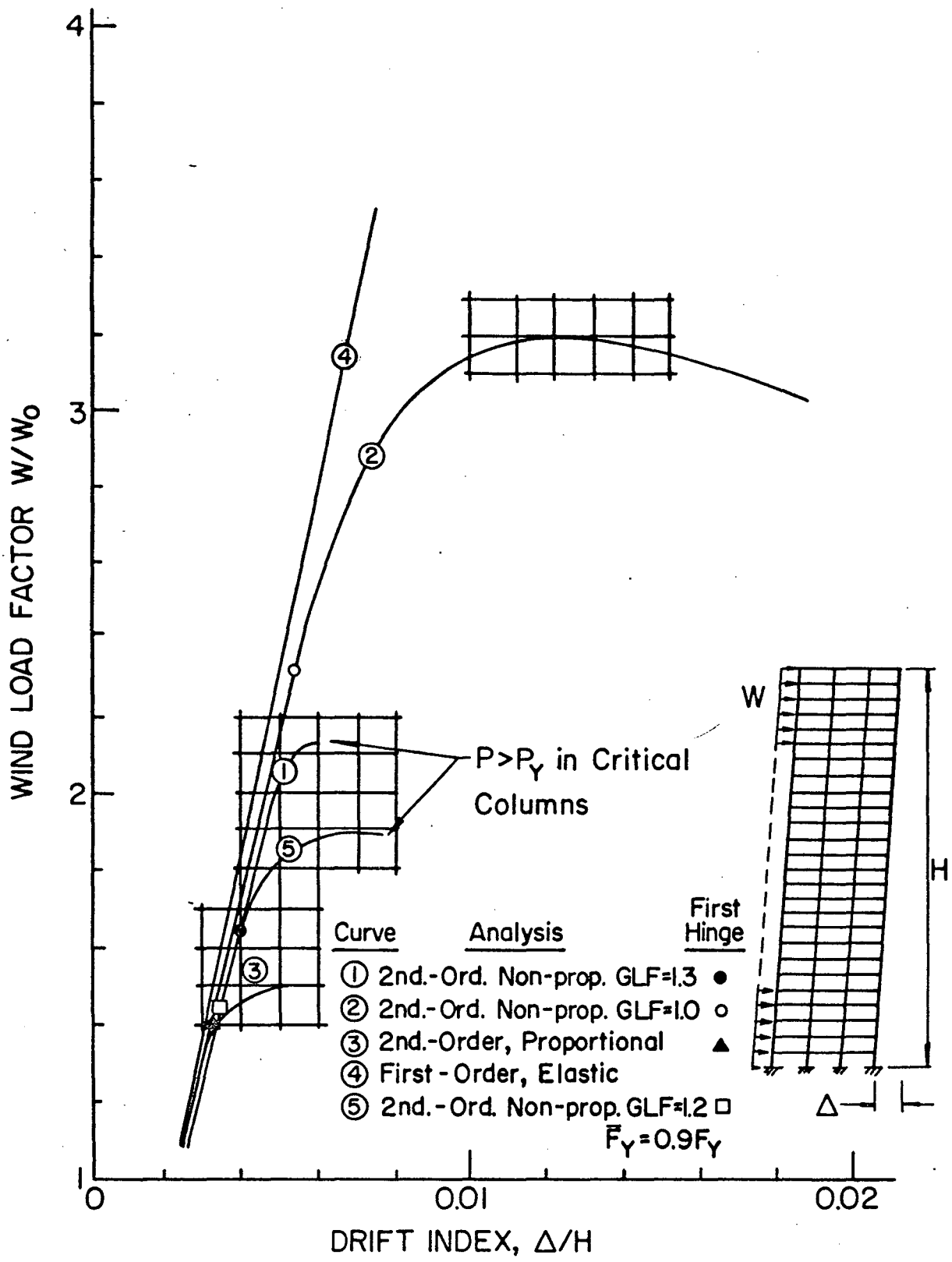


Fig. 10 Load - Drift Curves of Frame 2 - Design IV

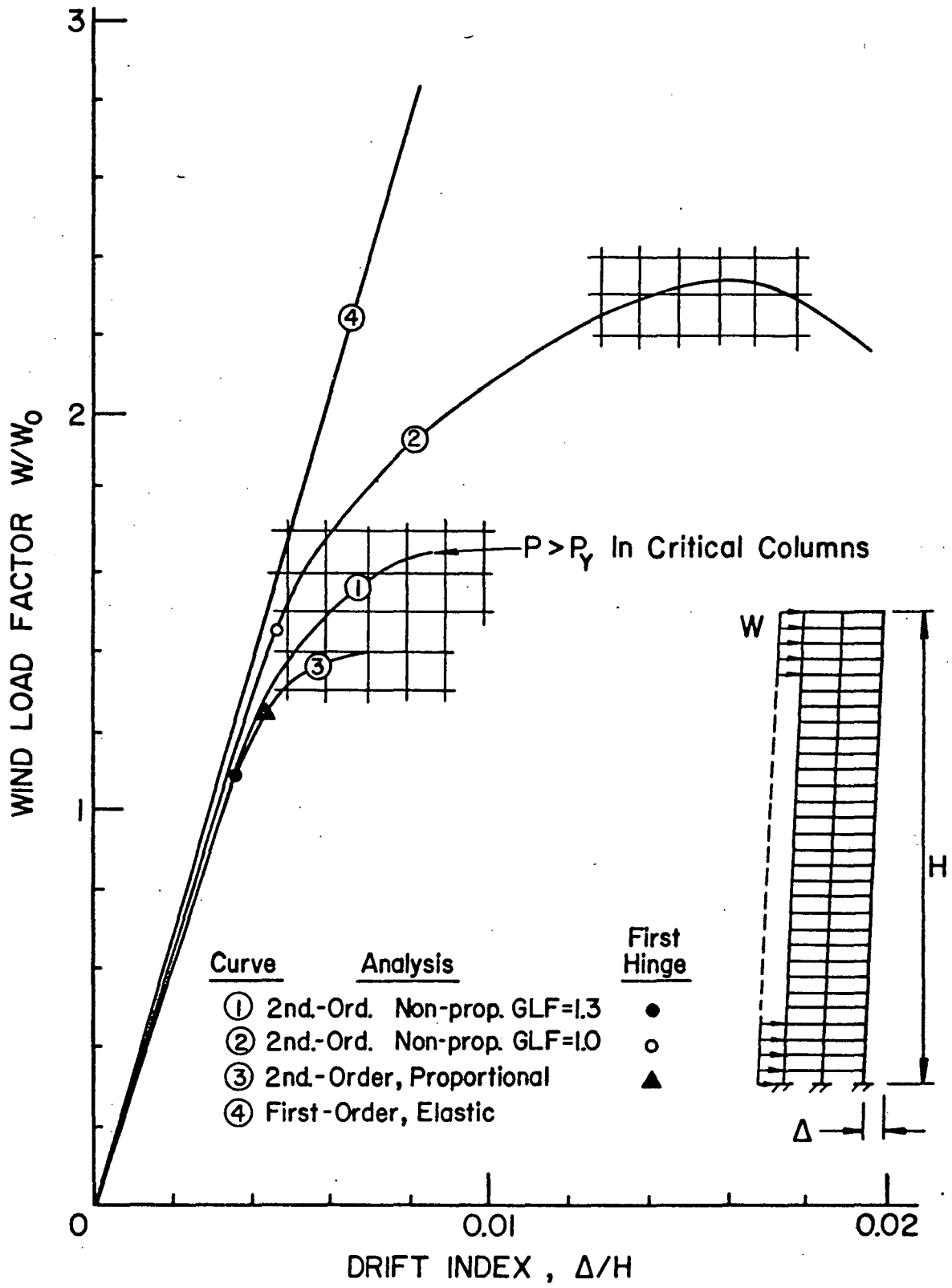


Fig. 11 Load - Drift Curves of Frame 3 - Designs I and III

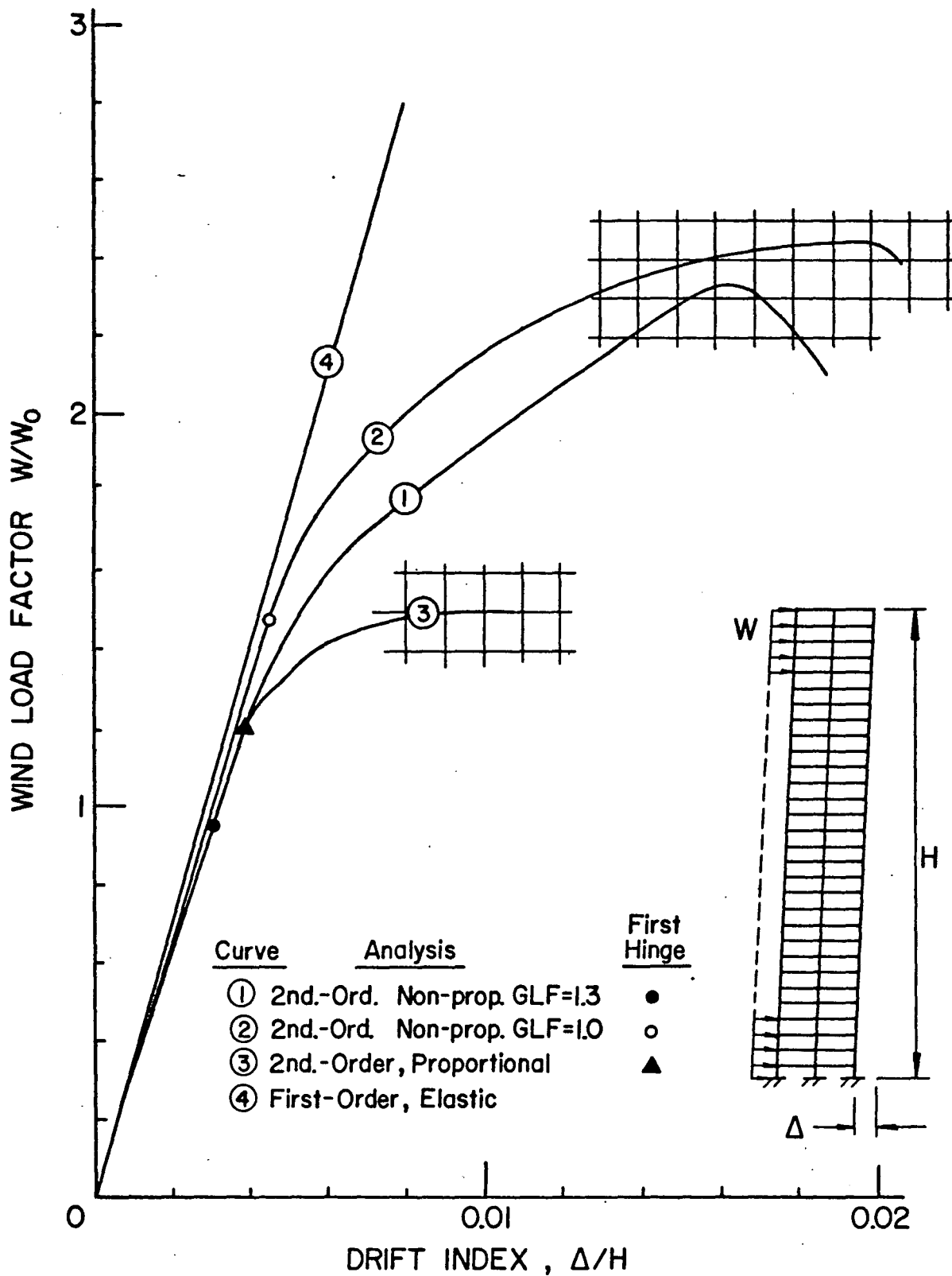


Fig. 12 Load - Drift Curves of Frame 3 - Design II

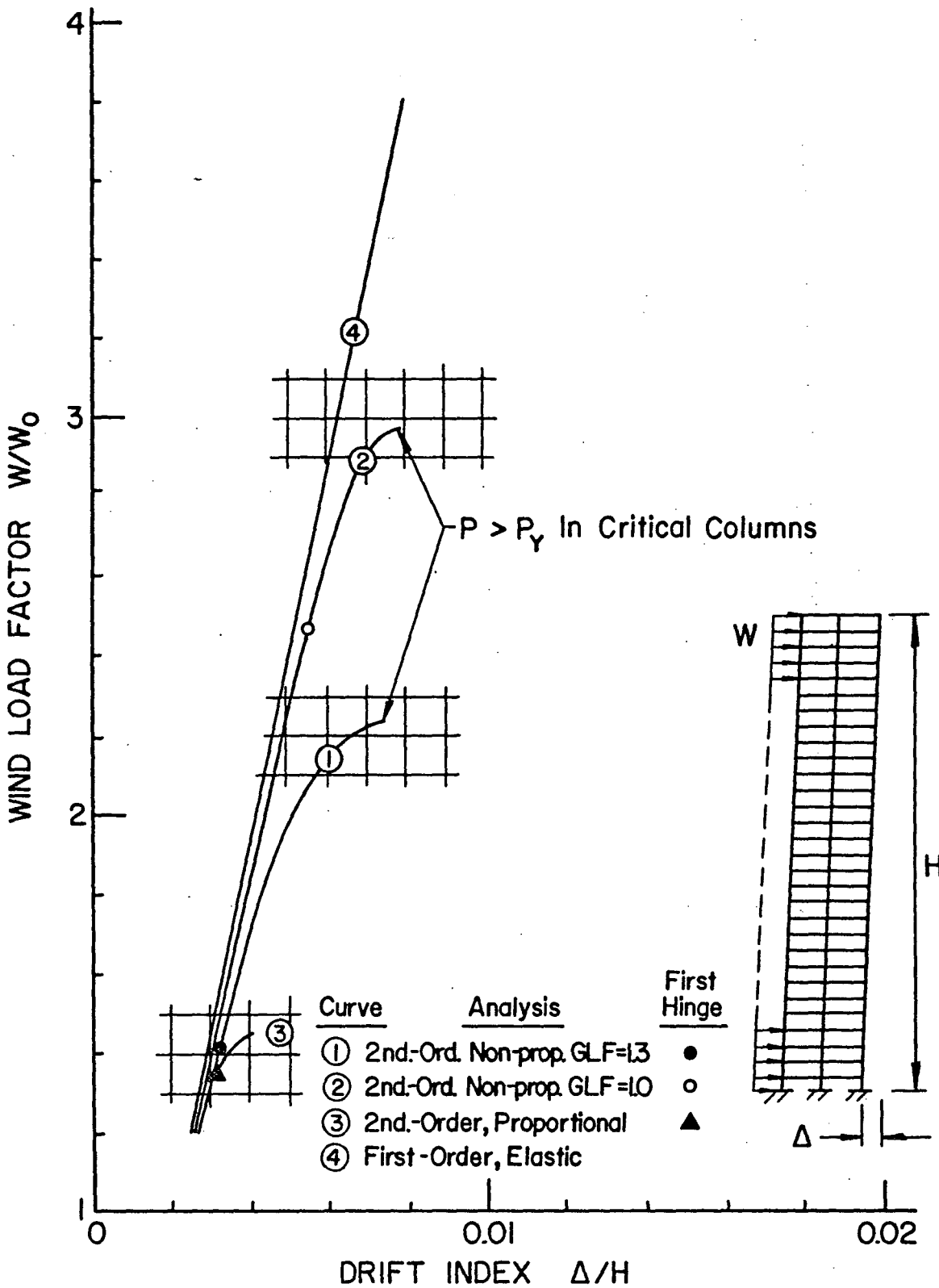


Fig. 13 Load - Drift Curves of Frame 3 - Design IV

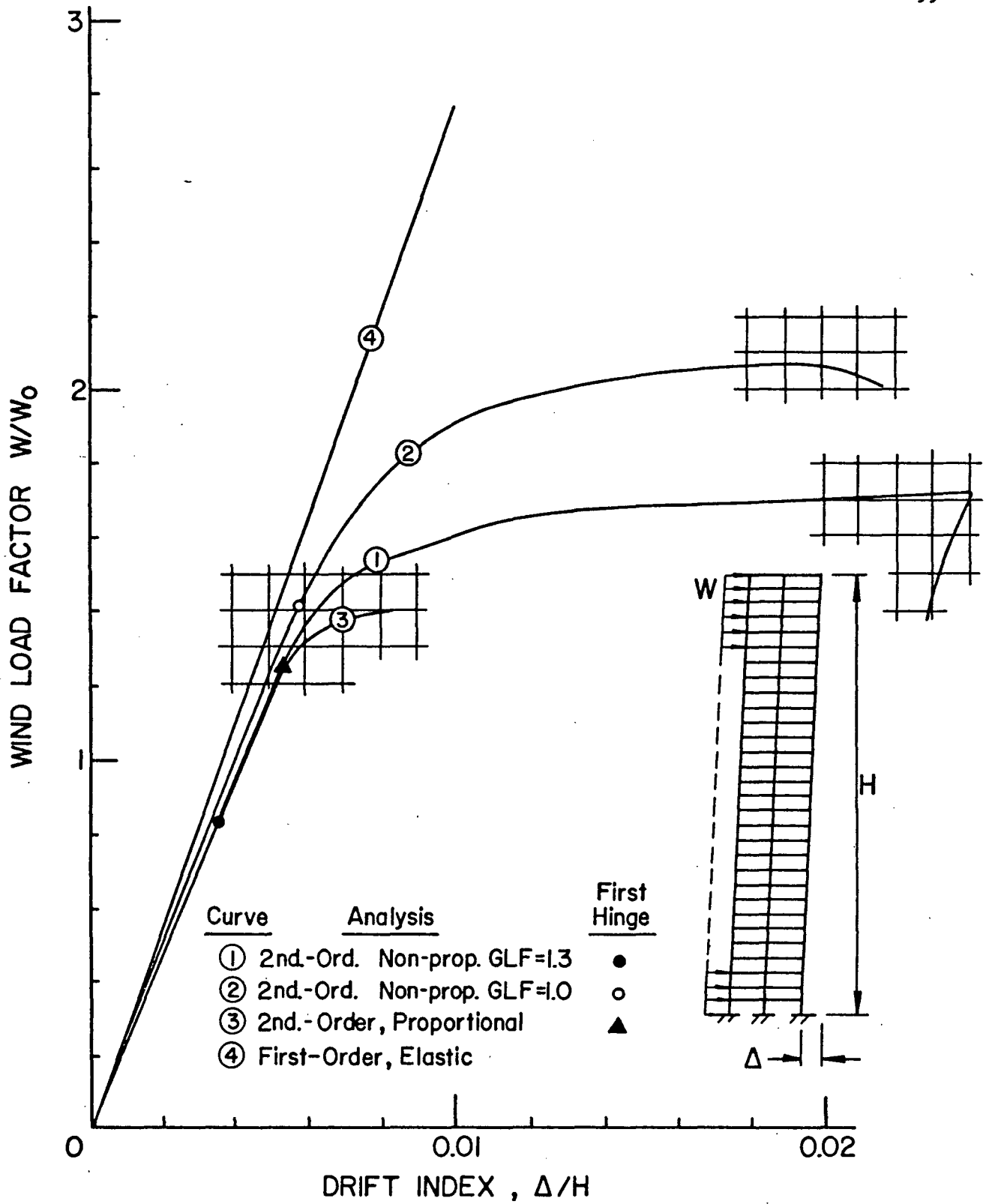


Fig. 14 Load - Drift Curves of Frame 4 - Designs I and III

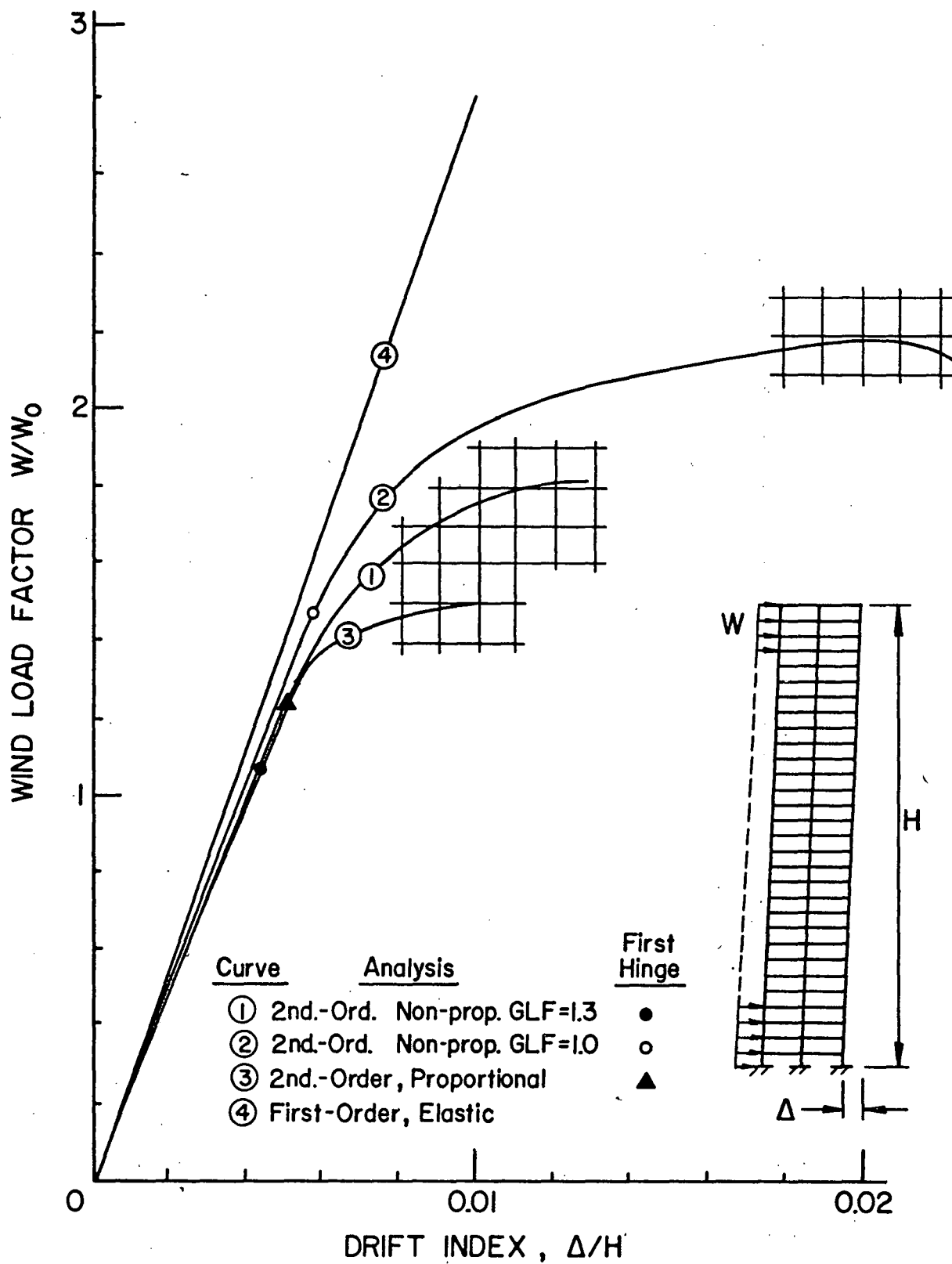


Fig. 15 Load - Drift Curves of Frame 4 - Design II

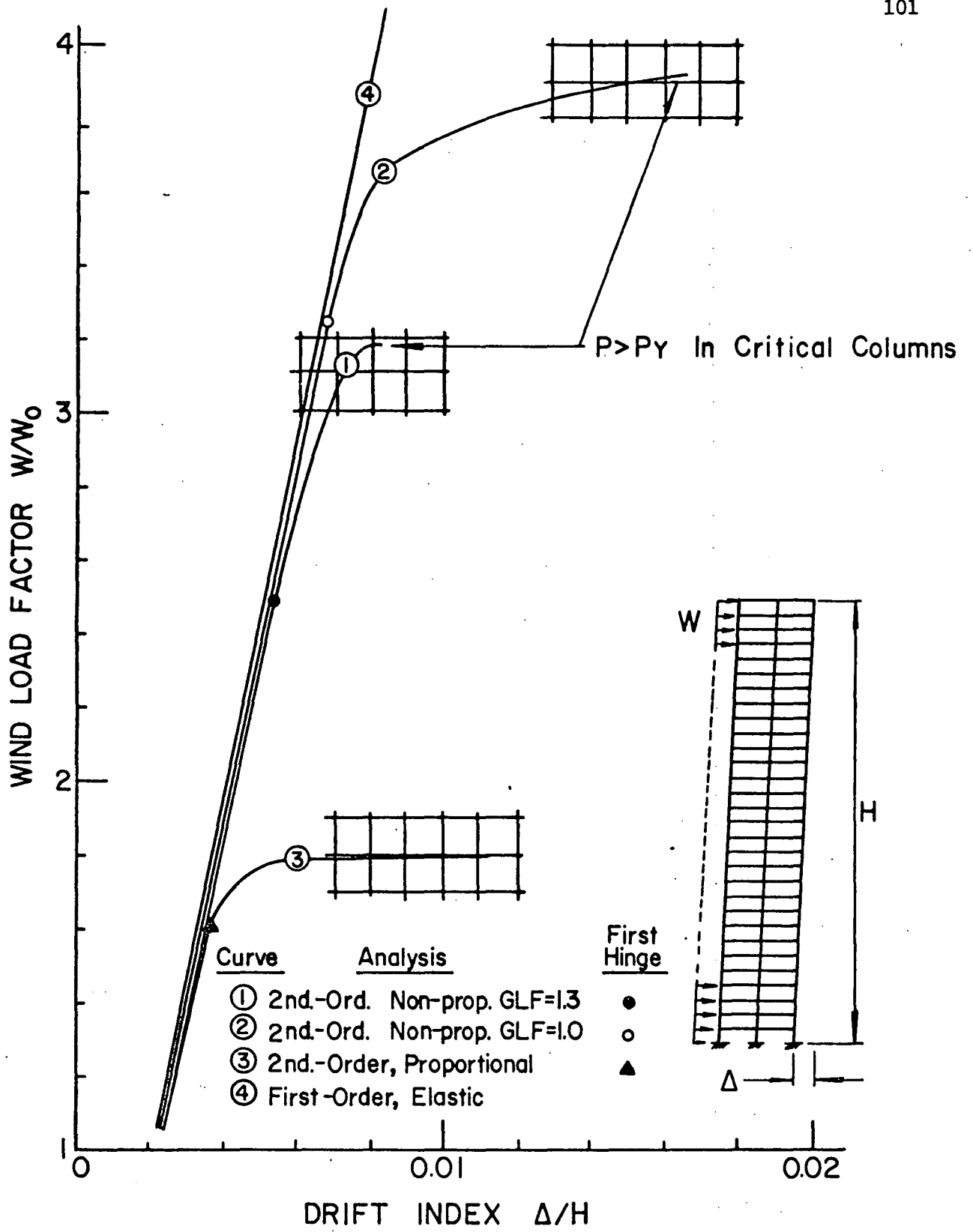


Fig. 16 Load - Drift Curves of Frame 4 - Design IV

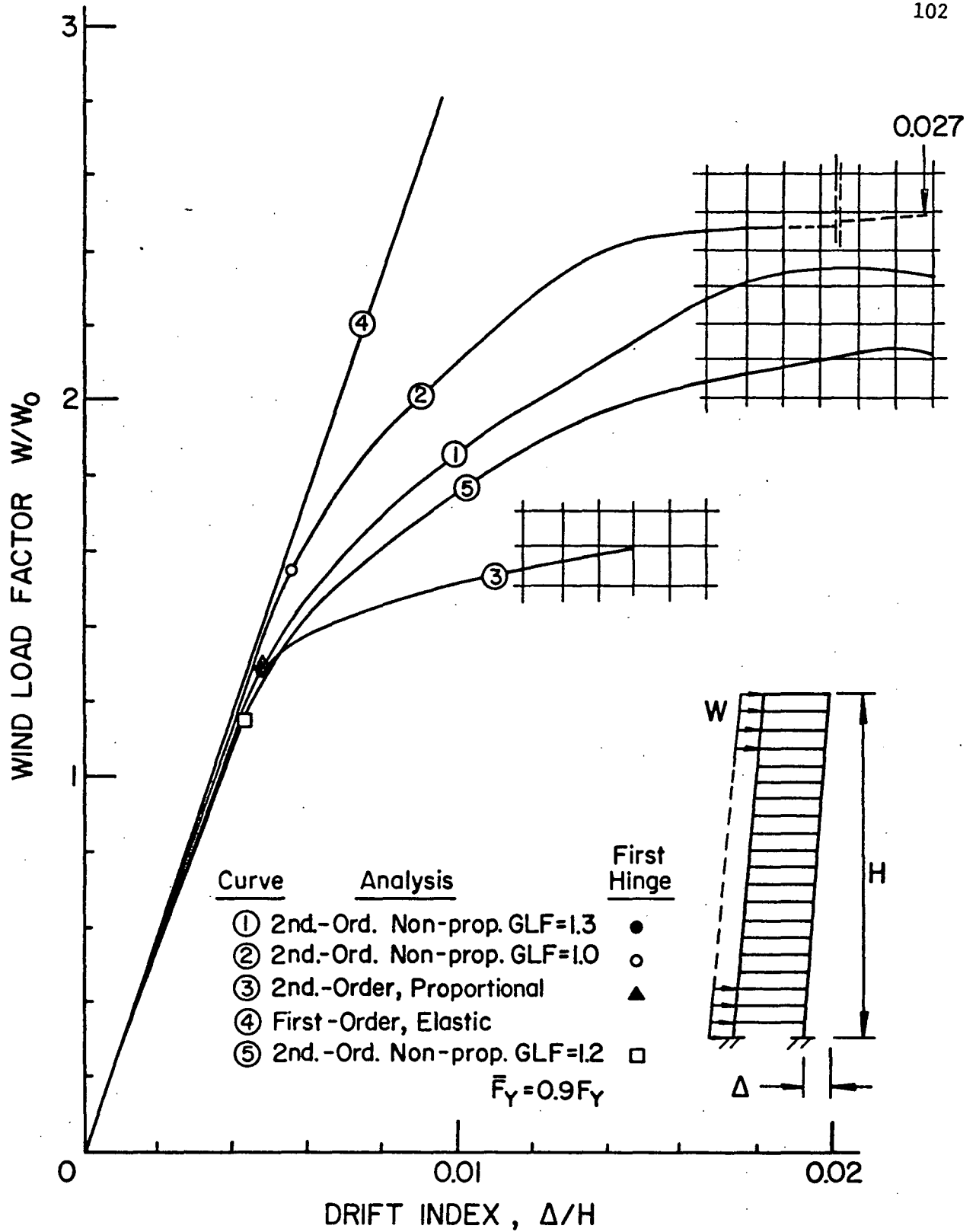


Fig. 17 Load - Drift Curves of Frame 5 - Designs I and III

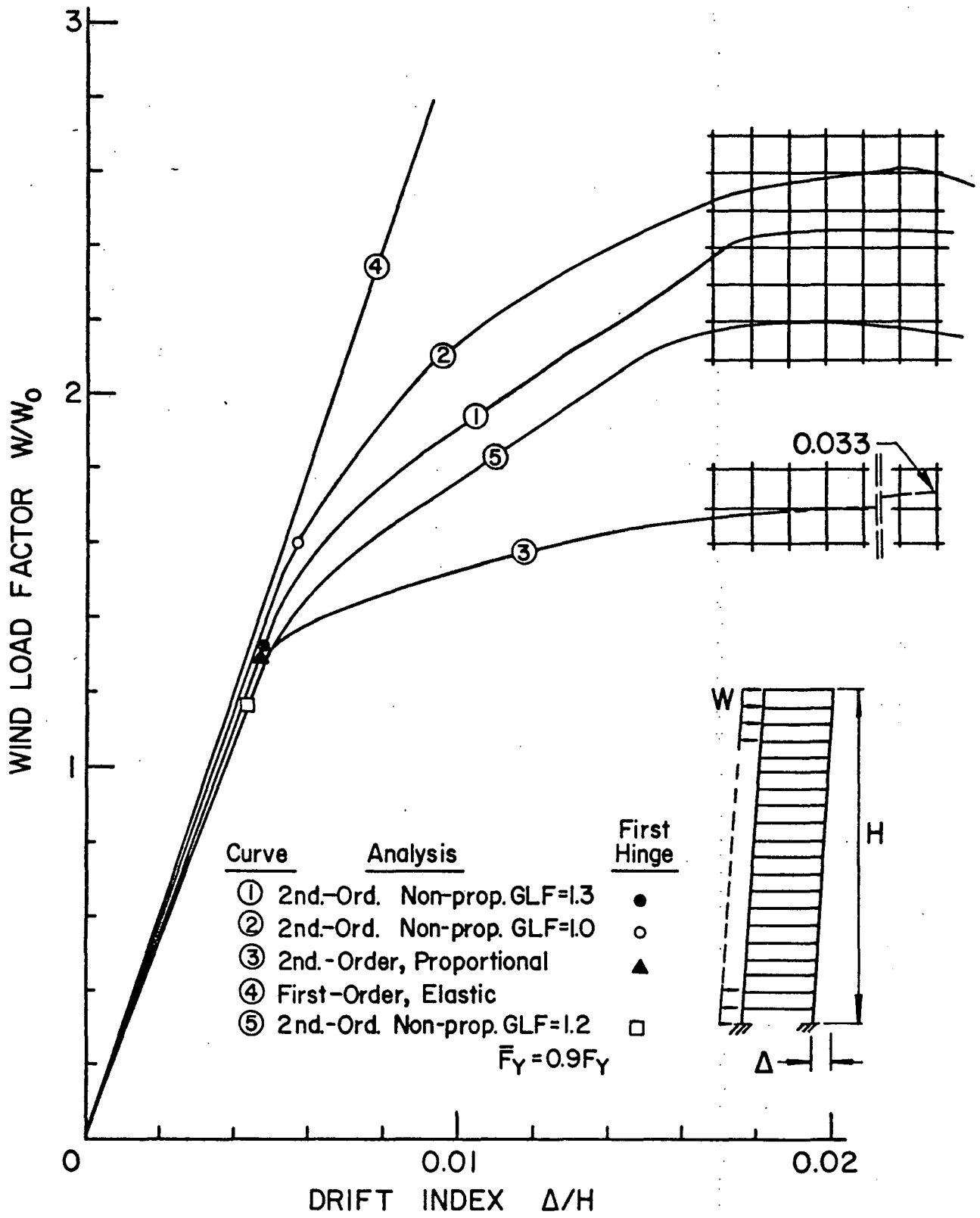


Fig. 18 Load - Drift Curves of Frame 5 - Design II

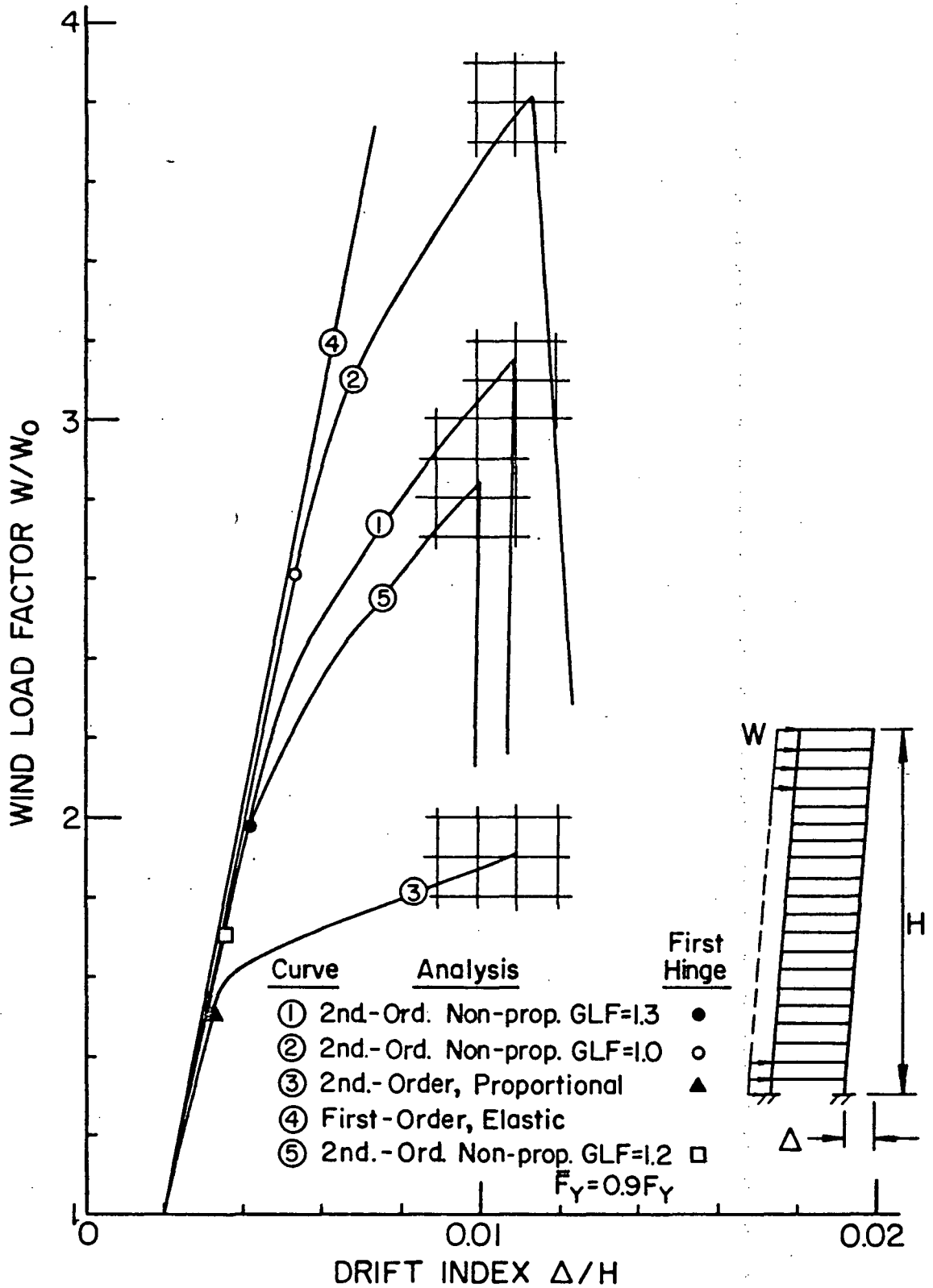


Fig. 19 Load - Drift Curves of Frame 5 - Design IV

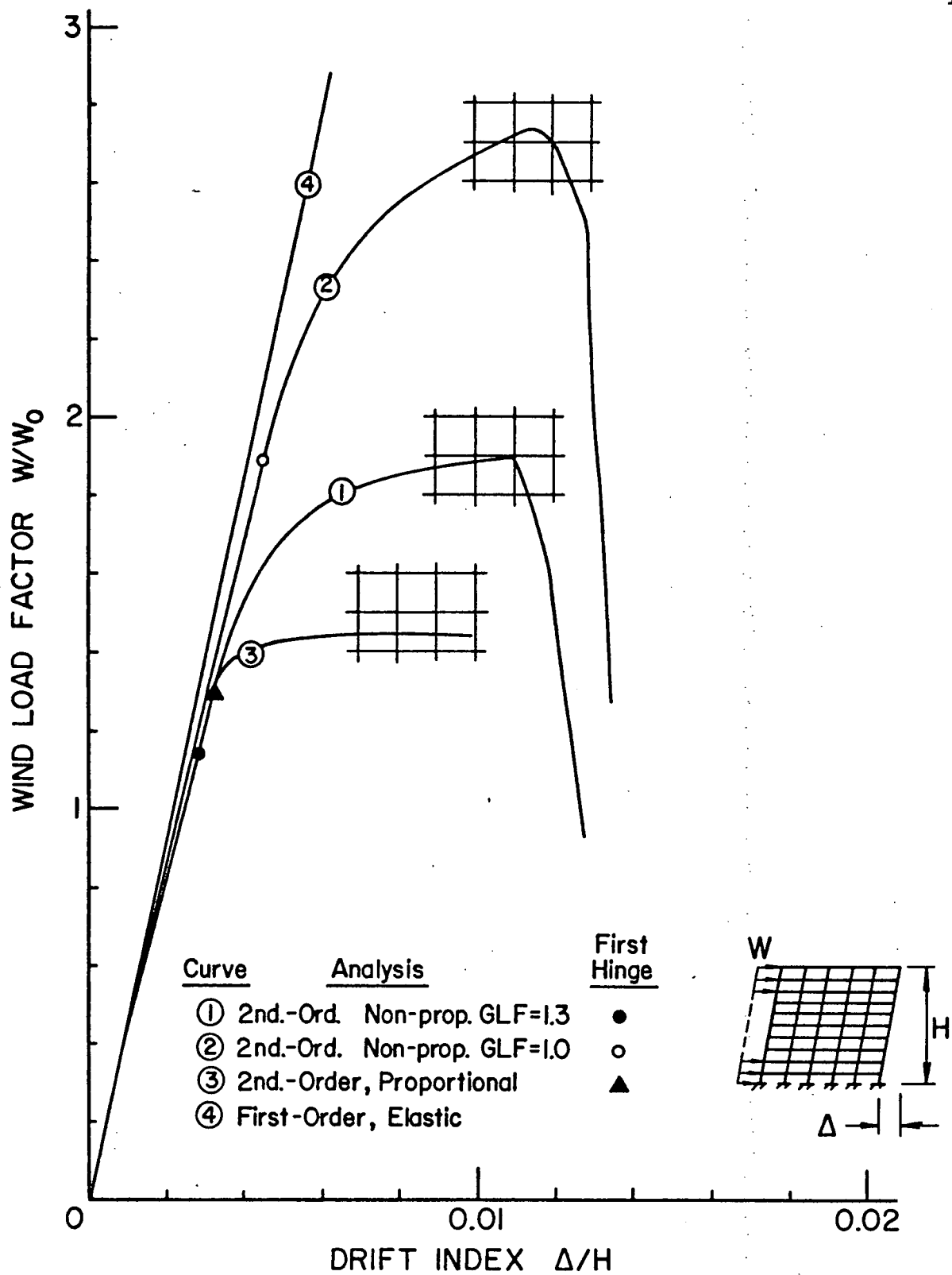


Fig. 20 Load - Drift Curves of Frame 6 - Designs I and IV

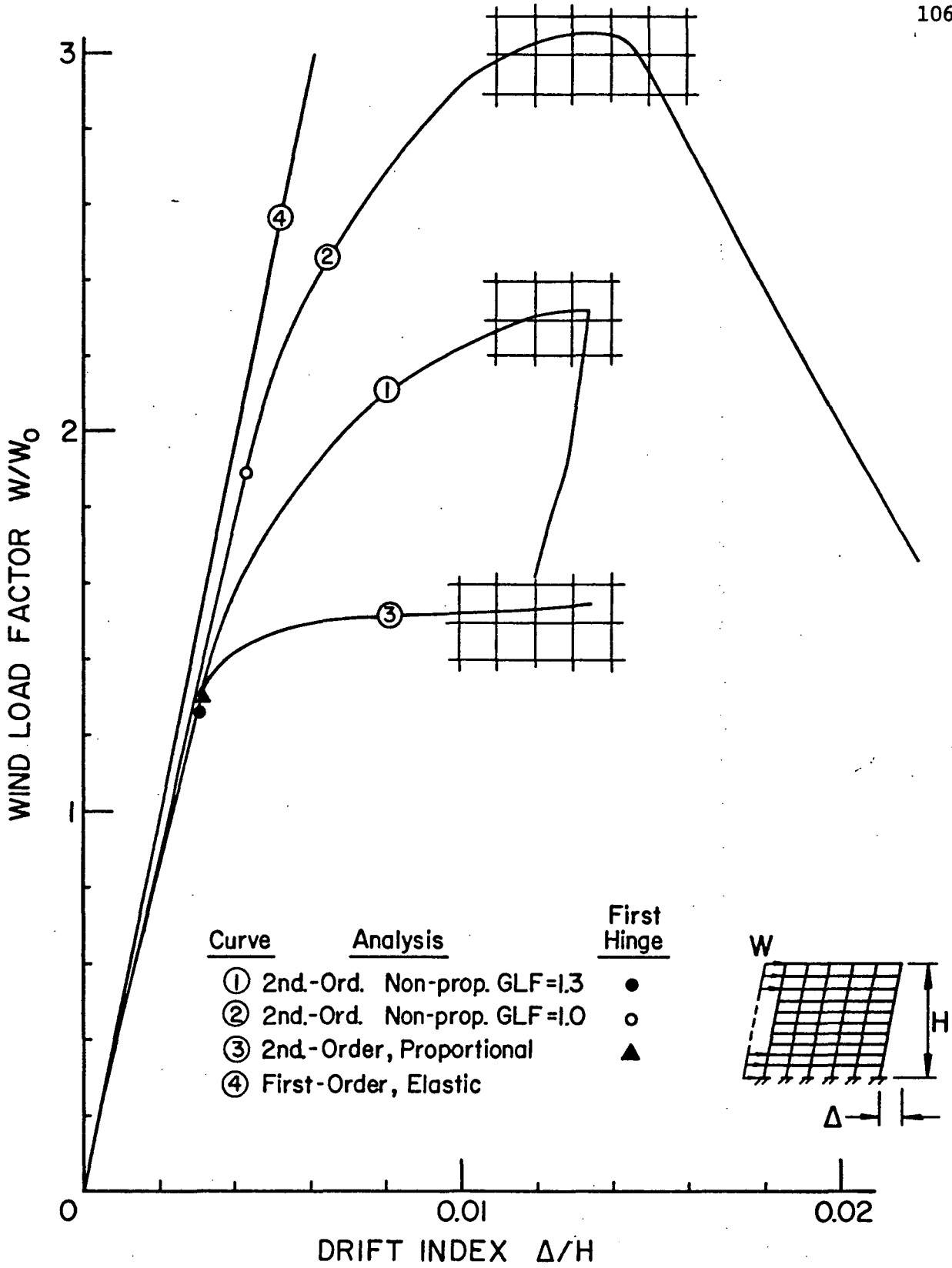


Fig. 21 Load - Drift Curves of Frame 6 - Design II

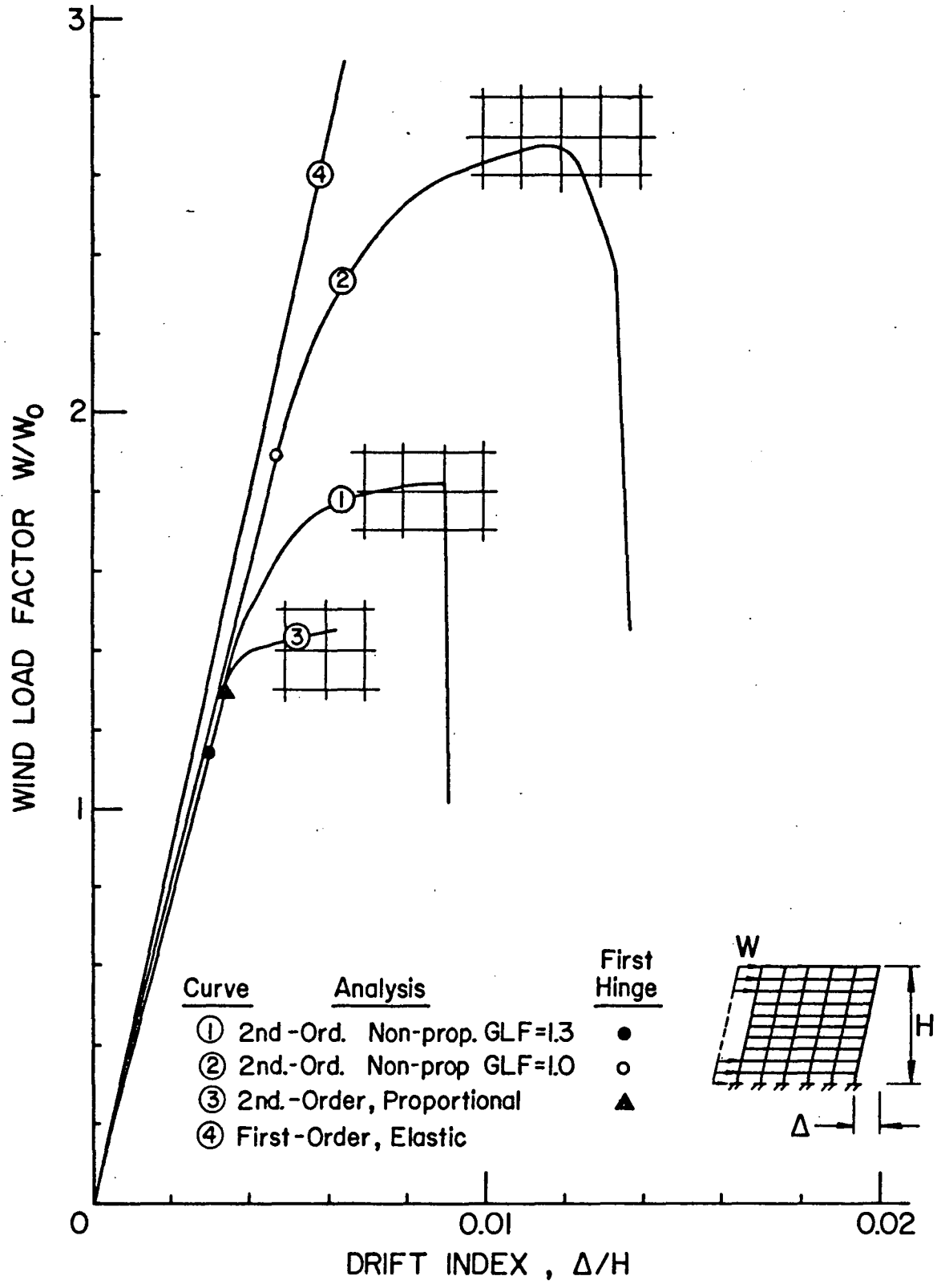


Fig. 22 Load - Drift Curves of Frame 6 - Design III

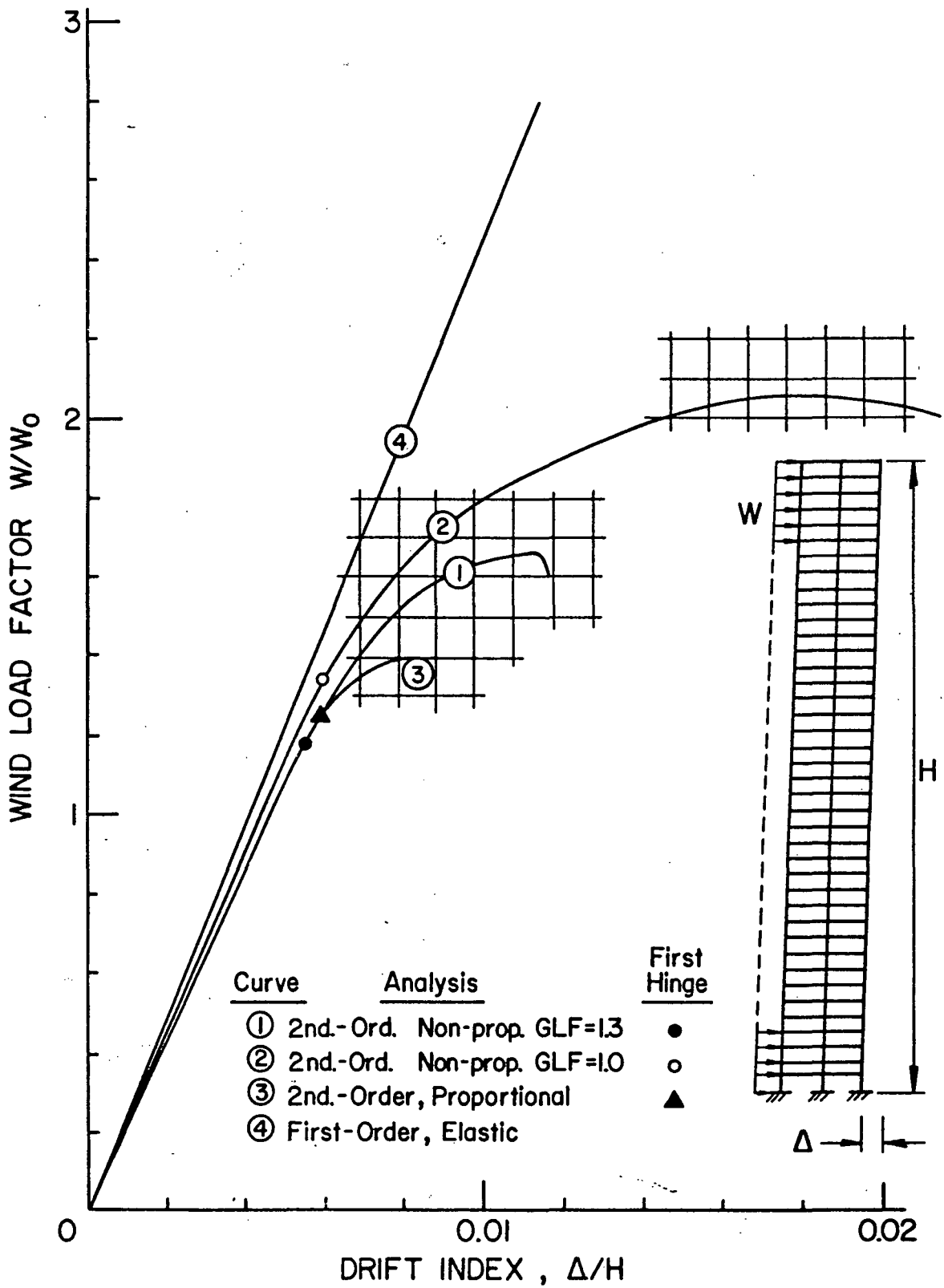


Fig. 23 Load - Drift Curves of Frame 7 - Designs I and III

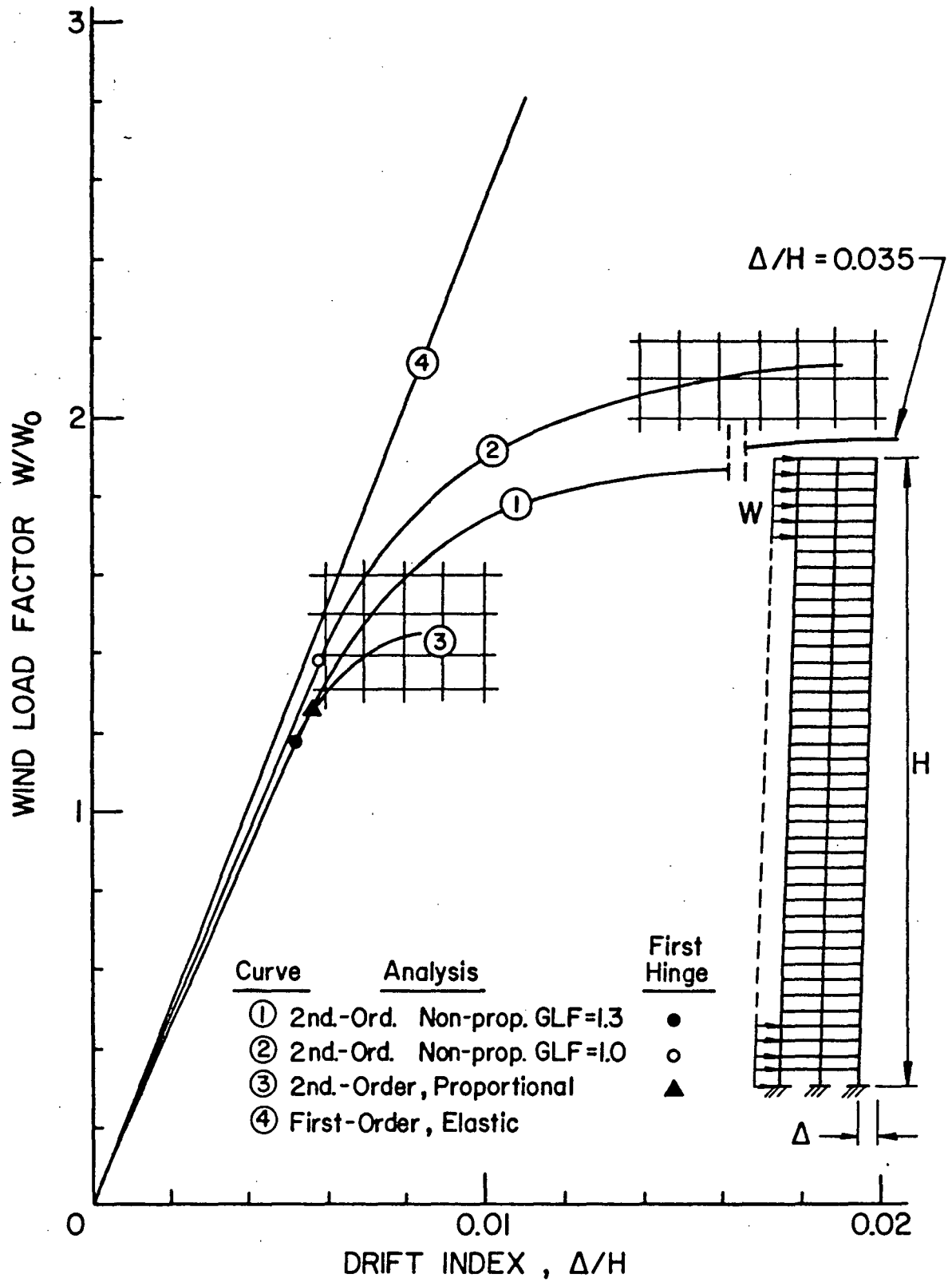


Fig. 24 Load - Drift Curves of Frame 7 - Design II

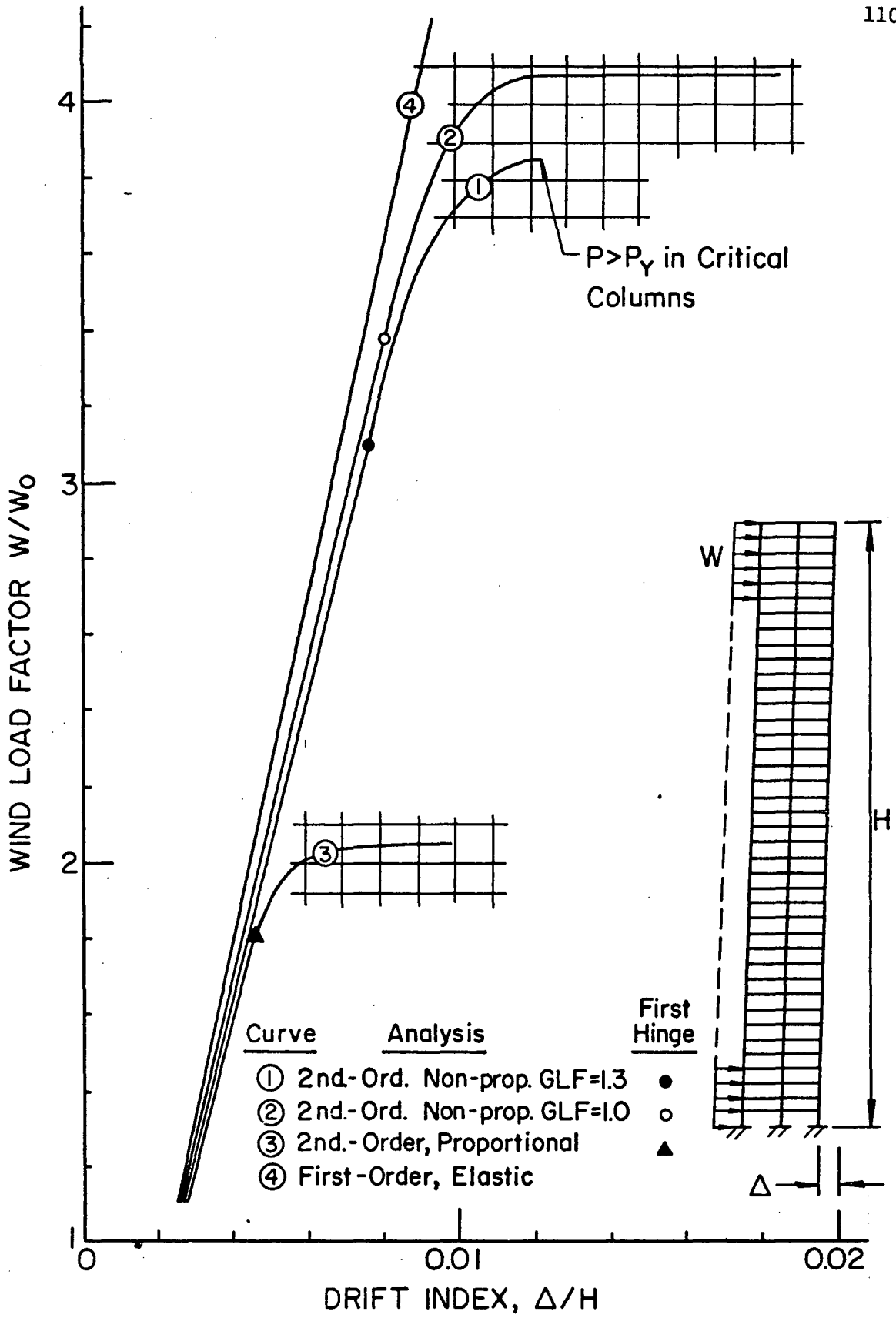


Fig. 25 Load - Drift Curves of Frame 7 - Design IV

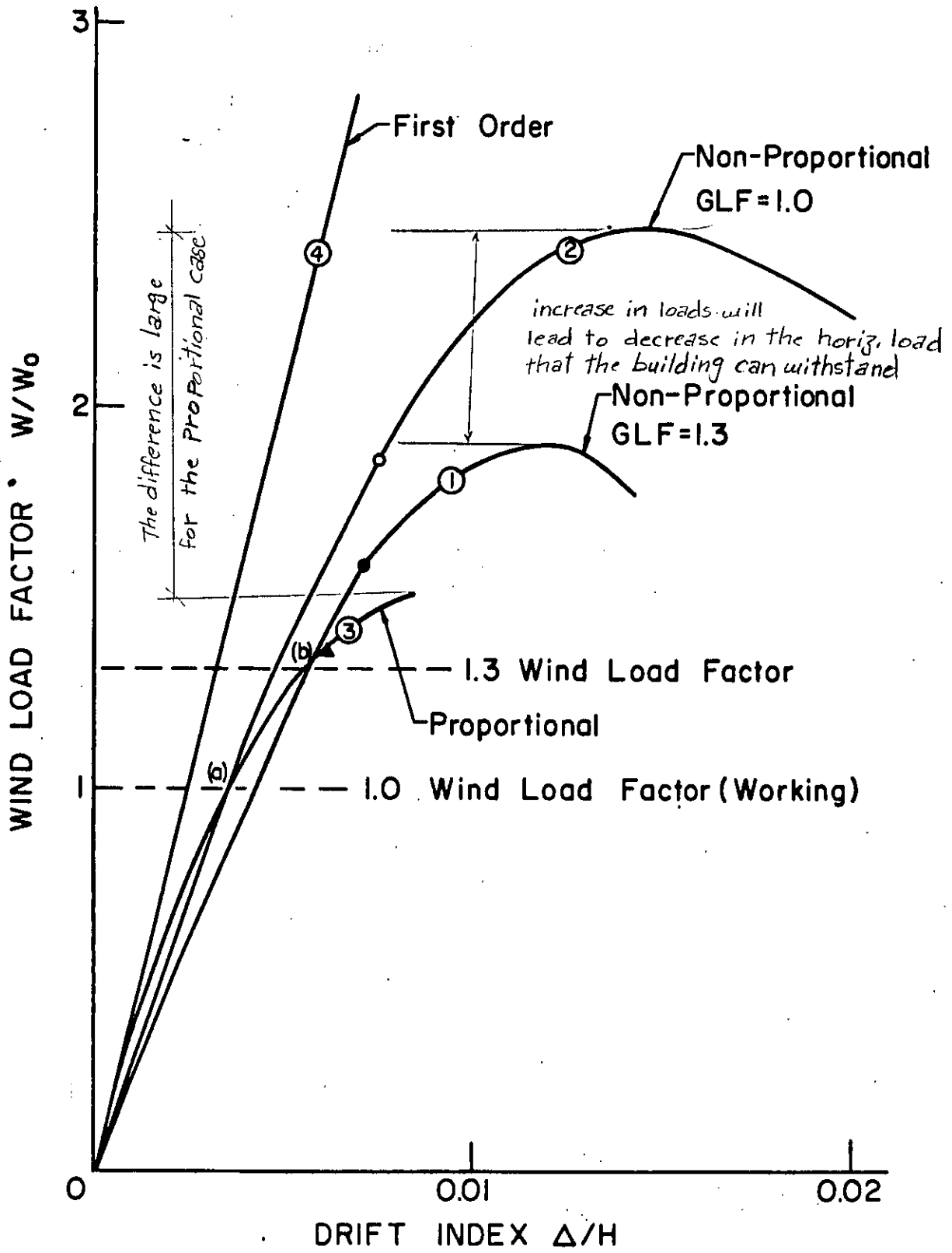


Fig. 26 Relationships Between Load-Drift Curves Determined by Proportional and Nonproportional Load Analysis

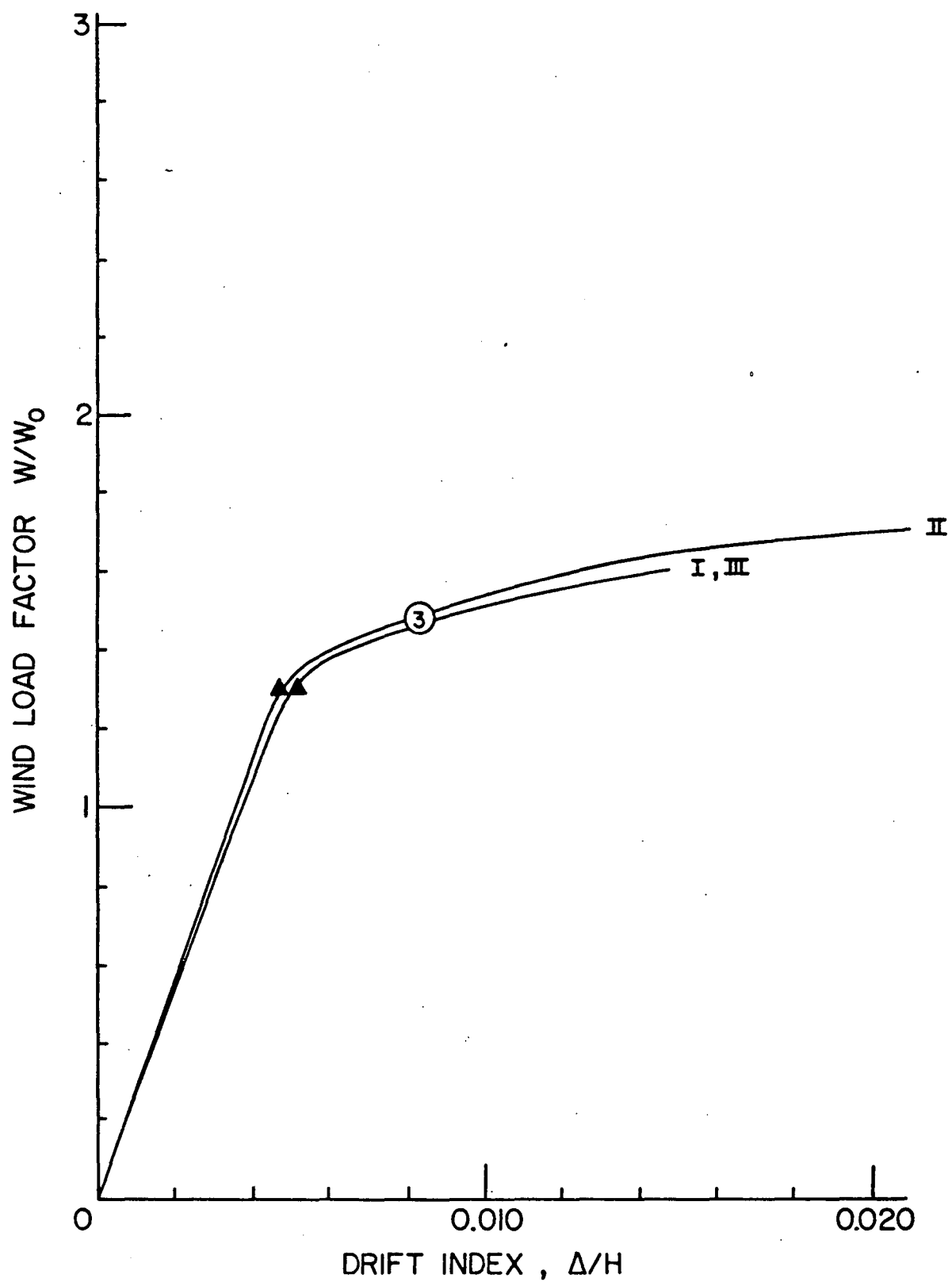


Fig. 27 Comparison of Load - Drift Curves of
Frame 5 - Designs I, II and III (Analysis 3)

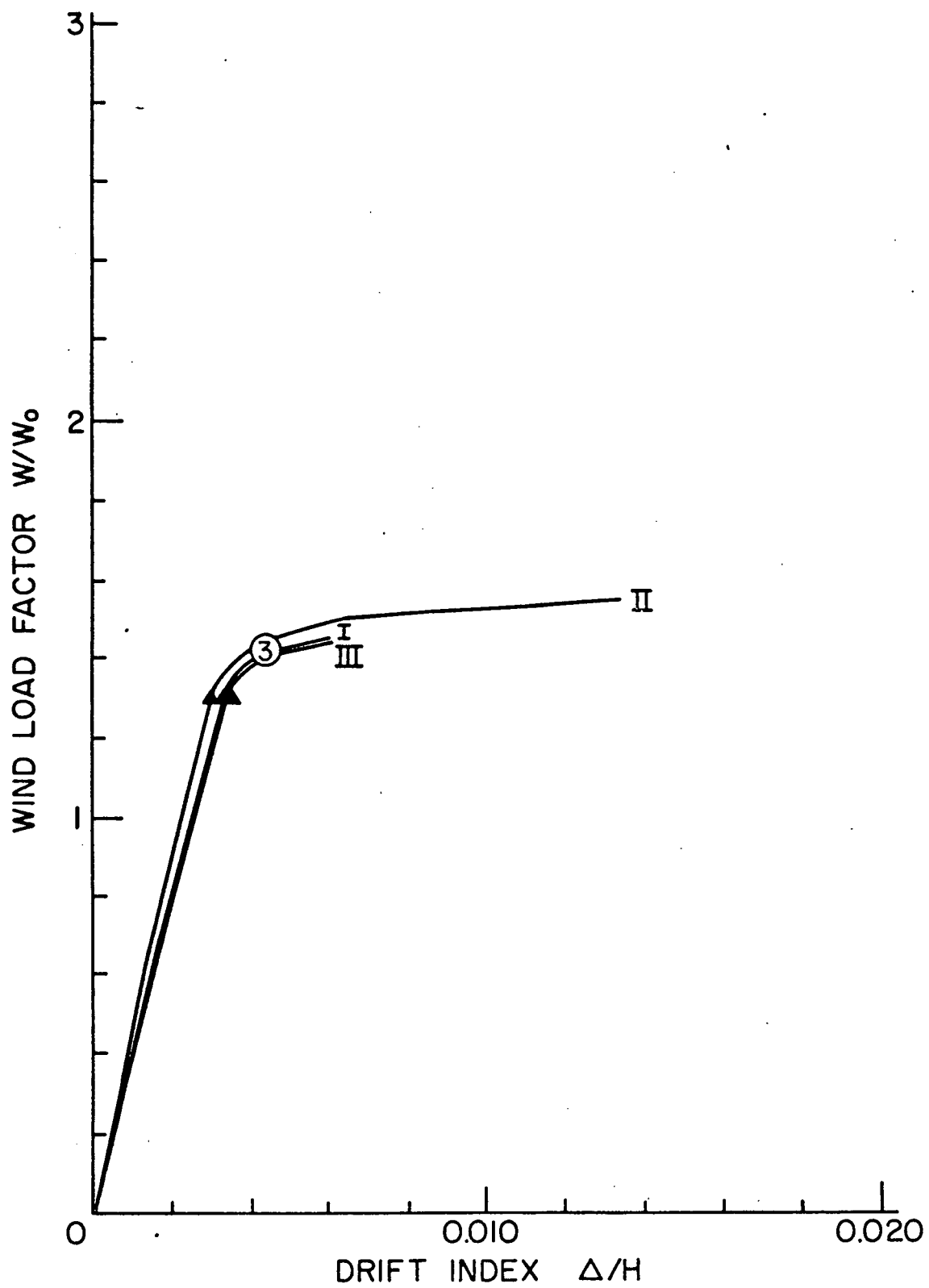


Fig. 28 Comparison of Load - Drift Curves of
Frame 6 - Designs I, II and III (Analysis 3)

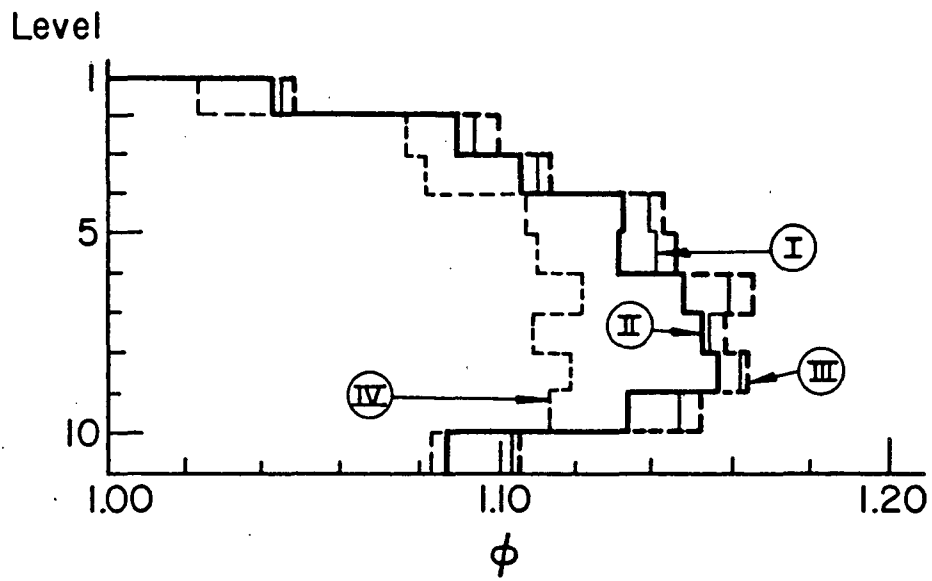


Fig. 29 Story P-Delta Moment Ratios at Factored Loads for Frame 1

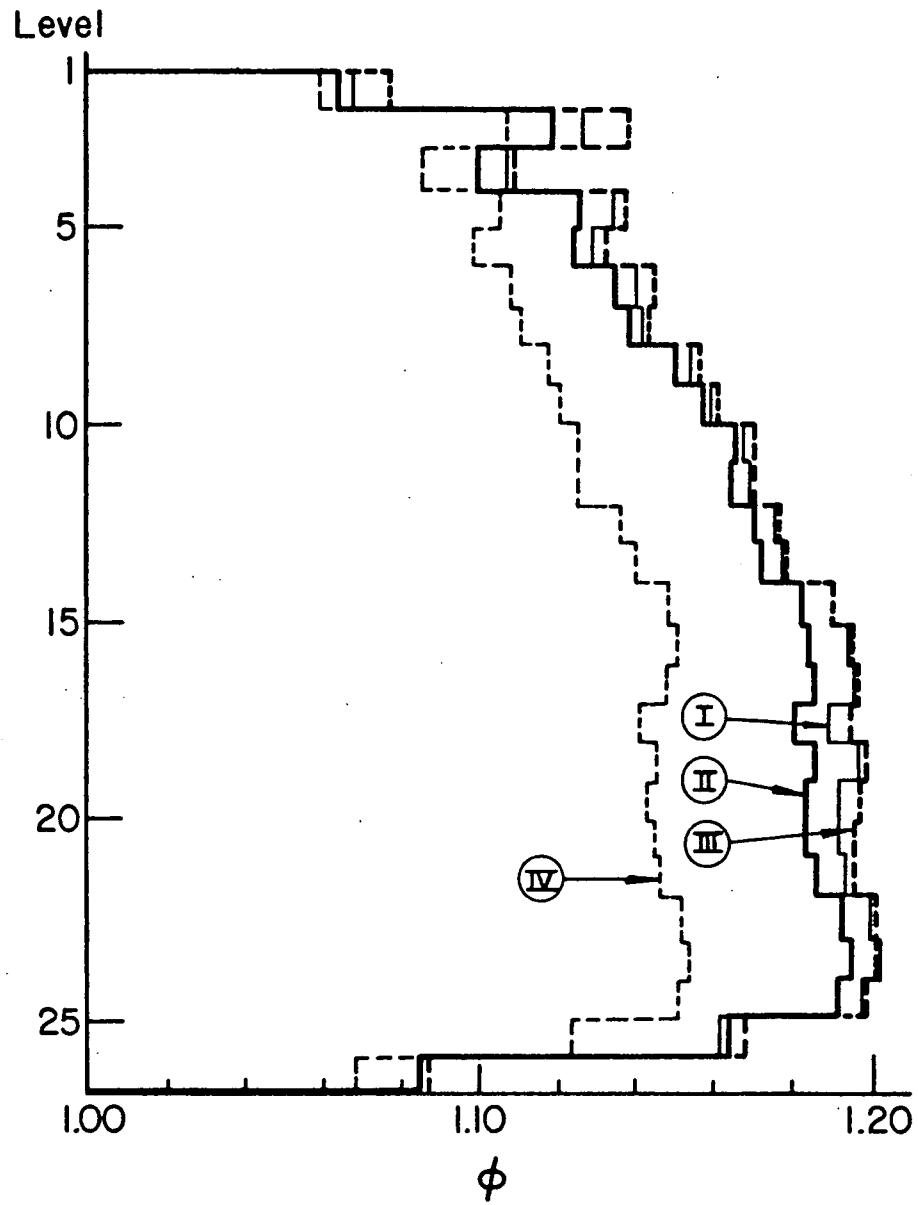


Fig. 30 Story P-Delta Moment Ratios at Factored Loads for Frame 2

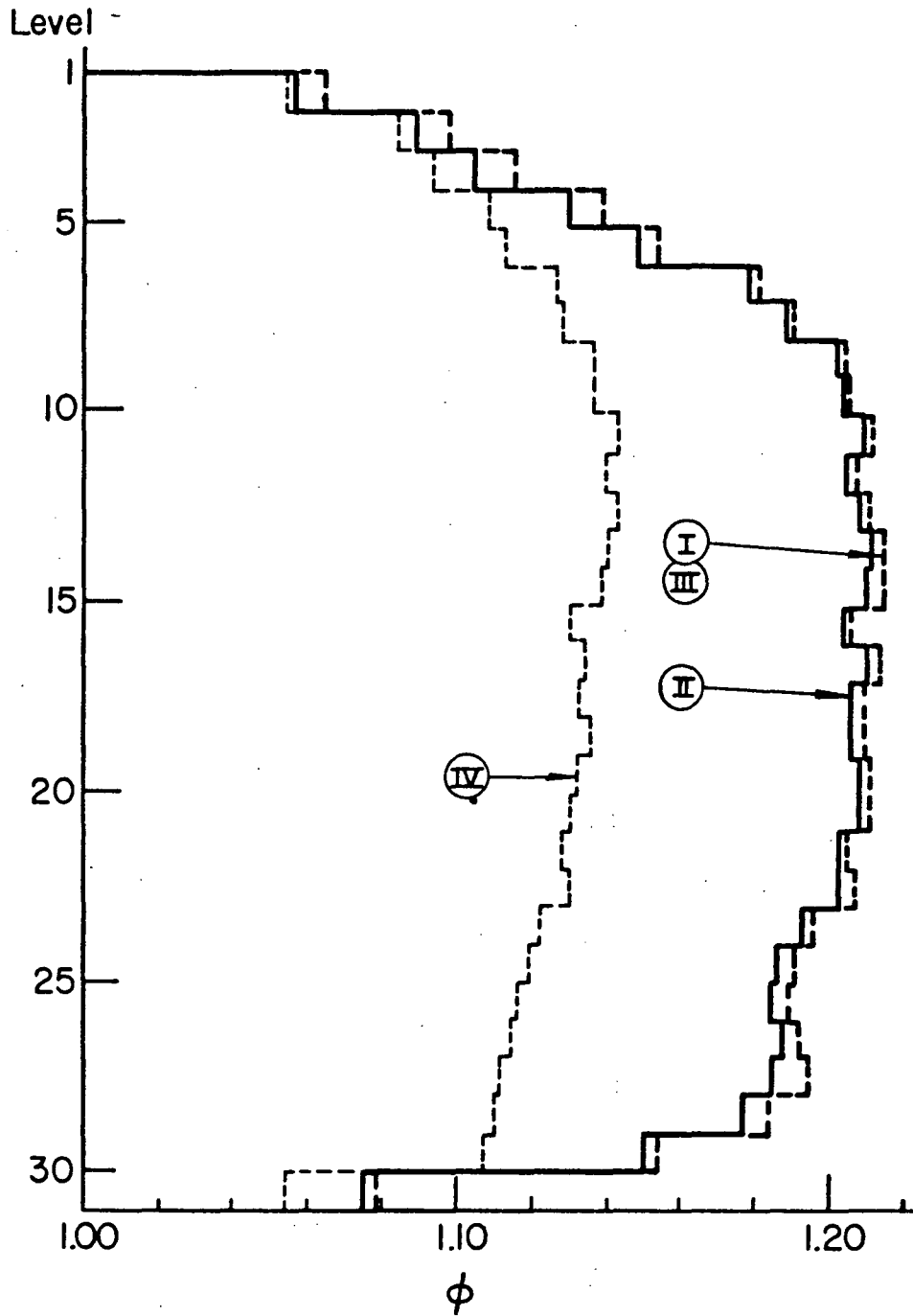


Fig. 31 Story P-Delta Moment Ratios at Factored Loads for Frame 3

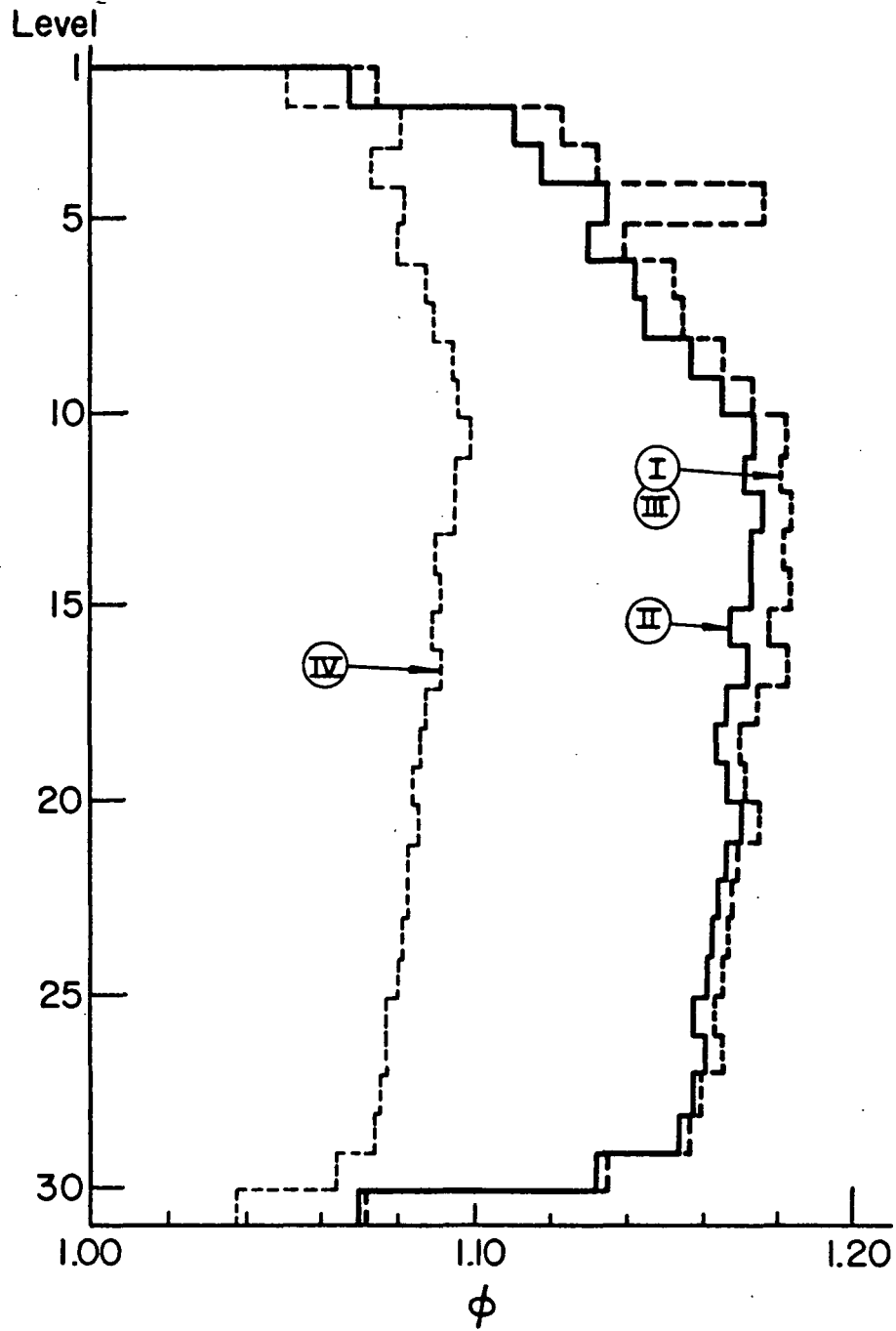


Fig. 32 Story P-Delta Moment Ratios at Factored Loads for Frame 4

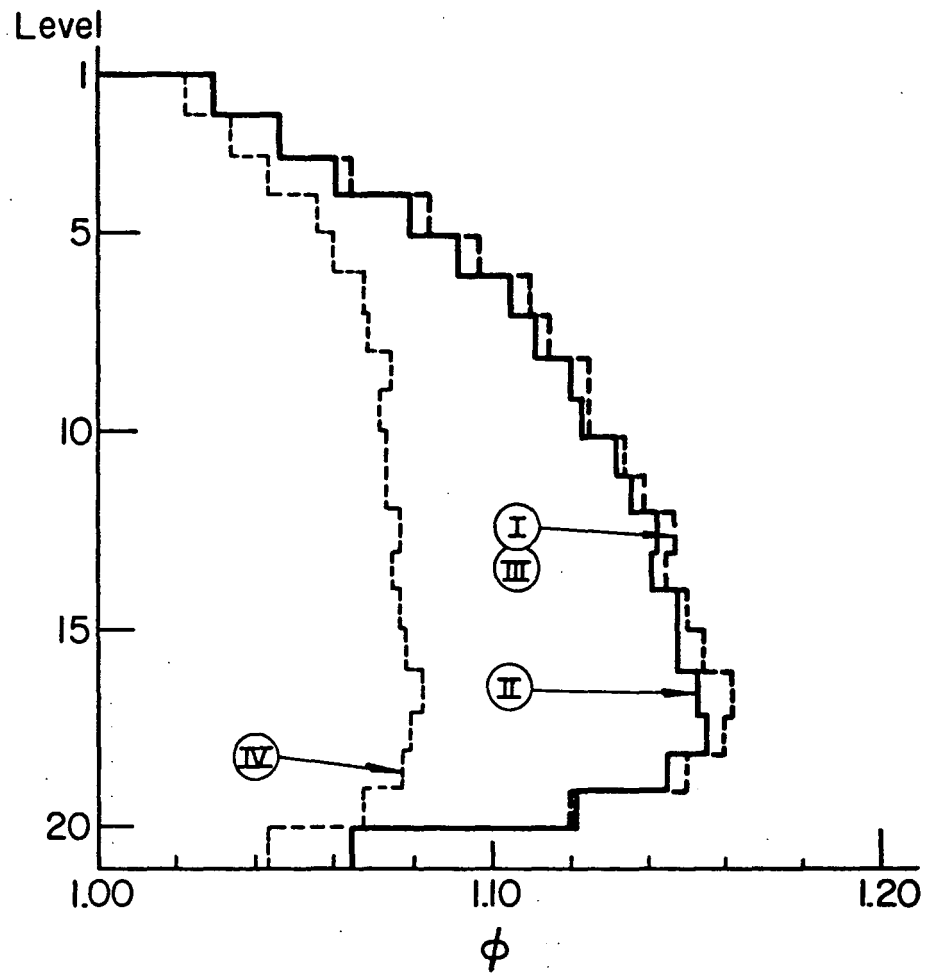


Fig. 33 Story P-Delta Moment Ratios at Factored Loads for Frame 5

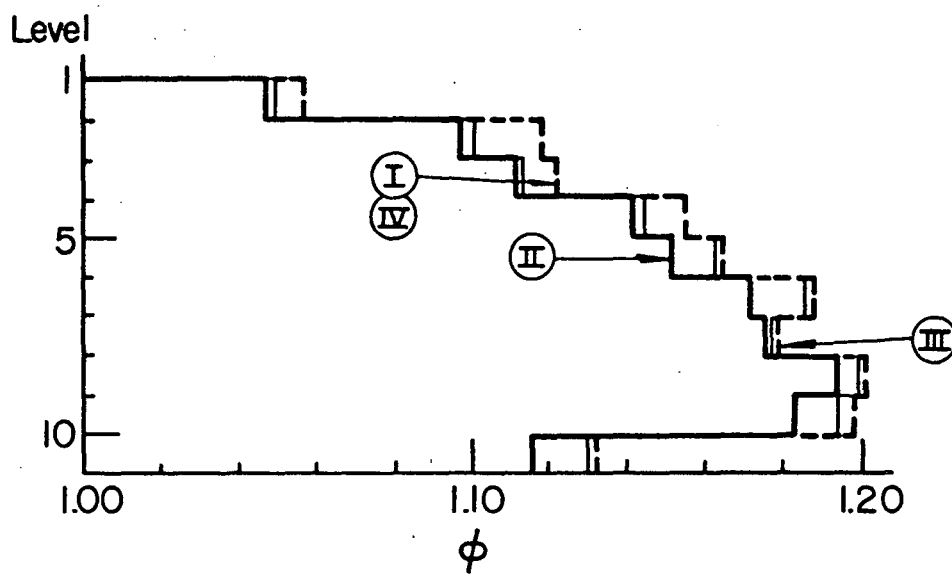


Fig. 34 Story P-Delta Moment Ratios at Factored Loads for Frame 6

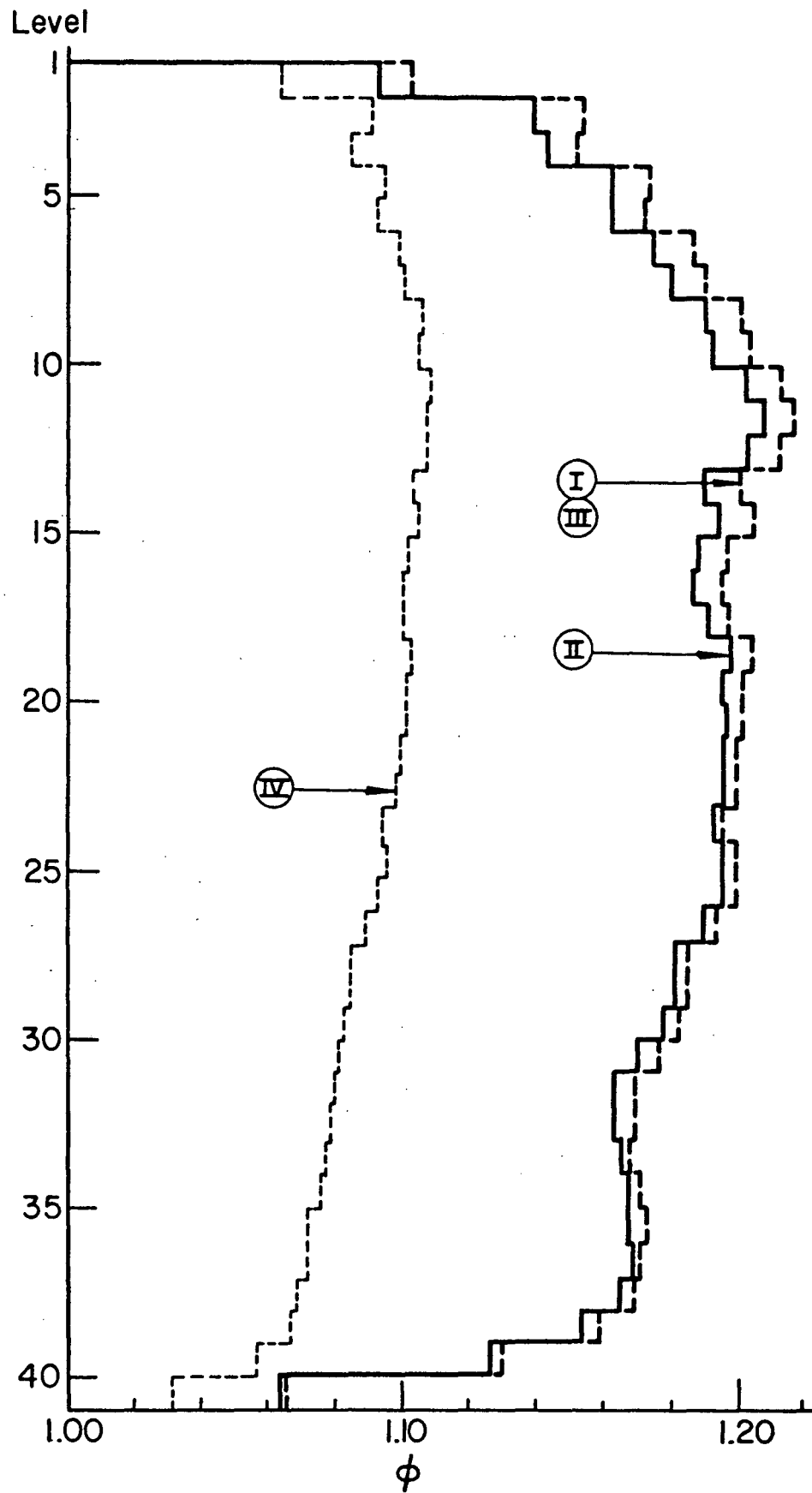


Fig. 35 Story P-Delta Moment Ratios at Factored Loads for Frame 7

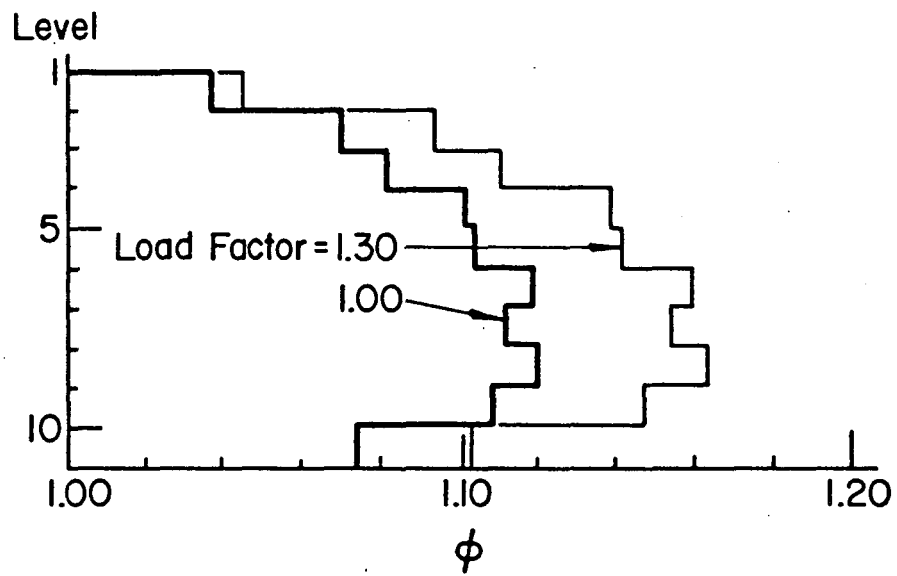


Fig. 36 Comparison of Story P-Delta Moment Ratios at Working and Factored Loads for Frame 1 - Design I

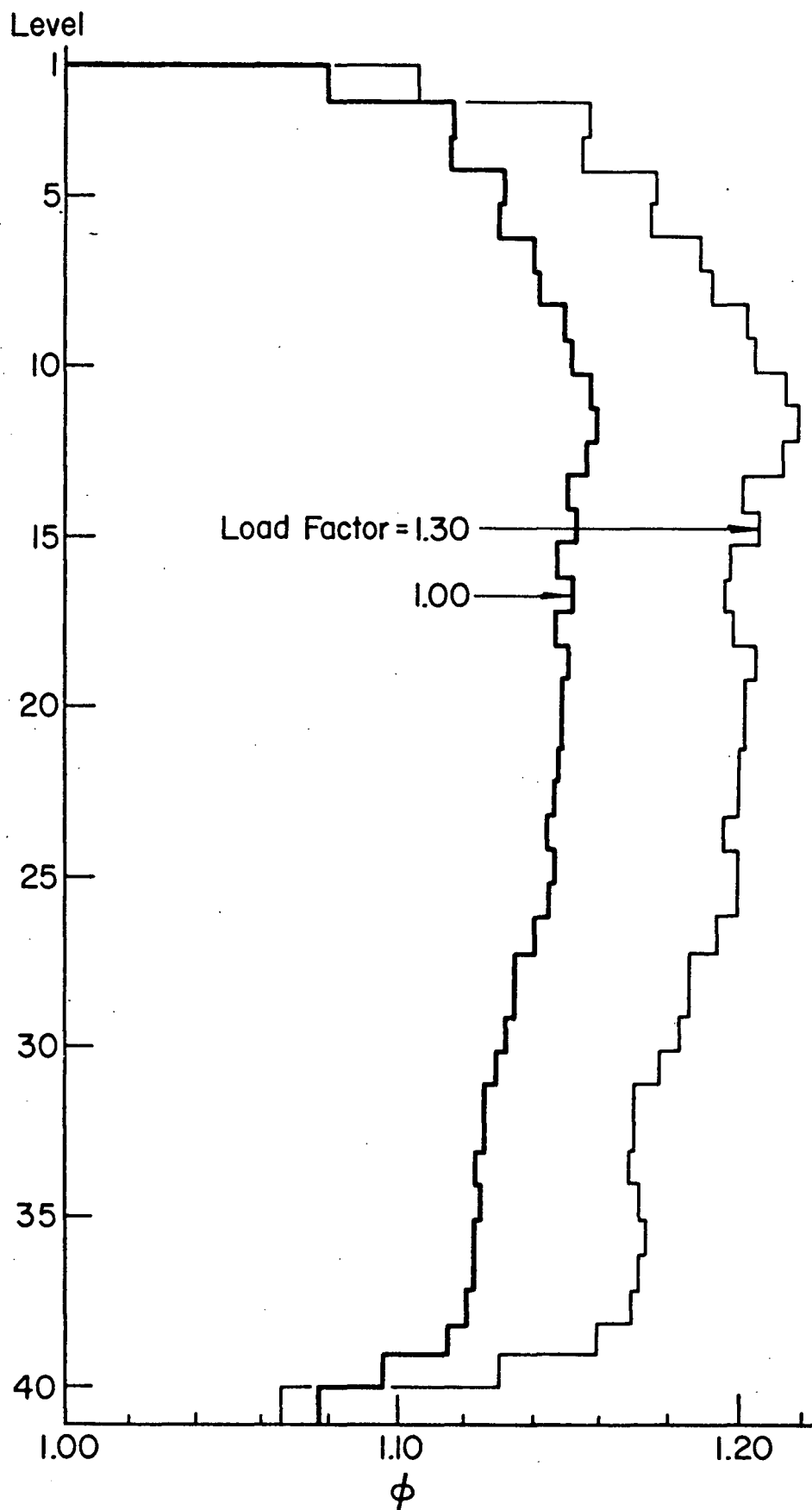


Fig. 37 Comparison of Story P-Delta Moment Ratios at Working and Factored Loads for Frame 7 - Design I

DESIGN I

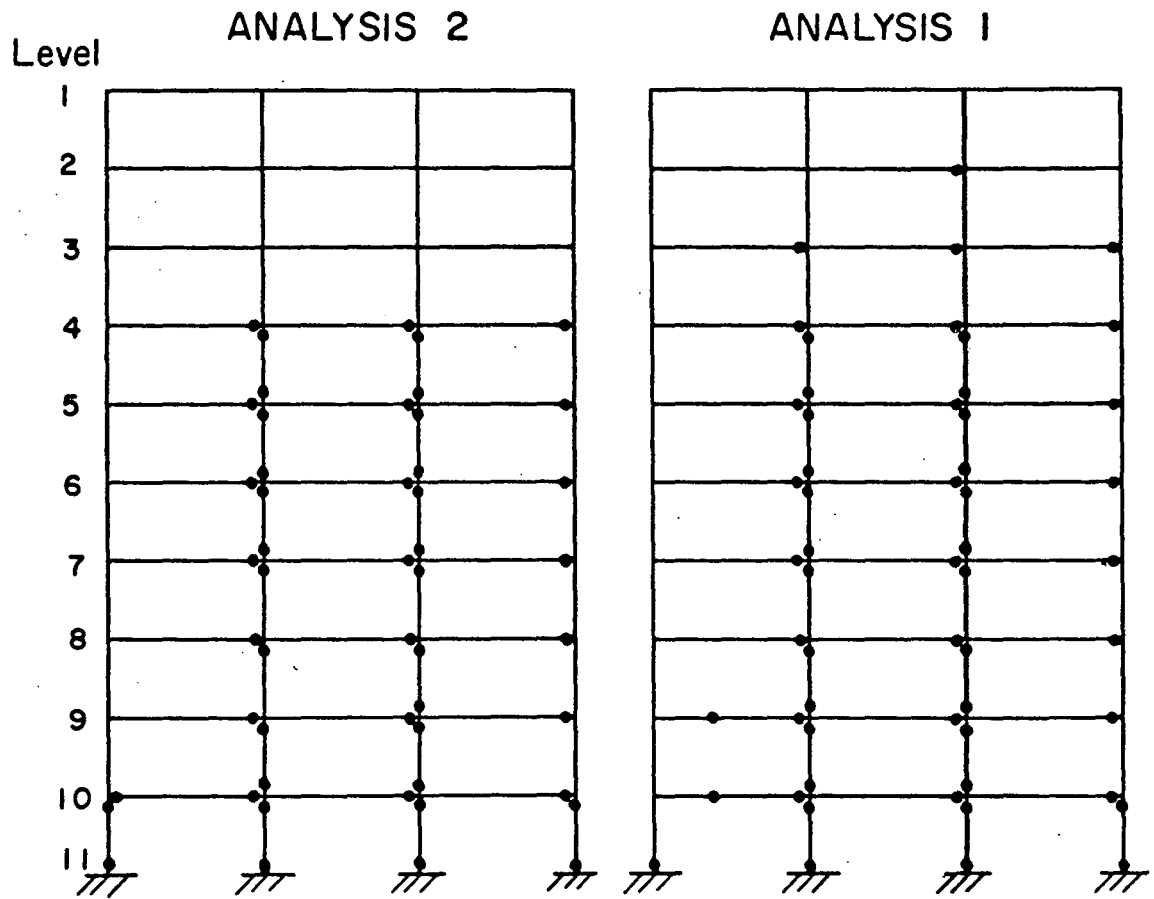


Fig. 38 Frame 1 - Plastic Hinge Patterns

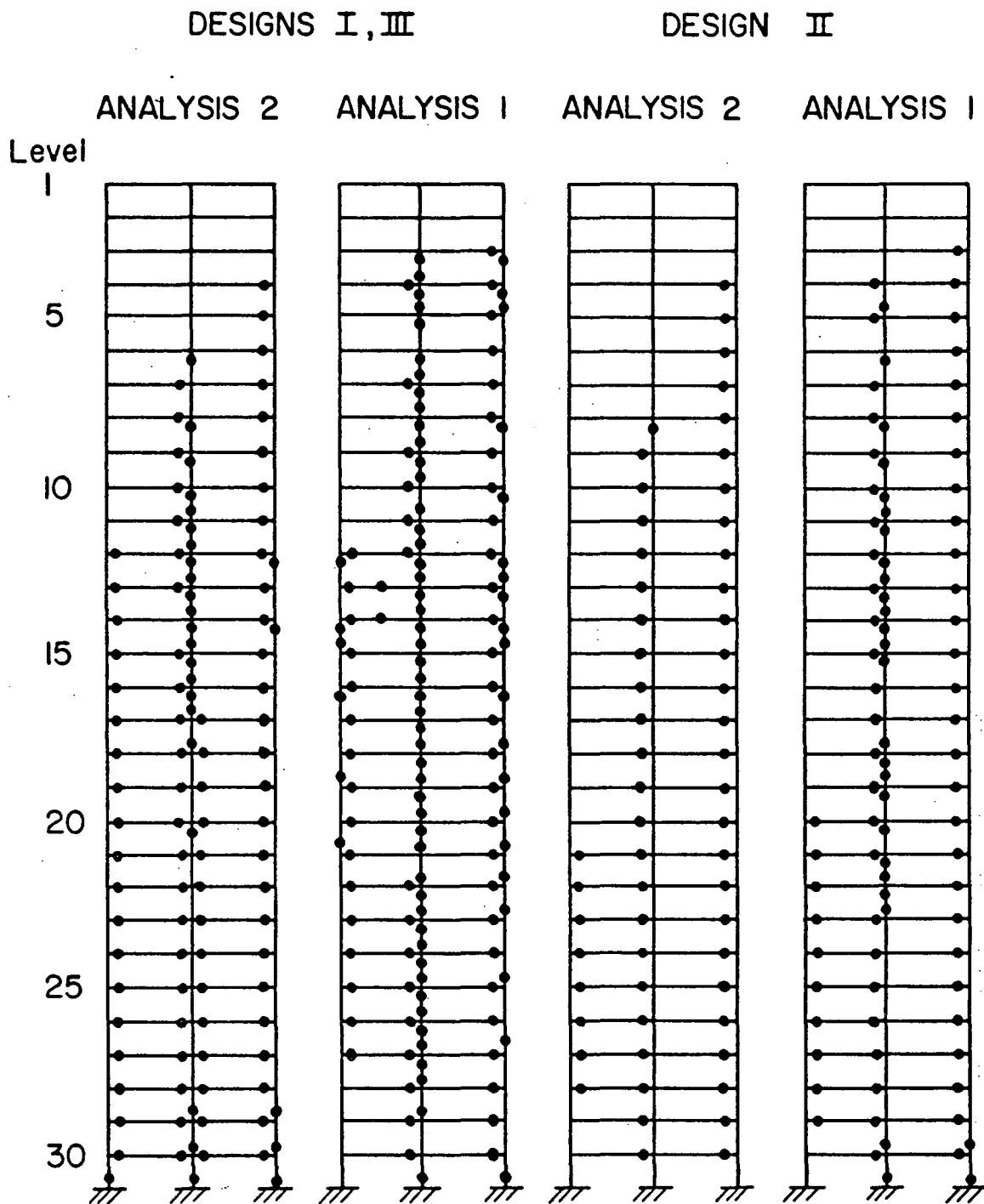


Fig. 39 Frame 4 - Plastic Hinge Patterns

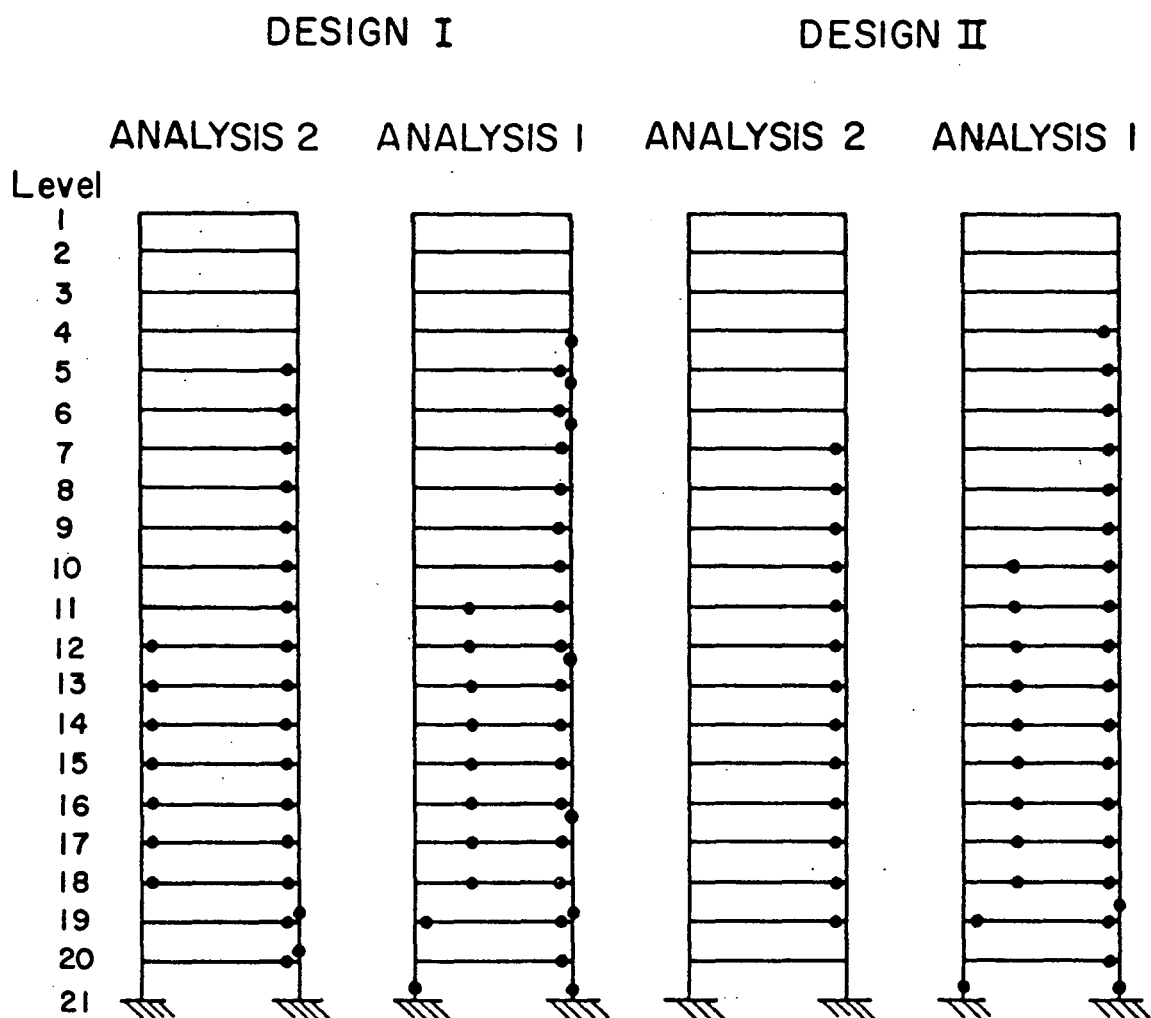


Fig. 40 Frame 5 - Plastic Hinge Patterns

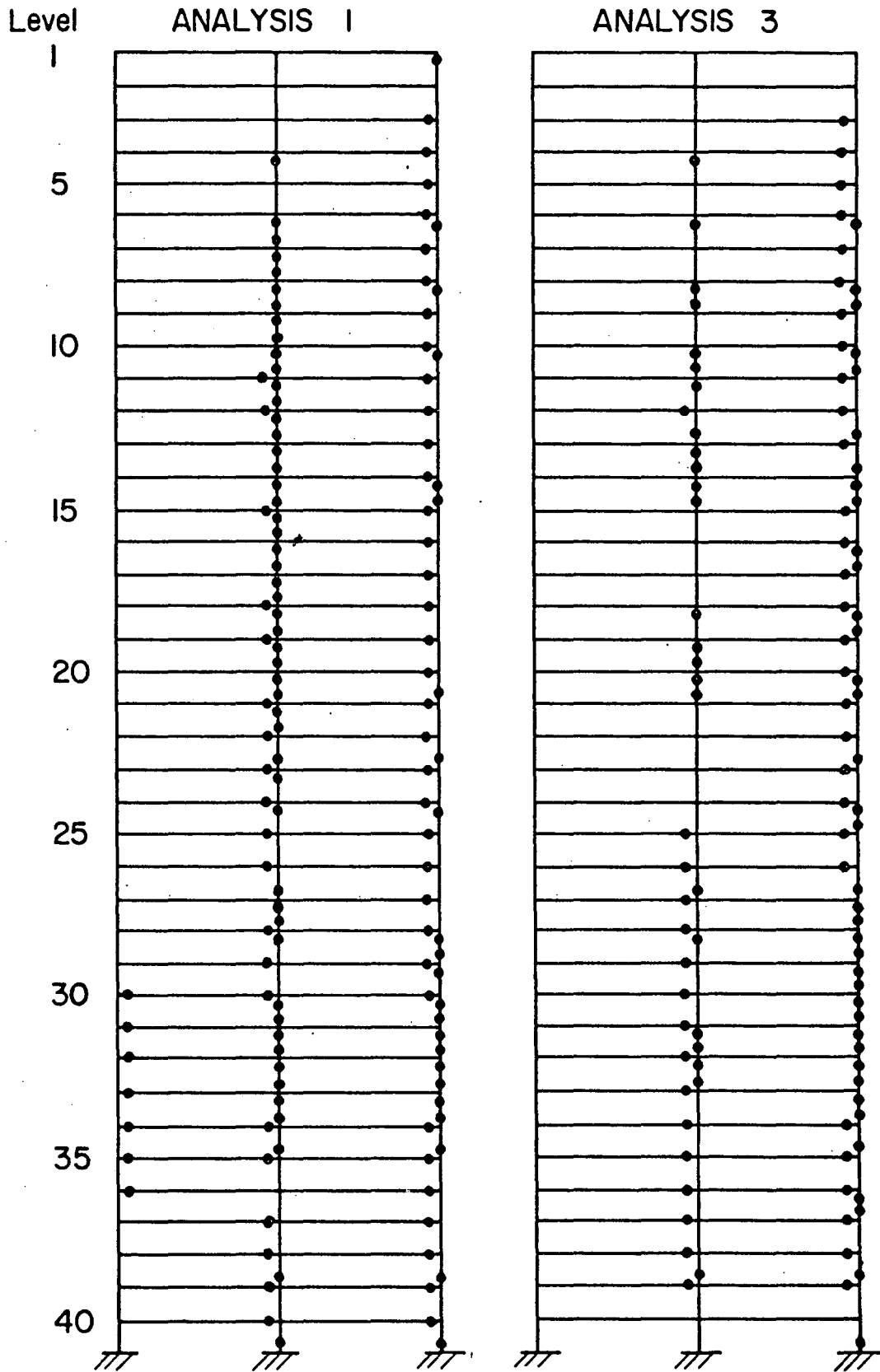


Fig. 41 Frame 7 - Plastic Hinge Patterns

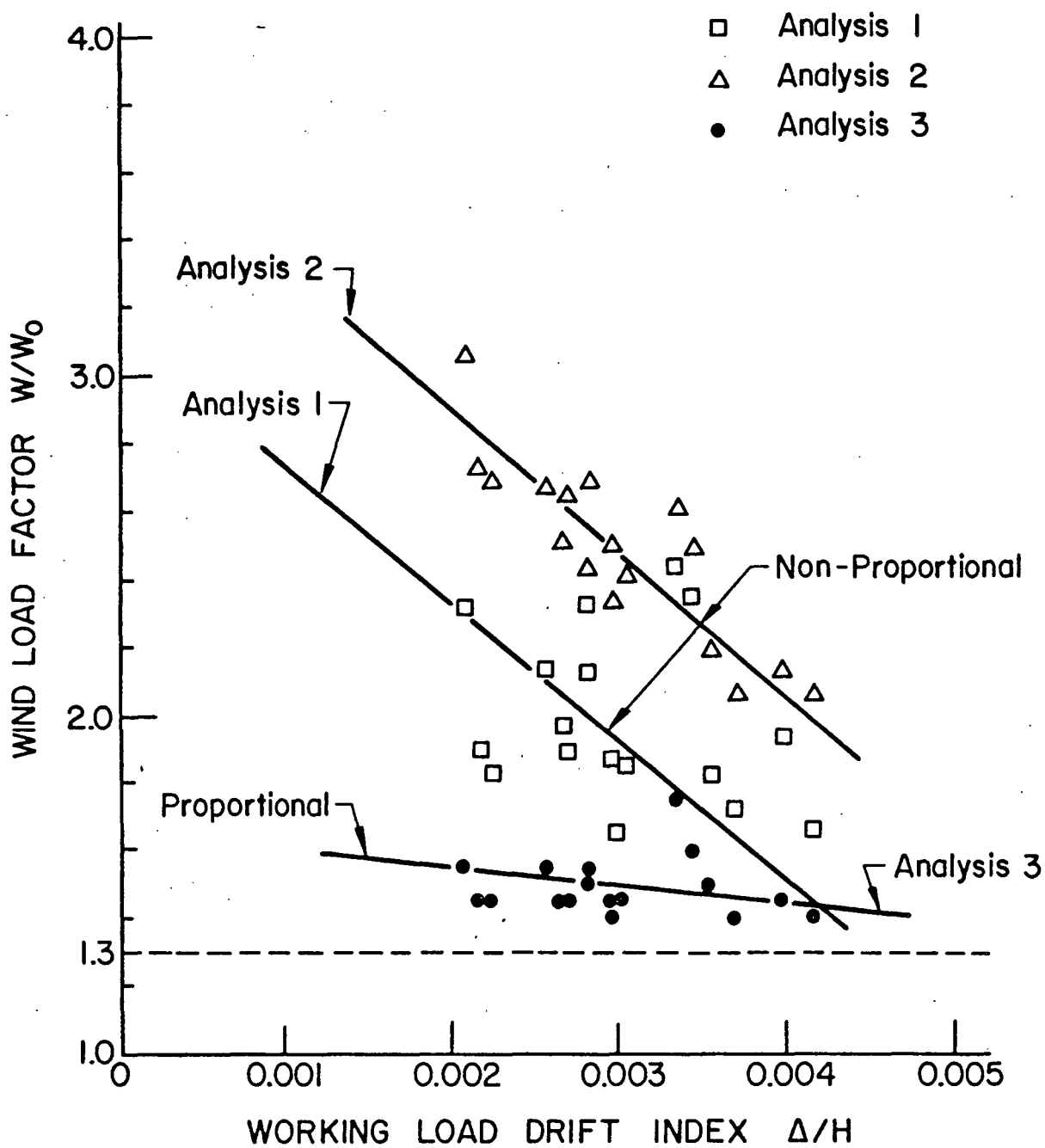
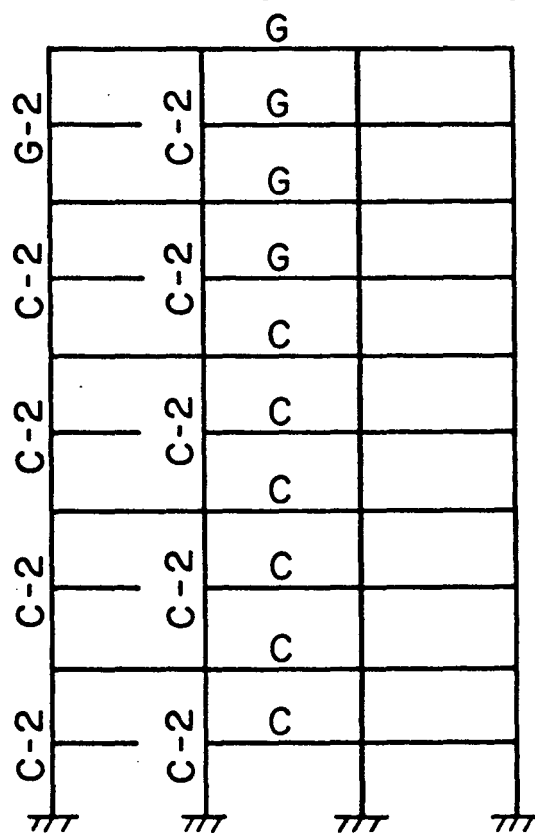
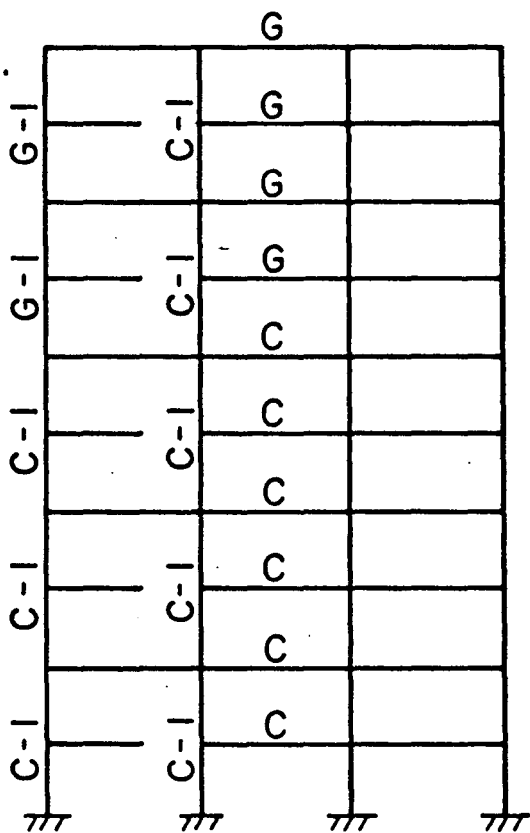


Fig. 42 Relationships Between Maximum Strength and Working Load Drift for Stress-Controlled Designs



G: Gravity Load

C: Combined Load

I: Equation I

2: Equation 2

Fig. 43 Loading Conditions and Column Formulas Governing Member Sizes in Frame 1, Designs II and III

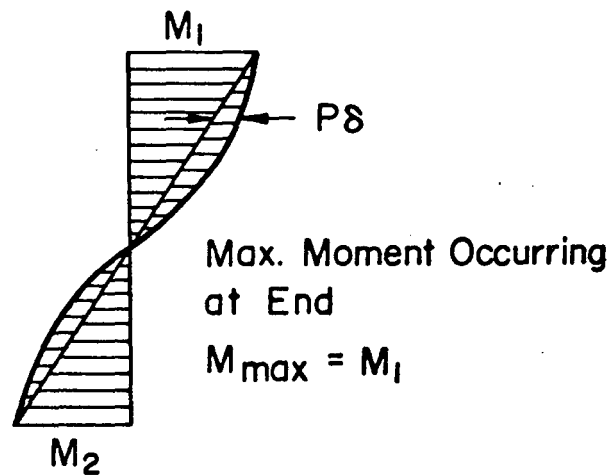
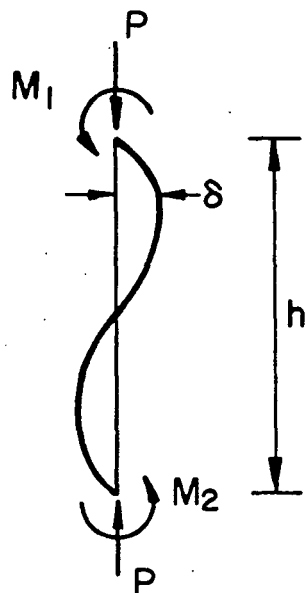


Fig. 44 Maximum Moment in Column Bent in Double Curvature

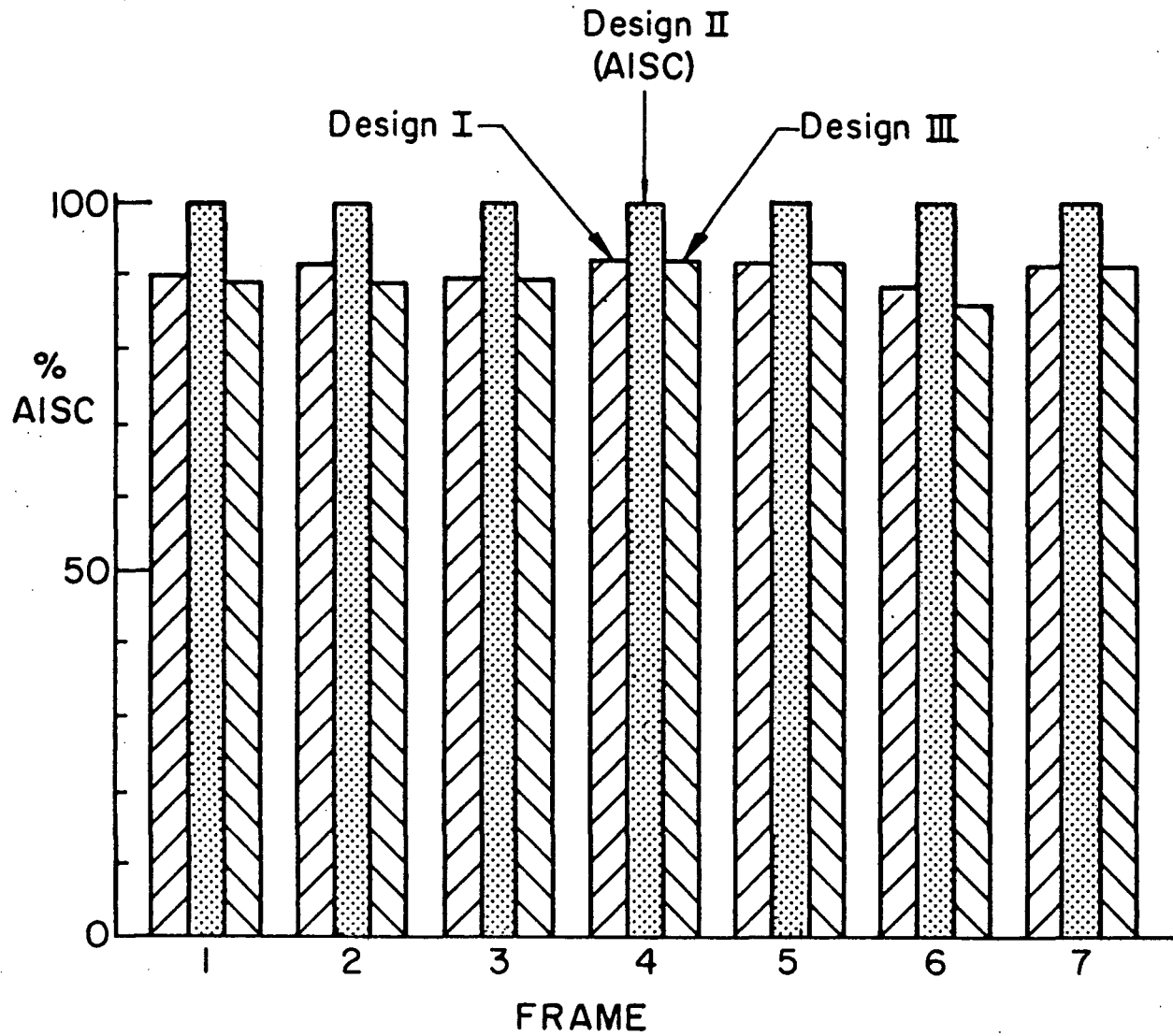


Fig. 45 Relative Column Weights of the Three Stress - Controlled Designs

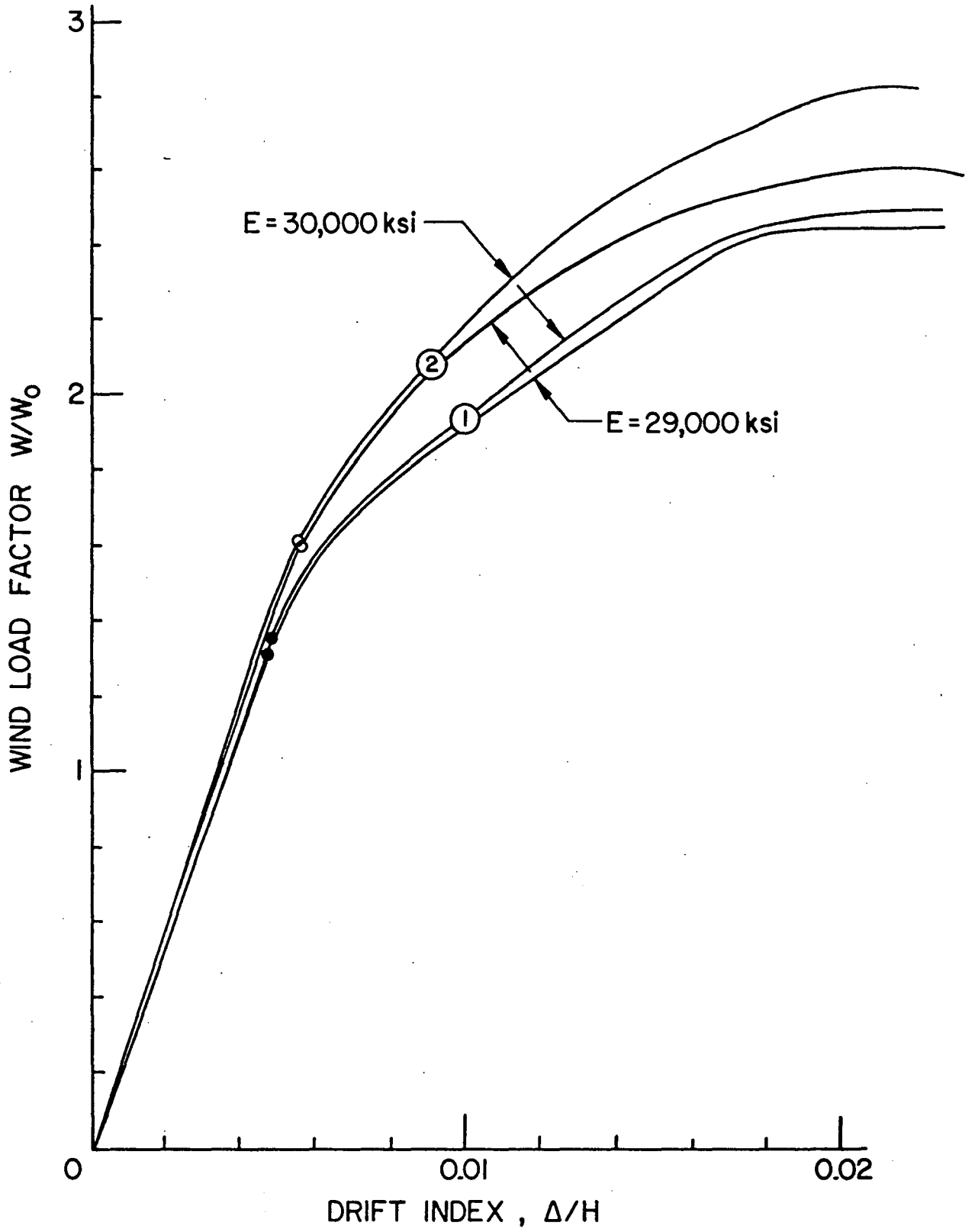


Fig. 46 Effect of Variation of Modulus of Elasticity
Frame 5 - Design II - Analyses 1 and 2

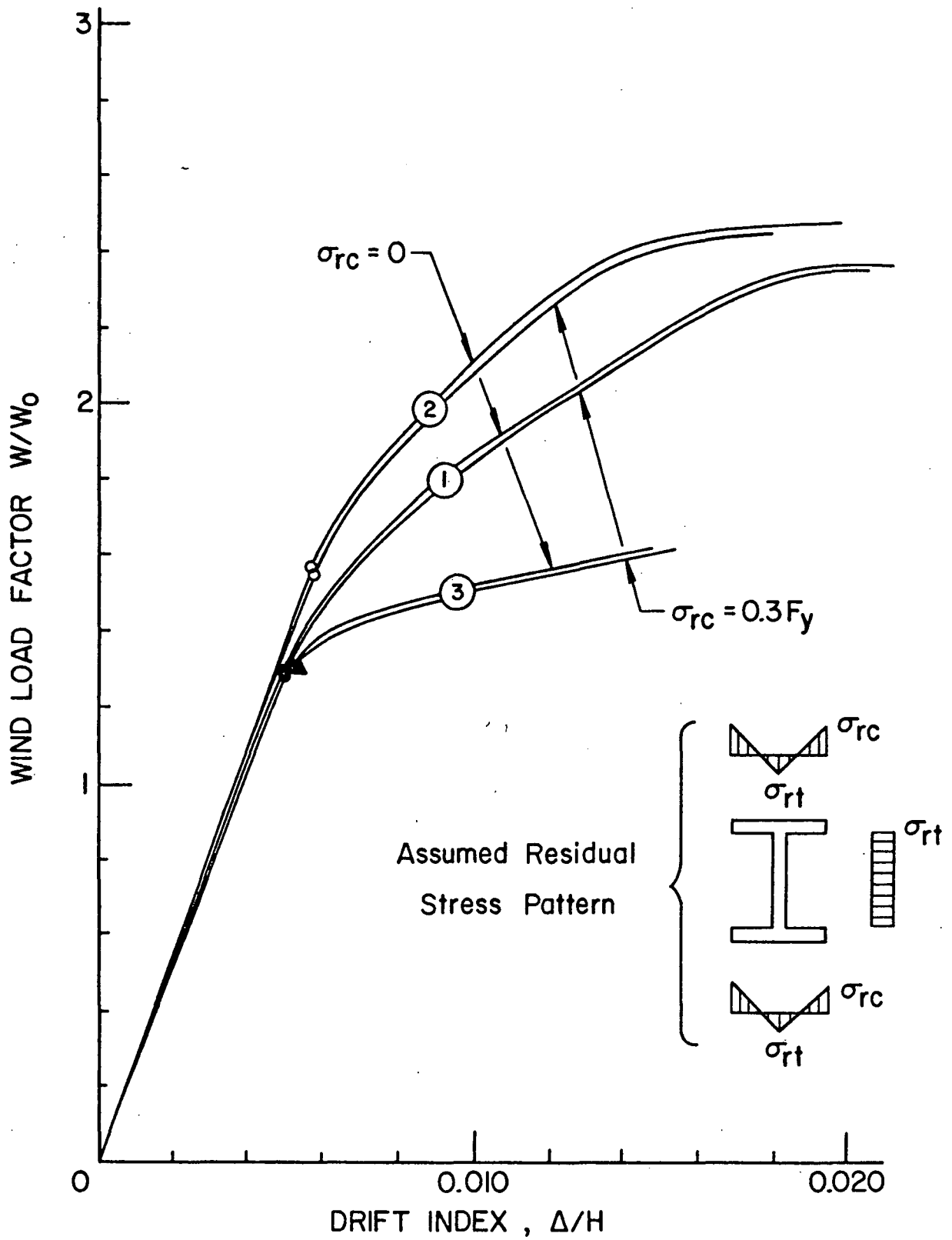
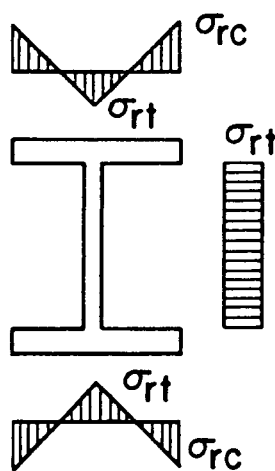


Fig. 47 Effect of Assumed Residual Stress Patterns
 Frame 5 - Design I - Analyses 1, 2 and 3

W8 x 31

$\phi/\phi_{pc} = 0.1$

$\sigma_{rc}/F_y = 0.3$



Assumed Residual Stress Pattern

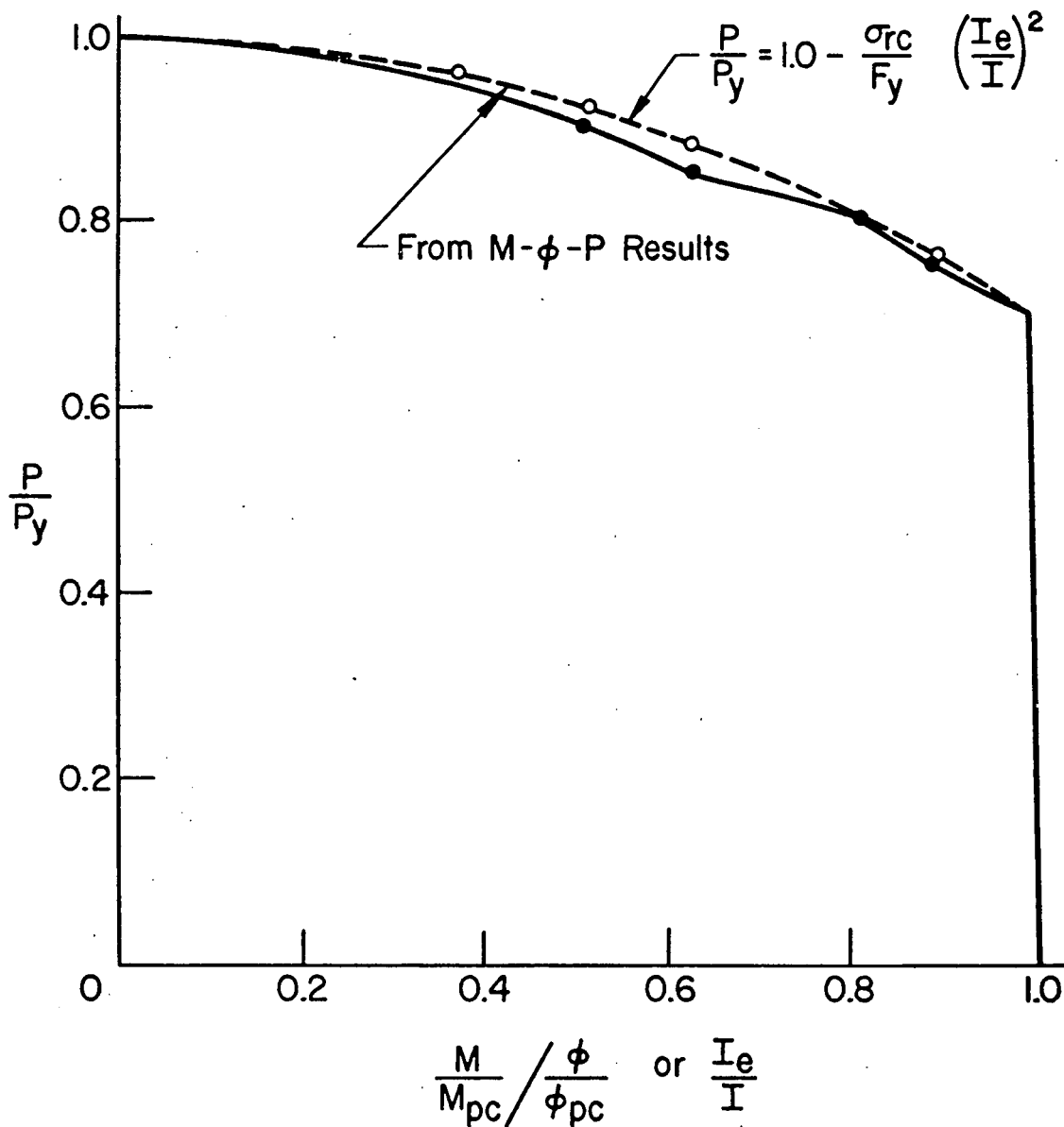


Fig. 48 Effective Moment of Inertia

11. REFERENCES

1. Lu, L. W.
STABILITY OF FRAMES UNDER BENDING MOMENTS, Journal of the Structural Division, ASCE, 89 (ST-3), p. 35, (June 1963)
2. Galambos, T. V.
STRUCTURAL MEMBERS AND FRAMES, Chapter 6, Prentice-Hall, Englewood Cliffs, N. J. 1968.
3. Lay, M. G.
THE BASIS FOR THE PLASTIC DESIGN RULES OF AS CAL.
Proceedings, Second Australian Conference on Mechanics of Structures and Materials, Adelaide, 1969
4. ASCE-WRC
PLASTIC DESIGN IN STEEL-A GUIDE AND COMMENTARY, ASCE Manual and Report on Engineering Practice No. 41, 1971
5. AISC
SPECIFICATION FOR THE DESIGN, FABRICATION AND ERECTION OF STRUCTURAL STEEL FOR BUILDINGS, American Institute of Steel Construction, New York, 1969.
6. ASCE Subcommittee No. 31
WIND BRACING IN STEEL BUILDINGS (FINAL REPORT), Trans. American Society of Civil Engineers, 105, pp. 1713-1738, (1940)
7. ANSI
BUILDING CODE REQUIREMENTS FOR MINIMUM DESIGN LOADS IN BUILDINGS AND OTHER STRUCTURES, American National Standard A58.1 - 1972
8. Driscoll, G. C., Jr.
MULTI-STORY FRAMES I, IN "STRUCTURAL STEEL DESIGN" Edited by L. Tall, Second Edition, Ronald Press, 1974.
9. Fleischer, W. F.
SIMPLIFIED HIGH-RISE DRIFT ANALYSIS AND OPTIMIZED ADJUSTMENT, Engineering Journal, American Institute of Steel Construction, Vol. 9, No. 2, pp. 50-69, April, 1972.
10. Parikh, B. P.
THE ELASTIC-PLASTIC ANALYSIS AND DESIGN OF UNBRACED MULTI-STORY STEEL FRAMES, Ph.D. Dissertation, Fritz Engineering Laboratory Report No. 273.44, Lehigh University, May, 1966.

11. Kim, S. W.
ELASTIC-PLASTIC ANALYSIS OF UNBRACED FRAMES, Ph.D. Dissertation, Fritz Engineering Laboratory Report No. 346.6, Lehigh University, March, 1971.
12. Lu, L. W. and Beedle, L. S.
RECENT RESEARCH ON THE STRENGTH, STIFFNESS AND DUCTILITY OF STEEL BUILDING FRAMES, Proceeding, Australian and New Zealand Conference on Tall Building, Sydney, p. 633, August, 1973.
13. Liapunov, S.
ULTIMATE STRENGTH OF MULTISTORY STEEL RIGID FRAMES, Journal of the Structural Division, ASCE, 100 (ST-8), p. 1643-1655, (August, 1974)
14. Parikh, B. P., Daniels, J. H. and Lu, L. W.
PLASTIC DESIGN OF MULTI-STORY FRAMES, DESIGN AIDS, Fritz Engineering Laboratory Report No. 273.24, 1965